Pulmonary atelectasis: computed tomography findings in healthy Beagles under general anaesthesia

by

Christelle le Roux

Submitted in partial fulfillment of the requirements for the degree MMedVet (Diagnostic Imaging)

Faculty of Veterinary Science
University of Pretoria

Pretoria, May 2016

SUPERVISOR:

Dr. Nicolette Cassel BSc, BVSc, MMedVet (DIM), DipECVDI
Diagnostic Imaging Section
Department of Companion Animal Clinical Studies
Faculty of Veterinary Science
University of Pretoria

CO-SUPERVISOR:

Prof. Robert M. Kirberger BVSc, DVSc, MMedvet (Rad), DipECVDI
Diagnostic Imaging Section
Department of Companion Animal Clinical Studies
Faculty of Veterinary Science
University of Pretoria

Table of Contents

Acknowledgements vi
List of tables viii
List of figures ix
List of abbreviations xiv
Summary 1
Chapter 1: Introduction 2
1.1 Background 2
1.2 Problem statements 2
1.3 Research questions 3
1.4 Hypotheses 4
1.5 Objectives 4
1.6 Benefits 5
Chapter 2: Literature review 6
2.1 Definition of pulmonary atelectasis 6
2.2 A review of respiratory physiology 6
2.3 Pathophysiology and clinical signs of atelectasis 8
2.4 Clinical importance 11
2.5 Anaesthesia and atelectasis formation 12
2.6 Imaging modalities and findings in atelectasis 15
2.7 Radiation safety in CT 17
2.8 Applications in veterinary science 18
2.9 Relevant canine thoracic anatomy pertaining to the study 20
2.10 Conclusions drawn from the literature review 21
Chapter 3: Materials and Methods 22
3.1 Experimental design 22
3.2 Experimental procedures 22
3.3 CT Protocol 24
3.4 Observations and analytical procedures 30
3.5 Data measurements 31
3.5.1 Image symmetry and interpretation 31
3.5.2 Trachea 32
3.5.3 Aortic root 34
3.5.4 Diaphragm 36

3.5.5 Lungs 39
3.6 Data and statistical analysis 42
Chapter 4: Results 43
4.1 Study population 43
4.2 Data acquisition 43
4.2.1 General anaesthesia 43
4.2.2 Computed tomography procedure 45
4.3 Data sets analysed 46
4.3.1 Image symmetry and interpretation 46
4.3.2 Trachea 53
4.3.3 Aortic root 56
4.3.4 Diaphragm 57
4.3.5 Lungs 60
4.3.5.1 General overview 60
4.3.5.2 Subjective visual assessment of lung lobes 63
4.3.5.3 Overall assessment of combined left and right lung lobes in RLR versus LLR 64
4.3.5.4 Findings on slice “a” 70
4.3.5.5 Findings on slice “b” 76
4.3.5.6 Findings on slice “c” 83
4.3.5.7 Findings on slice “d” 90
4.3.5.8 Findings on slice “e” 99
4.3.5.9 Summary of findings in dogs with visual attenuation changes 105
4.3.5.10 Summary of results for all lungs lobes 108
Chapter 5: Discussion 110
5.1 General thoracic assessment and anatomical findings 110
5.2 Trachea 113
5.3 Aortic root 114
5.4 Diaphragm 115
5.5 Lungs 116
5.5.1 Measurement technique 116
5.5.2 Overall lung findings 118
5.6 Limitations of the study 122
5.7 Clinical applications 123
5.8 Future studies 124

Chapter 6: Conclusion 126
References 128
Appendices 133
Appendix A: Beagle data 133
Appendix B: Timed scanning intervals 133

Acknowledgements

Without the help of the following people this dissertation would not have been possible. Heartfelt appreciation goes to:

Dr. Nicky Cassel, for being my promoter and always being positive and enthusiastic about the research.

Prof. Robert Kirberger, for his advice during the planning of the protocol, input to and revision of my dissertation, and his thoroughness and attention to detail.

Prof. Allison Zwingenberger for her well-thought out input into the study design.

Sr. Melanie McLean, for assistance with the computed tomography scans, willingness and enthusiasm, even while helping on weekends – your positivity made the research a pleasure!

Dr. Zandri Whitehead, for her meticulous attention to detail while administering and monitoring/recording the general anaesthesia, and being willing to help out during her own busy residency.

Sr. Anette van Veenhuyzen, for her co-ordination of the Beagles before and during the research.

The Onderstepoort Teaching Animal Unit for allowing me to use their Beagles in my study – their support was paramount to the success and completion of my research.

The Department of Companion Animal Clinical Studies and Head of Department, Prof. Johan Schoeman, for financial assistance.

The 2014 first-year veterinary nursing students, for assisting in the handling of the Beagles for clinical examinations, blood collection and ultrasounds. Also a special thank you to Dr. Wilco Botha, for his additional help and assistance with UVIS and the clinical pathology laboratory.

Prof. Geoffrey Fosgate, for doing the statistical analysis for this project and his patience with my data capture and tables.

Ms. Estelle Mayhew for her help with the bulk of editing the images, and my sister Adrie le Roux who helped with some unplanned image editing.

Louis, for your love and support over the past 3 years, even from across the ocean. Your support of my career means the world to me.

Ma and Pa, for your continuous support and love, for always being there through the hours of studying and work, for providing us with everything we need and more, your selflessness and willingness to sacrifice for your children, and all the weeks of dog-sitting.

List of tables

Table 1 Transverse Plane Images Indicating Visual and Anatomical Landmarks for the Five Anatomical Lung Sites Page 26

Table 2 The Effects of Study Variables on Hounsfield Units Measured in the Six Dogs over the Entire Duration of the Study Page 66

Table 3 The Effects of Study Variables on Cross-Sectional Area Measured in the Six Dogs over the Entire Duration of the Study Page 67

List of figures

Figure 1	Sagittal planning image for slices “a” to “e”	Page 27
Figure 2	a) TRA and b) DOR images: Left to right image symmetry	Page 31
Figure 3	SAG image: Image symmetry for tracheal assessment	Page 33
Figure 4	TRA image: Method of tracheal assessment	Page 34
Figure 5	TRA image: Method of aortic root assessment	Page 35
Figure 6	SAG image: Point of maximal diaphragmatic excursion and symmetry for lung assessment	Page 37
Figure 7	DOR image: Diaphragm cupular symmetry	Page 38
Figure 8	DOR image: Diaphragm crural symmetry	Page 38
Figure 9	SAG image: Assessment of lumbophrenic angle	Page 39
Figure 10	TRA image: ROIs of dorsal, middle, ventral, and whole lung lobe	Page 41
Figure 11	Photo of study set-up: Dog, gantry and shielding	Page 44
Figure 12	Photo of anaesthetist positioning and breath-hold technique	Page 44
Figure 13	Photo of tailored CT protocol	Page 45

Figure 14 a) and c) TRA, and b) and d) DOR images: Cardiac apex shift in RLR and LLR Page 49

Figure 15 a) and c) DOR, b) and b) SAG images: Pericardiophrenic ligament Page 50

Figure 16 TRA images: Dorsal left and right diaphragmatic crural displacement in a) LLR and b) RLR Page 52

Figure 17 Graph: Comparison of tracheal position combined for all 3 slices in RLR versus LLR Page 54

Figure 18 Graph: Comparison of aortic root position in RLR versus LLR Page 56

Figure 19 DOR image: Symmetrical diaphragmatic cupula Page 58

Figure 20 DOR image: Asymmetrical diaphragmatic cupula Page 59

Figure 21 DOR image: Asymmetrical diaphragmatic crura Page 59

Figure 22 TRA image: Intrusion of left cranial *pars caudalis* at slice “a” Page 61

Figure 23 a) and b) TRA images: Thoracic and accessory lung lobe shape changes in sternal versus lateral recumbency Page 62

Figure 24 Graph: Comparison of combined left and right lung lobes HU in RLR versus LLR Page 64

Figure 25 Graph: Comparison of the combined left and right lung lobes cross-sectional area in RLR versus LLR Page 65

Figure 26 Graph: Comparison of the left cranial *pars cranialis* lobe HU at slice "a" in RLR versus LLR Page 70

Figure 27 Graph: Comparison of the left cranial *pars cranialis* lobe CSA at slice "a" in RLR versus LLR Page 71

Figure 28 Graph: Comparison of the right cranial lobe HU at slice "a" in RLR versus LLR Page 73

Figure 29 Graph: Comparison of the right cranial lobe CSA at slice "a" in RLR versus LLR Page 74

Figure 30 Graph: Comparison of the left cranial *pars cranialis* Lobe HU at slice "b" in RLR versus LLR Page 76

Figure 31 Graph: Comparison of the left cranial *pars cranialis* lobe CSA at slice "b" in RLR versus LLR Page 77

Figure 32 TRA image: Dog 1 at slice “b”, left cranial *pars cranialis* increased attenuation ventrally Page 78

Figure 33 TRA image a) and b): Dog 2 at slice "b” demonstrating lack of resolution of attenuation changes in the left *pars cranialis* Page 79

Figure 34 Graph: Comparison of the right cranial lobe HU at slice "b" in RLR versus LLR Page 80

Figure 35 Graph: Comparison of the right cranial lobe CSA at slice "b" in RLR versus LLR Page 81

Figure 36 Graph: Comparison of the left cranial *pars caudalis* lobe HU at slice "c" in RLR versus LLR Page 83

Figure 37 Graph: Comparison of the left cranial *pars caudalis* lobe CSA at slice "c" in RLR versus LLR Page 84

Figure 38 TRA image: Dog 1 at slice “c”, left *pars caudalis* increased attenuation ventrally Page 85

Figure 39 Graph: Comparison of the right middle lobe HU at slice "c" in RLR versus LLR Page 87

Figure 40 Graph: Comparison of the right middle lobe CSA at slice "c" in RLR versus LLR Page 88

Figure 41 Graph: Comparison of the accessory lung lobe HU at slice "d" in RLR versus LLR Page 90

Figure 42 Graph: Comparison of the accessory lung lobe CSA at slice "d" in RLR versus LLR Page 91

Figure 43 Graph: Comparison of the left caudal lobe HU at slice "d" in RLR versus LLR Page 93

Figure 44 Graph: Comparison of the left caudal lobe CSA at Slice "d" in RLR versus LLR Page 94

Figure 45 TRA image: Dog 1 at slice “d”, left caudal lobe increased attenuation Page 95

Figure 46 Graph: Comparison of the right caudal lobe HU at slice "d" in RLR versus LLR Page 96

Figure 47 Graph: Comparison of the right caudal lobe CSA at slice "d" in RLR versus LLR Page 97

Figure 48 Graph: Comparison of the left caudal lobe HU at Slice "e" for RLR versus LLR Page 99

Figure 49 Graph: Comparison of the left caudal lobe CSA at slice "e" in RLR versus LLR Page 100

Figure 50 Graph: Comparison of the right caudal lobe HU at slice "e" in RLR versus LLR Page 102

Figure 51 Graph: Comparison of the right caudal lobe CSA at slice "e" in RLR versus LLR Page 103

Figure 52 TRA image: Dog 6 at slice “e”, right caudal lobe increased attenuation Page 104

Figure 53 TRA image: Dog 5 at slice “c”, left *pars caudalis* increased attenuation Page 107

Figure 54 TRA image: Proposed method for assessment of atelectasis in obviously affected lungs Page 125

List of abbreviations

CSA	Cross-sectional area (in cm^2)
CT	Computed tomography
CVC	Caudal vena cava
DOR	Dorsal plane images
Fig	Figure
FRC	Functional reserve capacity
HU	Hounsfield unit
ICS	Inter-costal space
kV or kVp	kilovolt
LLR	Left lateral recumbency
LLR_3	CT scan at 3 minutes after placement in LLR
LLR_8	CT scan at 8 minutes after placement in LLR
LLR_{13}	CT scan at 13 minutes after placement in LLR
LLR_{20}	CT scan at 20 minutes after placement in LLR
LLR_{30}	CT scan at 30 minutes after placement in LLR
mA	Milliampere
MPR	Multi-planar reformatting
P	Statistical level of significance (set at 5%)
RLR	Right lateral recumbency
RLR_3	CT scan at 3 minutes after placement in RLR
RLR_8	CT scan at 8 minutes after placement in RLR
RLR_{13}	CT scan at 13 minutes after placement in RLR
RLR_{20}	CT scan at 20 minutes after placement in RLR
RLR_{30}	CT scan at 30 minutes after placement in RLR
ROI	Region of interest
SAG	Sagittal plane images
T	Thoracic vertebra/e
S_5	Sternal transverse CT scan at 5 minutes after S_e
S_{10}	Sternal transverse CT scan at 10 minutes after S_e
S_{20}	Sternal transverse CT scan at 20 minutes after S_e

S_e	First full helical transverse CT sternal scan after lateral recumbency
S_i	Initial full helical transverse CT baseline sternal scan
TRA	Transverse plane images
V/Q	Ventilation perfusion ratio
WL	Window level
WW	Window width

Summary

Pulmonary atelectasis: computed tomography findings in healthy Beagles under general anaesthesia

Le Roux, C. University of Pretoria, 2016

Keywords: atelectasis, computed tomography, general anaesthesia, lateral recumbency, pulmonary

A large proportion of dogs undergoing computed tomography are anaesthetised and receive concurrent supplementary oxygen. Both factors promote the development of pulmonary atelectasis, which may mask or mimic lung pathology and compromise image quality, which is of concern to the radiologist. The aim of the study was firstly to determine whether significant atelectasis would develop using a commonly employed anaesthetic protocol in a typical hospital setting, especially where dogs may have been anaesthetised in lateral recumbency prior to scanning. Secondly, to determine whether a change in body position to sternal recumbency would be sufficient to resolve atelectasis.

Six healthy adult Beagles were anaesthetised in sternal recumbency and using a breath-hold technique, baseline helical transverse thoracic images were acquired. Dogs were then placed in either right or left lateral recumbency for 30 minutes, with scans performed at predetermined lung lobe locations and time intervals. Dogs were then repositioned in sternal recumbency for a further 20 minutes, with similar scans performed. The study was repeated two weeks later in the opposite lateral recumbency. Changes in Hounsfield units and cross-sectional area of all lung lobes were measured.

Lateral recumbency did not result in true atelectasis in healthy Beagles of normal body condition. Infrequently, patchy increased attenuation, which failed to resolve completely during sternal recumbency, was visualised in the left cranial lobe during left lateral recumbency. The degree of attenuation changes in healthy Beagles was minimal, and thus if dogs were anaesthetised in lateral recumbency prior to computed tomography, this should not preclude scanning.

Chapter 1: Introduction

1.1 Background

Computed tomography (CT) has become a popular and widely available imaging modality for companion animals worldwide. In humans, CT has proven to be the best imaging modality available to assess diffuse lung disease, pulmonary neoplasia and metastases, and these applications have found to be of similar value in companion animal lung studies.[1] The majority of animals undergoing CT are anaesthetised and receive concurrent oxygen supplementation. Both factors are major contributors to the development of atelectasis.[2–5] Furthermore, atelectasis may be enhanced in cases where dogs may already be anaesthetised in lateral recumbency for a period of time prior to CT scanning.[6]

Patchy increased soft tissue attenuation of the lungs is regularly seen in dogs undergoing CT at the Onderstepoort Veterinary Academic Hospital, assumed to be due to pulmonary atelectasis, which may mask or mimic lesions[6] (e.g. pulmonary metastases or pneumonia) in the lungs if the clinician is not attentive thereof. It is this potential image compromise which makes atelectasis of concern to the radiologist. Besides the potential to miss pathology, atelectasis may lead to pulmonary complications, particularly post-operatively and in patients with a compromised respiratory system.[2] Such complications are well documented in people, but a few studies have suggested that atelectasis may be a risk factor for post-operative pulmonary complications in dogs as well.[7,8]

1.2 Problem statements

- When faced with an animal that has been anaesthetised and positioned in lateral recumbency for a period of time prior to CT scanning, the radiologist needs to decide on the optimal manner to perform the scan, bearing in mind the possibility of atelectasis formation (with regard to lung studies), or whether to abort the study in total.
- Pulmonary atelectasis may mask clinical lung disease or pulmonary abnormalities.

- Ventilatory and anaesthetic strategies have been documented to resolve atelectasis, but currently only broad recommendations exist in dogs regarding positional changes that may resolve or prevent it.

1.3 Research questions

Appearance of the normal thoracic structures and lung

- What are the baseline Hounsfield units (HU) and cross-sectional area (CSA) values expected for each lobe, and do they occur in a vertical (dorsal to ventral) gradient? Do these values correlate with normal lung HU reported in the literature?
- Do HU and CSA findings support and correlate with each other (e.g. greater lung CSA should be better aerated, and thus have a more negative HU)?
- What are the baseline anatomical positions of the aortic root and the trachea?
- How does body position affect the position of the trachea and aortic root?
- Can diaphragmatic position give an indication of the stage of respiration (inspiratory versus expiratory)?
- Does diaphragmatic cupular and crural anatomical position on CT correlate with those described in radiology?
- Utilising our chosen study population, anaesthetic technique and CT protocol, will there be visually apparent HU and lung CSA changes?
- How does each lobe behave with regards to HU and CSA when it is dependent versus non-dependent?
- How will the HU and CSA of each lung change over time, and with change in body position?

Atelectasis formation

- What will be the range of HU of the most severely affected lung lobes, and will this be consistent with an atelectic lung?
- If atelectasis forms, will there be obvious secondary signs such as mediastinal or diaphragmatic excursion seen on CT?

- If atelectasis has formed, how long will it take to resolve with repositioning in sternal recumbency?
- If there are any significant HU or CSA changes, do they correlate with tracheal, aortic root and diaphragmatic findings/changes?

1.4 Hypotheses

- Pulmonary atelectasis will develop within five minutes in the dependent lobes after placement in lateral recumbency (following induction of general anaesthesia), and:
    - will progress in severity up to 20 minutes (post induction of general anaesthesia) whilst in lateral recumbency;
    - will not show progression after 20 minutes;
    - will be resolved within 10 minutes after return to sternal recumbency.
- With a decrease in CSA, an increase in HU would be expected (indicating decreased aeration, or atelectasis, depending on the magnitude), and vice versa.
- For the right lung lobes, the right middle lung lobe will be first to become atelectic and be most severely affected in right lateral recumbency (RLR).
- For the left lobes, the left cranial lobe will be most severely affected when in left lateral recumbency (LLR).
- The periphery of the lungs will be affected first and most severely.
- There will be indirect evidence of atelectasis, if present and severe enough, in the hemi-thorax where it occurs, seen as mediastinal shift towards the affected side and cranial excursion of the diaphragm on the affected side.

These hypotheses are based on the most common radiographic sites we have seen clinically, as well as relevant imaging and anatomical literature.[9–11]

1.5 Objectives

- To determine which lung lobes develop atelectasis at what time intervals, and most severely, if an animal is positioned in lateral recumbency prior to CT scan

(for example, an animal induced in another part of the hospital prior to CT, or undergoing CT after surgery).

- To assess how long it takes for atelectasis to resolve after repositioning in sternal recumbency, and which lung lobes resolve first.
- To collect information which may not form part of the main objectives but may be utilised at a later stage (e.g. thoracic CT anatomy).
- All studies will be done using the standard general anaesthetic protocol employed for dogs undergoing CT at the Onderstepoort Veterinary Academic Hospital.

1.6 Benefits

- To determine if repositioning an animal (after atelectasis has formed or is suspected of having formed), will resolve atelectasis and thus allow imaging of the lungs without confusing artefactual pathology, utilising a standardised anaesthetic technique in a clinical hospital setting.
- To improve diagnostic accuracy by ensuring that atelectasis does not form or is resolved before pursuing a CT scan.
- To decrease unnecessary radiation exposure, frequency of general anaesthesia and time wastage encountered with repeat CT scans where atelectasis has already formed.
- To pre-empt atelectasis in compromised dogs and improve clinical management of such dogs.
- This research project will fulfil one of the requirements for completion of the MMedVet (DIM) degree for the primary investigator.

Chapter 2: Literature review

2.1 Definition of pulmonary atelectasis

Pulmonary atelectasis is broadly defined as collapse of the alveoli[2,4] or absence of gas from portions of the lungs,[4] and the lack of ventilation to a collapsed lung.[12]

This is not to be confused with pulmonary hypostasis, which is sometimes been used erroneously to refer to atelectasis. Hypostasis refers to the gravitational accumulation of fluid or blood in the dependent parts of organs or the body, due to poor circulation or as occurs after death (http://www.oxforddictionaries.com). Hypostasis may be a contributing factor in passive atelectasis formation, but there are other causes of atelectasis that are not due to hypostasis.[10]

2.2 A review of respiratory physiology

The respiratory system is designed to distribute oxygen obtained from the atmosphere to the body, and to remove carbon dioxide, the body's main metabolic waste product.[13] Ventilation is the process by which air, containing oxygen, is taken into the lungs, where gaseous exchange can take place, and ends with air, containing carbon dioxide, being released back into the environment.[12] Ventilation can be quantified by the formula:

$$VE = VT \times f$$

Where
VE = minute ventilation, the total volume of air breathed per minute
VT = tidal volume, or the volume of air taken in with each breath, and
f = ventilation frequency, or breaths per minute.

Inhalation is an active process that relies on muscular energy and adequately functioning respiratory muscles, the most important ones being the diaphragm and the external intercostal muscles.[12] Active contraction of the laryngeal muscles widens the glottis, and active contraction of the diaphragm and external intercostal muscles

expand the thorax and thus increases thoracic volume. This leads to a reduction in the intrathoracic pressure which is necessary for the lungs to expand. Exhalation occurs immediately after inhalation after tidal volume has been reached, and relies on the elastic recoil of the thorax and thus is largely independent of muscular activity.[12]

At the end of exhalation, some air will remain within the alveoli to prevent collapse of the lung. This is known as the functional reserve capacity, or FRC. The lungs are kept from collapsing at the end of expiration due to negative intrapleural pressure, which is about minus 5 centimetres water. Loss of this negative pressure will lead to collapse of the lungs due to their elasticity. Elastic and collagen tissue content of the lung, as well as their surface tension, are responsible for this elasticity. To counter this elasticity, the lung has a surfactant lining which decreases the surface tension.[12]

Lung compliance is the measure of the elastic properties of the lung, and the respiratory muscles must work to overcome this elasticity in order for inspiration to be effective. A compliant lung is easy to inflate, whilst a non-compliant lung is difficult to inflate. Lung compliance is the most important factor causing resistance to inhalation during low respiratory and low flow rates, for example at rest.[12] A diseased lung, as occurs with pulmonary fibrosis or pneumonia, will also lead to a decrease in compliance. Such a diseased lung has an increase in elastic recoil which leads to rapid exhalation, which the body tries to prevent by using respiratory muscles to “break” the exhalation process. This will lead to a terminal expiratory push which can encroach into the normal FRC and increase the work required to initiate the next inspiratory cycle.[13] At higher respiratory rates, for example during exercise, frictional resistance of the airways play a more important role and needs to be overcome by muscular energy.[12]

Gaseous exchange can only occur within the lung alveolus. Alveolar dead space refers to poorly perfused alveoli that prevent gas exchange.[12] Gaseous exchange depends on the close relationship between the alveoli and the pulmonary capillaries. Preferably, ventilation (V) and perfusion (Q) should be matched closely, meaning that each alveolus should receive air and blood in proportions that are ideal for gas exchange to occur (called the V/Q ratio). Even in the healthy animal this does not occur, as there is some V/Q mismatching due to gravity and the normal branching of bronchi, bronchioli and blood vessels. A V/Q of 0.8 is acceptable in a healthy patient. In diseased lung, V/Q mismatches become significant and may lead to hypoxaemia due to impaired gas exchange. Low V/Q occurs in lung disease, for example

pneumonia and obstructive disease, due to decreased ventilation. High V/Q occurs when ventilation is relatively increased, as may occur when there is decreased blood flow or obstruction to blood flow. Low V/Q occur in atelectasis, or when there is blood supply but no ventilation. V/Q may be close to zero in either case.[12]

Distribution of ventilation is normally unequal in the healthy animal, but becomes even more so in disease states. This can be due to decrease in lung compliance, such as in pneumonia and obstructive airway disease. Distribution of ventilation also varies in recumbent animals, more notably in larger species such as the horse. Airway walls are not rigid and thus can be influenced by external compression due to the weight of mediastinal and abdominal structures.[12]

Dogs and cats lack significant interlobular septae[1] and thus have extensive collateral ventilation between lung lobes,[9] versus the pig and bovine which do not.[12] The healthy human lung has well-defined interlobular septae that demarcate the secondary lung lobules,[1] and thus also appears to have no significant collateral ventilation, except in disease states such as emphysema and obstruction. Collateral ventilation ensures that the lung receives air even when the parent bronchi are obstructed. In species where collateral ventilation is poor, such as man, the pulmonary arterial walls have well developed muscular walls that can vasoconstrict in response to hypoxia.[14]

2.3 Pathophysiology and clinical signs of atelectasis

Several different mechanisms have been described leading to the formation of atelectasis in man and dog. These include passive, compression, resorption (obstructive), adhesive and cicatrisation atelectasis[3,10] and all are due to the loss of lung volume by air loss. Non-inflation or non-expansion atelectasis, as occurs in the neonate due to the lack of surfactant,[9] will not be considered here.

Passive atelectasis occurs when the extra-alveolar pressure is moderately increased. This often occurs when the dependent lung portion collapses under the weight of non-dependent structures when the full capacity of the lung is not utilised. This is termed hypostatic collapse and is a normal physiological process.[10] An example of this occurs when an animal is placed in lateral recumbency for radiographs, and the dependent lung collapses due to the heart compressing the

lungs, decreased movement of the dependent thoracic cage due to compression, and because of the cranial shift of the dependent portion of the diaphragm. This occurs relatively rapidly in sedated, anaesthetised and even awake dogs.[15] Other causes of increased extra-alveolar pressure include pleural effusion or pneumothorax, or prolonged recumbency (especially important in anaesthetised patients).[10] The lungs retract from the thoracic wall due to their inherent elastic recoil which can no longer be counterbalanced by the natural recoil of the thoracic wall due to the disturbance in the integrity of the pleural space. The lungs maintain their shape but are deflated, thus appear as smaller replicas of their natural inflated state.[9]

Compression atelectasis occurs when the external transmural pressure is much greater than that required to keep the alveolus distended (it exceeds atmospheric pressure), and thus the alveolus collapses.[3] There is considerable loss of lung volume which cannot be reversed by the normal elastic recoil. Examples of causes include tension pneumothorax and large pleural effusions,[10] or with extra-pulmonary or pulmonary parenchymal lesions that impinge on surrounding alveoli.[9]

Neither passive nor compression atelectasis is obstructive. Both may be reversed with normalisation of extra-alveolar pressures[10] and thus generally have a good prognosis with no secondary involvement of tissues having occurred.[9]

Resorption atelectasis, also known as “gas” or obstructive atelectasis occurs if gas is removed from the alveolus (by capillaries) more rapidly than the rate at which it enters the alveolus. It may either occur due to airway obstruction, for example bronchial foreign bodies or mucous plugs in pneumonia, or due to non-obstructive causes, such as administration of supplemental oxygen. In airway obstruction, no fresh inflow of gas can occur distal to the obstruction and gas that is trapped distally will continue to be absorbed as blood flow continues.[10] Obstruction has to be complete in order to lead to alveolar collapse, thus collateral air supply has to be obstructed by exudates or inflammation. Other more complex factors can contribute to the formation of obstructive atelectasis in dogs, and include drying of airways, thick mucus secretions, decreased mucociliary action, inhibited cough reflexes, prolonged recumbency or absence of intermittent deep inspiration. These factors are most important in animals that undergo prolonged general anaesthesia, are unconscious, have impaired central respiratory control or have serious thoracic wall injuries. The prognosis in these cases may be guarded, with atelectasis leading to potential infection, which may become chronic, potentially leading to fibrosis.[9] In non-

obstructive causes of atelectasis, supplemental oxygen will replace nitrogen as the main component of inhaled and thus alveolar gas. As oxygen diffuses more readily into the blood, it is rapidly removed from the alveolus leading to a reduction in alveolar volume and progressive alveolar collapse. This is a normal physiological process.[10] This process may be accentuated when the alveoli have relatively low V/Qs.[3]

Adhesive atelectasis (not to be confused with atelectasis due to scarring or adhesion formation), due to decreased surfactant production or function, may contribute to atelectasis formation but this is the least important but also the least understood of the mechanisms.[3,9] Conditions leading to adhesive atelectasis include pneumonia and acute respiratory distress syndrome.[10]

Cicatrisation atelectasis occurs due to reduced lung compliance in cases of fibrosis or scar formation of lung tissue, such as occurs in idiopathic pulmonary fibrosis, chronic pneumonia or adhesive pleuritis.[10] The term cicatrisation atelectasis is of limited use and is controversial, and these cases usually have a poor prognosis.[9]

Atelectasis may involve only one lobe, or all lobes of a hemithorax, and may involve an entire lobe or only a part or segment of a lobe. It may also be partial or complete, depending on the amount of residual air and volume of lung left. Due to the dogs' well-developed collateral ventilation in the lung, segmental atelectasis in the healthy lung is uncommon and not clinically significant.[9]

Lung lobe collapse is rarely of similar degree between the lobes. The smaller lobes tend to collapse first, due to their larger surface-area-to-volume ratio. The right middle lobe and left cranial lobe are the smallest in the dog. The middle lobe is hypothesised to be predisposed to collapse due to less effective collateral ventilation, likely to be associated with its larger surface-area to volume ratio. The disease state of a lung also can influence degree of collapse - contused lung collapse to a greater degree than adjacent healthy lung, whilst emphysematous lobes tend not to collapse due to chronic over-inflation.[9]

The consequences of atelectasis depend on the type and duration of collapse, and pre-existing or concurrent pulmonary pathology. It may be resolved by re-inflation or lead to further complications such as fibrosis, pneumonia, bronchietasis or abscess formation.[9]

In humans, atelectasis has been associated with a decrease in lung compliance, impaired oxygenation, increased pulmonary vascular resistance and development of lung injury.[3] In dogs, more severe atelectasis or atelectasis in the diseased lung, may

be responsible for the formation of arteriovenous shunting, which causes respiratory distress.[9]

Clinical signs attributed to atelectasis in man may range from subclinical, to decreased breath sounds, crackles, coughing, and increased mucous production.[2] Impaired systemic oxygenation is the most striking effect of atelectasis in man[3] and has been described in obese dogs.[16] There are studies[7,8] that indicate that hypoxemia during the postoperative period in dogs without pre-existing pulmonary disease may be an important complication when surgery is performed using 100% oxygen supplementation along with inhalation anaesthetic agents. At this stage however the relationship between post-operative hypoxaemia and the development of atelectasis during anaesthesia has not been proven.

2.4 Clinical importance

Pulmonary atelectasis is the most common peri-anaesthetic and post-operative complication described in human patients, and considerable research has already focussed on its clinical significance, prevention and management.[3,17] In most cases, anaesthesia-induced and post-operative atelectasis is not clinically significant and disappears as the patient resumes natural breathing,[17] but in major surgery atelectasis may persist for up to 2 days.[3] The term “clinically significant atelectasis” has been used to describe atelectasis which persists or progresses in a patient and leads to clinically appreciable and significant hypoxaemia, dyspnoea or any other identifiable distress to the patient.[17]

Extensive research into prevention and treatment of atelectasis has been done, with treatment modalities including the use of voluntary deep breathing, spirometry, intermittent positive pressure breathing, chest physical therapy, bronchoscopy, aerosol therapy and intermittent continuous positive airway pressure.[17] Frequent turning and changes in body position are well known to be effective methods to decrease atelectasis formation.[2] In dogs, ventilation techniques have also been studied, and recruitment techniques (inflation techniques to re-expand all previously collapsed lung) continue to be developed and analysed.[18]

In several human studies, atelectasis and pneumonia have been dealt with together, as many of the pathophysiological changes attributed to atelectasis may

essentially predispose a patient to pneumonia. Atelectasis leads to altered surfactant production, making re-expansion of the lung difficult. Additionally, due to decreased mucociliary transport, bacterial growth may be aided. Thus a continuum from non-infectious (i.e. atelectasis) to infectious (i.e. pneumonia) pulmonary complications is established.[2] Atelectasis, in the same way, may potentiate damage in an already diseased or compromised lung by increased neutrophil activation.[3]

Pulmonary complications remain the leading cause of post-operative morbidity and death in humans, and development of post-operative pneumonia has been associated with a 30-46% mortality rate. Complications lead to increased healthcare costs by increasing the length of hospital stay and increased use of personnel and technology,[2] hence the interest in the topic of atelectasis in humans.

In canines, there is little information in the literature regarding the clinical importance of atelectasis, except for the importance of differentiating it from pneumonia, due to the vastly differing aetiologies and treatments.[9] Past research has assumed a relationship between post-operative hypoxaemia and atelectasis in the dog.[7,8]

2.5 Anaesthesia and atelectasis formation

Anaesthesia is a key factor that leads to atelectasis.

Ninety percent of human patients that have normal lung function before undergoing GA, will have atelectasis develop in the dependent lung portions during general anaesthesia.[19] Up to 20-50% of lung tissue in basal regions of human lungs may collapse[19] and atelectasis has been shown to appear on CT within 5 minutes of induction of anaesthesia.[20] In anesthetised dogs, notable CT attenuation changes occur within 7 minutes in lateral recumbency, but HU values could return to normal values within 7 minutes of repositioning into sternal recumbency.[11]

Atelectasis can develop with both intravenous and inhalation anaesthesia, and in both spontaneously breathing or mechanically ventilated patients.[2,3] Intravenous and inhalation anaesthesia cause a decrease in respiratory drive, due to suppression of the brainstem control centres of respiration, leading to hypoventilation.[21] No correlation has yet been found with the length of general anaesthesia and the degree of atelectasis formation in man.[22] In most human patients, and likely the same in

animals, the development of atelectasis is partly attributable to decreased or complete absence of periodic “deep breaths”, and in most cases these patients are not able to perform deep breathing manoeuvres due to factors such as administration of general anaesthesia, residual respiratory depression from anaesthesia or peri-operative pain.[3,17]

A major cause of anaesthesia-induced atelectasis in man is the use of high oxygen concentration during induction and maintenance of anaesthesia, in conjunction with anaesthetic agents that cause a fall in FRC. Thus absorption atelectasis is a convincing proven mechanism of atelectasis formation in general anaesthesia.[22] Oxygen is a highly soluble gas and rapidly gets removed from the alveoli, leading to collapse.[3] A common practice amongst anaesthesiologists is to use a high concentration of oxygen (approaching 100%) as pre-oxygenation prior to general anaesthesia, or along with inhalation anaesthetic during general anaesthesia, which can be correlated to more severe atelectasis formation. If a patient is not pre-oxygenated, atelectasis is not seen directly after induction. Similar findings are seen with increased oxygenation at the end of surgery before extubation,[3] or “post-oxygenation”.[22] In one study, the rate of atelectasis formation was three times greater when 100% oxygen was used during induction and maintenance of general anaesthesia, versus a 30% concentration.[23] Pre-oxygenation with oxygen appears to be a major determining factor in atelectasis formation in man. Despite maintenance of anaesthesia at a lower oxygen concentration (e.g. 40%), if pre-oxygenation at 100% was performed, it will result in the same degree of atelectasis in groups maintained at 40% or at 100% oxygen.[22] Re-expanding atelectic lung with 100% oxygen also results in a rapid return to the pre-expansion degree of atelectasis.[23] Despite these findings, anaesthetists still use a higher oxygen concentration as it provides a safety margin in cases of apnoea or difficulty in airway management which may lead to hypoxaemia.[3,24] Supplementation of 100% oxygen is also a common practice in veterinary anaesthesia and in dogs, supplementation at 40% significantly maintained better aeration and gas exchange compared to a 100% concentration (determined by blood gas parameters and degree of atelectasis on CT).[4] A recent study which assessed radiographic changes of atelectasis in sedated dogs breathing room air versus 100% oxygen, supported the findings that oxygen supplementation leads to a higher degree of atelectasis in dogs as well.[5]

Other contributing factors to atelectasis formation in humans include the relaxation and cephalad displacement of the diaphragm during anaesthesia, allowing less effective maintenance of the differential pressures between the thorax and abdomen. The pleural pressures are especially increased in the dependent lung regions and can compress the adjacent alveoli. In children, inhalation agents have shown to decrease the activity of intercostal muscles which contributes to a decrease in FRC. A net shift of blood from the thorax, which appeared to pool in the abdomen, has also been suggested as an additional source of pressure on the diaphragm and thus thorax.[3]

In humans, morbid obesity has shown to increase the occurrence of atelectasis due to decreased chest wall and lung compliance (the excess weight of the abdomen and torso increases cranial diaphragmatic excursion and makes excursion more difficult, leading to compression atelectasis). This leads to decreased functional reserve capacity, which promotes airway closure[3,25] and which leads to resorption atelectasis.[22] Pregnancy may have similar effects of FRC.[3] In sedated dogs, it has been shown that obesity has a significant effect on oxygenation, but not ventilation, and that after weight loss oxygenation significantly improves.[16] In this study, the reason for impaired oxygenation was not determined, but it was suggested to be due to atelectasis formation (as extrapolated from human studies). The amount of thoracic fat was shown to have the greatest effect on oxygen indices.

In diseased lung, such as in acute respiratory distress syndrome, there is poor lung compliance which will lead to hypoventilation.[12] Due to poor compliance in these cases, a low tidal volume will lead to increased atelectasis, as well as if a low tidal volume ventilatory strategy (as is the accepted standard for treatment) is employed.[3]

The dog has frequently been used as an animal model to study lung function during anaesthesia in humans, and it has been questioned whether or not the dog lung responds in a similar way to anaesthesia as the human lung does.[26] In a study on barbiturate anaesthesia and formation of atelectasis in dogs, it was demonstrated that in dogs anaesthetised with sodium pentobarbital and ventilated with room air, 75% did not show any atelectasis, and in those which did, the changes were very mild compared to humans.[26] A limitation to this study was that a significant proportion of the dogs had cardiac abnormalities or had been given digoxin or dobutamine prior to the study. The effects of the cardiac abnormalities and drugs on the formation of atelectasis, if any, were not investigated, and no positional changes were investigated.

Humans undergoing anaesthesia usually receive agents other than barbiturates for anaesthesia, usually receive muscle relaxants if ventilated, and are given supplemental oxygen as a routine. The effect of these differences in relation to human findings has been briefly alluded to,[26] but no concrete findings established.

2.6 Imaging modalities and findings in atelectasis

Radiographs are often a first step in evaluating canine patients with pulmonary or thoracic disease, but findings may be confused by the presence of a pleural effusion, involvement of multiple thoracic compartments or structures, and superimposition of structures.[27]

On radiographs of the canine lungs, pulmonary atelectasis is described as an alveolar pattern with increased focal or lobar opacity of the lungs (often triangular in shape), air bronchograms and border effacement.[9] A mediastinal shift[2] and sometimes over-inflation of the remaining aerated lung segments may also seen in severe human cases.[28] The affected lobes may be retracted from the thoracic boundaries by varying degrees, with cranial displacement of the hemi-diaphragm on the affected side, and crowding of blood vessels and bronchi seen due to loss of volume of the lung.[9]

Radiographs help to classify atelectasis according to the extent and location into massive unilateral lung atelectasis, lobar atelectasis, segmental atelectasis, plate-like linear atelectasis and small atelectic foci. Massive and lobar atelectasis are the most severe, as the rest are usually prevented by the dog's well developed collateral ventilation. Presumed plate-like atelectasis has recently been described in the non-anaesthetised dog and cat.[29] An important factor in the appearance of atelectasis in dogs and cats, versus in man, is body position immediately preceding radiographs. In man, patients are usually radiographed in an upright position, whilst animals are radiographed using lateral recumbency as one of the views obtained. Diseased lung tends to collapse rapidly in recumbency and may remain so for a period of time after being returned to sternal recumbency.[9] Similarly, animals under prolonged anaesthesia in lateral recumbency, or critically ill recumbent animals, are also predisposed to developing atelectasis prior to radiography.[9] Radiographs should thus be obtained in sternal or dorsal recumbency prior to lateral recumbency, and the

animal induced in sternal recumbency if radiographs are to be obtained with sedation or under general anaesthesia.[10]

Radiographic differential diagnoses in dogs for atelectasis include pneumonia, haemorrhage, contusion, and neoplasia, and a number of artefacts, such as resulting from rotated views. These may have subtle signs that can differentiate them, or may benefit from positional or sequential radiographs to differentiate them.[9]

Computed tomography has several advantages over conventional radiography[27] and is the preferred imaging modality when imaging the lungs in dogs as in humans. Its popularity is due to its increasing availability, elimination of superimposition, good contrast resolution, high signal to noise ratio for lung, and the ability to reconstruct the image into multiple planes (called multi-planar reformatting or MPR), three-dimensional images or volume rendered techniques. A patient can be scanned rapidly using helical CT, and lung volumes and aeration distribution can be calculated using inherent software programmes.[3,30] Computed tomography has demonstrated the occurrence of atelectasis in humans as early as the 1980's and is said to be the gold standard to detect lung aeration and atelectasis.[31] In man, a CT scale was devised to detect differences in lung inflation, enabling the user to identify and distinguish between hyperinflated (–1,000 to –901 HU), normally aerated (–900 to –501 HU), poorly aerated (–500 to –101 HU), and non-aerated (–100 to +100 HU) areas of lungs.[31] This scale has also been successfully and consistently used in dogs by one author.[4,32] Small variations of the scale exist depending on the literature consulted, with generally either -300 to 200 HU or -100 to +100 HU accepted as being consistent with atelectasis.[19,28,33,34] In companion animals, mean HU of -713 has been established for expiration and -846 for inspiration.[35] In man and dog, signs of atelectasis, seen as increased attenuation, appear in the dependent regions of lungs on CT.[3,11,26] The HU of these areas correspond to that of blood and connective tissue, thus indicating the absence of air.[3] Concomitant changes, as already described occurring in radiographs, may also be seen on CT.

Limitations to the use of CT are relatively few, and include motion artefact from respiration or from a patient that cannot be sedated, especially important in animals, and differences in operator techniques that may influence the conclusion of the study (e.g. use of contrast, use of a pressure injector).[27] The technique of sedation or general anaesthesia used may also be a limitation for thoracic studies, for example, atelectasis formation if a patient was induced in lateral recumbency (as may occur in animal

patients). Limiting factors pertaining more specifically to lung studies, where one may need to distinguish between lung tissue and surrounding soft tissue, include the partial volume artefact,[31,36] the lung's irregular borders, and sharp density gradients within the lung and surrounding tissues, leading to beam hardening. These factors may not be significant in studies where repeat scans of the same region are being performed, or in areas where the lung is well aerated.[31,37] It also has been documented that CT underestimates lung volume by up to 34% versus a helium dilution measurement technique, but that serial measurements are highly reproducible in experimental studies.[37]

CT may aid in determination of the cause of atelectasis, if caused by bronchial obstruction or if associated with a pleural effusion, thereby guiding the next investigative step.[38]

2.7 Radiation safety in CT

Advances in CT technology and availability have led to an exponential increase in the number of CT scans performed in the human population per year, both for diagnosis in symptomatic patients and as a screening tool in asymptomatic patients. This has led to an increase in interest in radiation safety associated with CT as it is related to an increased radiation dose compared to traditional radiography (up to 50 times increase for abdominal CT versus standard abdominal radiography).[39] There is also an increase in the number of children being scanned, thus the potential risk of cancer in this population due to CT is of importance.[39]

Steps are in place to decrease unnecessary patient exposure. CT should only be performed if no other modality will provide the same information, and the number of studies should be kept to a minimum.[39] Other methods include the use of automated exposure control (termed CARE dose by Siemens), a technique in which the automated tube current is adapted to the individual patient's size and anatomic shape. Thus for example, the thinner parts of the patient will receive less radiation than thicker parts, where a higher dose is needed to penetrate the tissue.[40]

Because CT is a genuine risk factor for radiation induced carcinogenesis, albeit a small one, it would appear logical to pre-empt the formation of atelectasis in a patient

and take the necessary steps to prevent or remedy it in order to prevent unnecessary repeat scanning.

2.8 Applications in veterinary science

As the majority of our patients undergoing CT studies receive general anaesthesia or deep sedation, presumptive atelectasis is something that is often seen with variable severity on CT images (including in the Onderstepoort Veterinary Academic Hospital). This is not only of clinical concern in patients with primary lung pathology undergoing imaging, but also for patients with abdominal or musculoskeletal pathology undergoing thoracic imaging. Cognisance to the fact that pulmonary atelectasis may, or will occur is especially important in aged or debilitated patients where there is a potential risk of transition from subclinical atelectasis to clinical pneumopathy.[7,8] Pulmonary atelectasis has not been extensively studied from the point of view that it may cause respiratory complications in the animal, as has been done in human studies, but it remains a possibility in especially the respiratory compromised animal.

References are available that allude briefly to positioning animals in sternal recumbency for CT and giving several manual inflations by endotracheal tube prior to the CT scan in order to reduce the incidence of pulmonary atelectasis.[10,41] References are available that also question the development of significant atelectasis in dogs under anaesthesia. These have already been discussed.[26]

A German study assessed the progression and regression of obstructive atelectasis in crossbreed dogs using radiography versus CT.[42] The investigators totally occluded either one or both main stem bronchi, using a double endotracheal tube, and documented the changes in HU, lung CSA and secondary evidence of mediastinal shift. Attenuation changes were seen to occur within 30 seconds of total occlusion, with total atelectasis occurring within 5.5 ± 1.1 minutes. Mediastinal shift towards the affected side was noted within 30 to 60 seconds. Resolution of atelectasis was observed over a 1 to 2 hour period with spontaneous respiration. The study proved that CT was more sensitive than conventional radiography at assessing the progression and regression of atelectasis over time, as would be expected, however its main focus was obstructive atelectasis.

In 1985, a canine CT study looked at the volume and CT attenuation values of lungs of three anaesthetised but spontaneously-breathing Beagle dogs placed in various body positions.[11] They found that changes in lung volume and CT attenuation values were detectable within seven minutes after placing the dog in lateral recumbency with no further changes occurring after this time. Lung volume of the dependent lung in lateral recumbency decreased to 50% of its volume in sternal recumbency, and its CT attenuation was increased in lateral recumbency versus in sternal or dorsal recumbency. After returning the dog to sternal recumbency, complete resolution of changes occurred within seven minutes. Unfortunately no specific lung lobes were alluded to, and were referred to simply as left or right lobes by the author. Interestingly, the authors found differences in regional attenuation when the dogs were in dorsal recumbency (i.e. higher HU values dorsally and lower values ventrally, versus the middle zone of the lungs); however, this was not found in sternal recumbency. The reason for this remains obscure.[11]

In dogs undergoing CT, it has been demonstrated that oxygen supplementation at 40% significantly maintained better aeration and gas exchange in the lungs compared to a 100% concentration.[4] The caudal lobes were the most severely affected when dogs were scanned in dorsal recumbency and showed signs of atelectasis. This was attributed to due to diaphragmatic shift that occurs with dorsal recumbency. The CT scans in this study however were performed after abdominal surgery of approximately one hour's duration.

Although not a CT study, as previously mentioned, radiologically visible positional atelectasis was demonstrated in dogs breathing both room air and supplemental oxygen, with oxygen supplementation causing more severe changes.[5] What was striking in this study was the degree of radiologically visible mediastinal shift and pulmonary interstitial/alveolar pattern that occurred. The dogs received different sedation protocols, but were not intubated. An interesting finding, which has often been demonstrated in human studies, was that the dogs with the highest body condition scores showed more severe atelectasis than those with lower scores. The authors mentioned the lack of CT in their study as a limitation, although the reason for this was justified.

It has been demonstrated using CT, that abdominal surgery greatly promotes the formation of atelectasis in dogs due to the increase in intra-abdominal pressure induced by the surgery, and the resultant cranial shift of the diaphragm.[32]

All these studies investigate the most important factors in a clinical environment, namely anaesthesia or sedation, inspired gas composition and oxygen supplementation, and body position; however, none replicate a typical clinical hospital set up. Many are found to be irrelevant from the radiologist's viewpoint regarding modern CT scanners, modern anaesthetic agents as well as relevant information on the affected lung lobes.

2.9 Relevant canine thoracic anatomy pertaining to the study

Comprehensive references exist with regards to general canine thoracic anatomy,[43] as well as radiological[44,45] and CT anatomy.[46]

The canine diaphragm may have a variable appearance on radiographs, which was the focus of a radiological study by Grandage.[47] He made many observations regarding the radiological anatomy and factors that may affect its appearance, including body position, most of which are still relevant today.

The radiological appearance of the diaphragm is ascribed to the divergent nature of the x-ray beam and where in the patient it is centred, which usually is either for the thorax or abdomen.[47] Anatomically, the left diaphragmatic crus is naturally always located in a more cranial position compared to the right crus in the sternal recumbent dog (e.g. standing).[47] However, the dependent crus is always more cranially located when in lateral recumbency, and this can be seen on standard RLR or LLR radiographs. The right side of the diaphragmatic cupular dome is as a rule more cranially located on a radiological dorsoventral view, whereas the two crura do not contribute to the diaphragmatic silhouette on this view.[47,48]

The angle between the ventral border of the vertebral bodies and the slope of the crura, dorsal to the caudal vena cava (CVC), was described on radiographs and normal values measured between 40° to 70°. This was found to be dependent on body position, thoracic conformation, and degree of inspiration.[47]

The pericardiophrenic ligament does not receive much attention in most references or literature. Description on the visualisation of the ligament with diagnostic imaging in the dog is sparse,[49–51] and it is usually only briefly mentioned in anatomy texts.[52] The ligament is described as a continuation of the apex of the fibrous pericardium to the ventral muscular periphery of the diaphragm. It is a dorsoventrally

flattened band of elastic fibres that is 1 cm wide, up to 5 cm long, but less than 1 mm thick, and is not radiographically visible.[52] The caudoventral mediastinal reflection is often erroneously referred to as the pericardiophrenic ligament, which was also a mistake made by Grandage in his original research on the canine diaphragm. Its function in that specific research was believed to minimise right lateral motion of the heart, however no further detail or reference was given to the finding.[47] More recent texts only mention that the ligaments' function is to severely restrict any cardiac motion.[53]

2.10 Conclusions drawn from the literature review

- Controversy exists about the degree of atelectasis formation in dogs, and there are few studies relating to possible respiratory complications in healthy or respiratory compromised dogs that have developed atelectasis.
- Studies evaluating time to development and severity of atelectasis in each lung lobe in dogs in a clinical hospital setting, using a standardised useful anaesthetic protocol (used for CT), are lacking. Most values are extrapolated from human studies, or have involved various outdated anaesthetic/oxygen protocols, outdated CT scanners or porcine models. The available canine studies fail to give information about specific lobes.[11]
- Radiographs have shown visible atelectic changes within a short period of time,[5] and thus it is expected that CT will show more pronounced changes.
- Computed tomography is the best modality for assessing the lung.
- No risk studies have been performed concerning acceptable radiation exposure to animals, and in humans it also remains a controversial topic.

Chapter 3: Materials and Methods

3.1 Experimental design

The study was approved by the University of Pretoria's Animal Ethics Committee (approval number V023-14). Radiation safety and as low as reasonably achievable (ALARA) principles were employed throughout as necessary.

Six adult sterilised female Beagles belonging to the Onderstepoort Teaching Animal Unit were used in this prospective descriptive study and served as their own controls (summarised in Appendix A). All dogs were in good body condition (5 to 6 out of 9, using the Nestlé® Purina body condition score chart, available from http://www.purina.co.uk), the median (range) age was 8 (8-9) years and body weight was 13 (10.8 – 13.7) kg. All dogs could be correctly identified by their microchips, and wore collars with tags that displayed their names. Older dogs were used due to greater inherent risk of radiation exposure in younger versus older animals, and thus only six dogs were made available by the Onderstepoort Teaching Animal Unit.

Each dog had a clinical examination performed by the author, as well as a blood smear, full blood count, basic biochemistry panel (total serum protein count, albumin, urea, creatinine, alanine aminotransferase, alkaline phosphatase, cholesterol and glucose), urinalysis (urine dipstick, specific gravity), and abdominal ultrasound performed two days prior to each component of the study (i.e. each CT study for LLR versus RLR). Lung pathology was ruled out by means of the survey CT scan (which formed part of each study). Pre-CT radiographs were not taken in order to decrease frequency of sedation or general anaesthesia for each dog, to decrease additional radiation exposure, and because CT is more sensitive at detecting pulmonary pathology. All six dogs were found to be clinically healthy.

3.2 Experimental procedures

Each dog (dog 1 - 6) underwent two CT studies separated by two weeks, one each for RLR and LLR. The dogs were randomly assigned into two groups by flipping a coin. Group 1 was scanned in RLR first, followed by LLR. Group 2 had the CT exams conducted in the reverse order. Each group (3 dogs) was scanned consecutively on

one day. The dogs were starved for 8-12 hours (water freely available) prior to induction of anaesthesia.

A 22-gauge intravenous catheter was placed in the cephalic vein of either the left or right thoracic limb and secured with Elastoplast®. Dogs were anaesthetised using the following anaesthetic protocol, which is routinely employed for dogs at the Onderstepoort Veterinary Academic Hospital:

- Premedication with morphine sulphate *(Fresenius Kabi, South Africa)* given at 0.2 mg/kg intramuscularly 15 minutes prior to intravenous catheter placement (although an opioid is not consistently given as premedication for anaesthesia of short duration for CT, it was added for this study to ensure a smoother more stable anaesthesia, due to the longer anaesthesia time (GE Zeiler (MMedVet Anaesthesiology), pers. comm. 12 March 2014).
- Diazepam *(Pax® 10mg/2ml, Pharmacare Ltd, South Africa)* given at 0.2 mg/kg intravenously.
- Induction followed within two minutes in sternal recumbency with propofol *(Propofol 1%®, Fresenius Kabi, South Africa)* given at 4-6 mg/kg intravenously.
- Endotracheal intubation was performed as soon as possible.
- Maintenance with 100% oxygen at 1 litre per minute, and 2 – 2.5% isofluorane *(Isofor®, Safeline Pharmaceutical [Pty] Ltd., South Africa)*.
- Monitoring of anaesthesia

The time of induction was recorded for each dog, as well as the time taken from induction to the first sternal scan in order to assess for time consistency between dogs.

Sternal recumbency was used as it is the most common orientation used for thoracic CT scans at the Onderstepoort Veterinary Academic Hospital and other institutions.

All dogs received an intravenous crystalloid *(Sabax® Ringers Lactate, Adcock Ingram)* at approximately 10 ml/kg/hr in order to combat insensible fluid loss due to the length of the general anaesthesia, evaporative losses due to maintenance on gas, and to prevent relative hypovolaemia due to vasodilation by the anaesthetic drugs (GE Zeiler (MMedVet Anaesthesiology), pers. comm. 12 March 2014). In retrospect this rate was probably slightly in excess of what is advocated for general anaesthesia

based on more recent fluid therapy recommendations,[54] however no dogs demonstrated evidence of volume overload on clinical monitoring. Each dog was covered by a blanket for the duration of the scan.

Anaesthesia was monitored and recorded on the standard hospital monitoring sheet (heart rate, respiration rate, body temperature), and the dogs were connected to a Datex-Ohmeda Cardiocap™ 5 multi-parameter monitor *(GE Healthcare, Finland)* in order to collect data on peripheral capillary oxygen saturation (SpO_2), end-tidal carbon dioxide and exhaled isofluorane concentration (data not used in this study). Maintenance of end-tidal isofluorane concentration between 1.4 and 1.6 was used in this study to ensure stability and similarity of anaesthetic plane between dogs (GE Zeiler (MMedVet Anaesthesiology), pers. comm. 12 March 2014).[55]

3.3 CT Protocol

Prior to each day's studies, the dual-slice CT machine (*Siemens SOMATOM Emotion Duo, Forchheim Germany*) was calibrated with the standard calibration phantom provided by the manufacturer, performed as per pre-set machine protocol.

Immediately after induction of general anaesthesia, a lateral topogram (in order to more easily visualise the ribs and vertebral bodies for selection of scan regions) of the thorax was performed, followed by a full helical thoracic CT scan in sternal recumbency with breath-holding, to rule out any pre-existing pathology and to act as a baseline for any subsequent measurements and comparisons. The scan field extended from the thoracic inlet to the second lumbar vertebra.

Scan parameters were as follows:

- lung window (window level (WL) = -600, window width (WW) = 1200)
- sharp kernel (B70s)
- feet first sternal/prone position
- kV = 130 and effective mAs = 38-48
- slice thickness of 3 mm (2 x 2.5 collimator setting)
- tube rotation time: 0.8 seconds
- caudocranial direction

- isocentre determined using the machine's laser marker and centred within the mid-thorax
- pitch automatically set by Siemens' software (at 1.85)
- reconstruction interval set at 1.5 mm, hence a 50% reconstruction increment
- field of view: 300 x 300 mm
- matrix dimensions: 1024 x 1024 pixels

None of the dogs had any lung changes that would have excluded them from the study.

Each dog was then placed in the designated lateral recumbency and the topogram scan repeated. The dogs were allowed to lie in a natural position in lateral recumbency without positioning aids. Slices were acquired at five selected anatomical lung sites, which were preselected to include representative samples of all lung lobes (right cranial lobe on slices "a" and "b", left cranial *pars cranialis* on slices "a" and "b", left cranial *pars caudalis* on slice "c", right middle lobe on slice "c", right and left caudal lobes on slices "d" and "e", and the accessory lobe on slice "d") from the topogram. The approximate landmarks are shown in Table 1 and Fig.1.

TABLE 1. Transverse Plane Images Indicating Visual and Anatomical Landmarks for the Five Anatomical Lung Sites

Lung lobes	Vertebral body reference points	Anatomical location (see Fig. 1 for SAG orientation)	Visual CT appearance (lung window: WL -600, WW 1200, patient's left is to the left of the image)
Left (*pars cranialis*) and right cranial lobes	C7 to T1 IVD space, may extend to caudal T1	Box a. Cranioventral mediastinal fold	
Left (*pars cranialis*) and right cranial lobes	Mid-body of T3 (variation from T2–3 IVD space to T3–4 IVD space)	Box b. Lobes located at the level of the terminal trachea, over the cranial third of the heart.	
Left (*pars caudalis*) and right middle lobes	T4–5 IVD space (variation from mid-T4 to mid-T5)	Box c. Region where either bronchus of the right middle or left *pars caudalis* lobes are visualised within a few slices of each other, over caudal third of heart.	
Accessory lobe, left and right caudal lobes	Mid-body of T7 (variation from T6–7 IVD space to T7-8 IVD space)	Box d. Region in between diaphragm and heart where the accessory lobe appears largest.	
Left and right caudal lobes	T8-T9 IVD space (variation from mid-T8 to mid-T9)	Box e. Immediately caudal to the caudal most extent of the xiphoid process.	

T- thoracic vertebra; IVD - intervertebral disk space

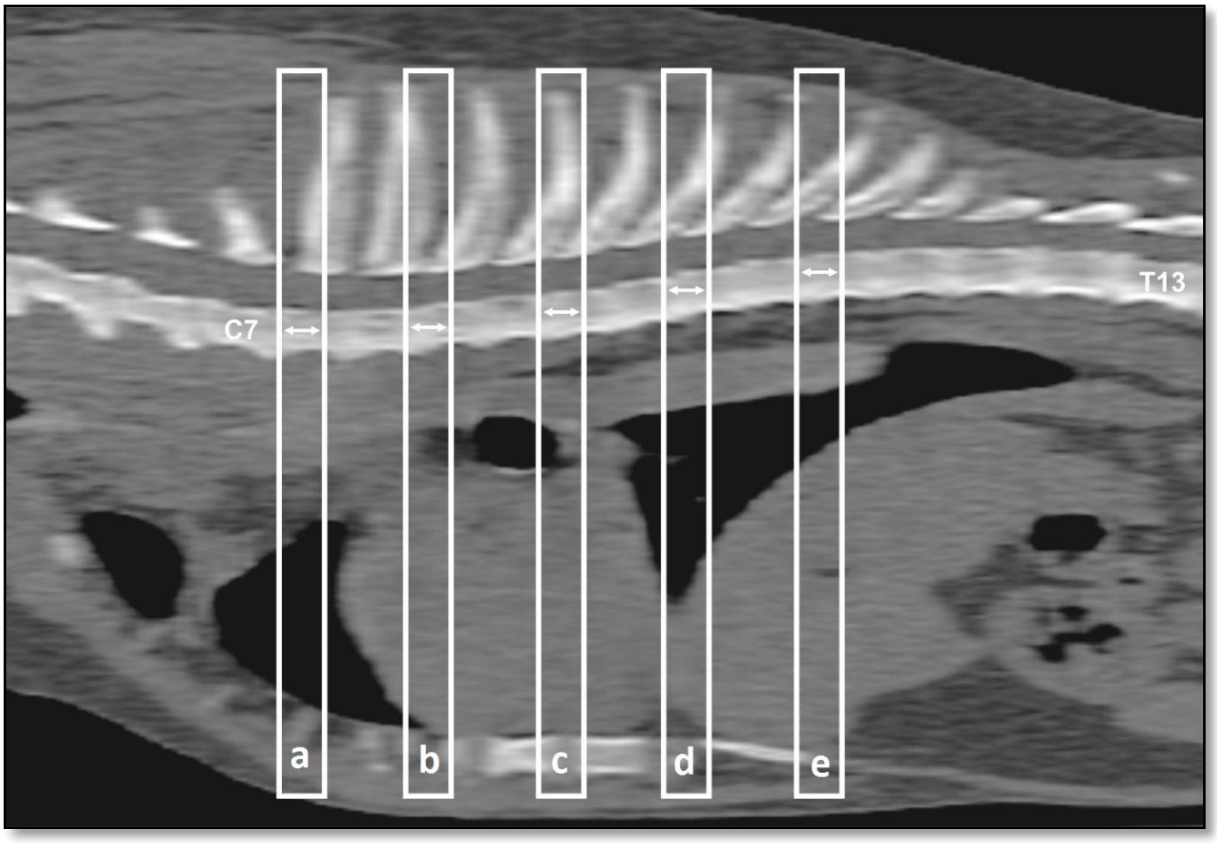

FIG. 1. Sagittal CT with white boxes labelled “a” to “e”, indicating regions where the lobes of interest were most likely to occur, compared to the vertebral bodies. The 5 boxes cross-reference with Table 1 (however are not in the same window). The image is in a bone window (WL 450, WW 1500) and was acquired in sternal recumbency.

Each box or set of slices consisted of approximately 14 – 21 slices of 1.5 mm reconstructed images (50% reconstruction intervals), resulting in an average total box length of 2.1 to 3.15 cm. Total length of the individual boxes added together (“a” to “e”) resulted in scan length of between 10.2 and 13.4 cm, out of total thoracic length of approximately 22.6 cm (on average) for a full thoracic helical scan, thus leading to scan reduction of between 45 to 60% for the 5 boxes, versus a full scan.

Total radiation dose to the patient and machine heating was thus reduced by only scanning certain regions versus repeating a full thoracic CT at each point in time, and by using the automated exposure control function (termed CARE Dose function by Siemens). Helical slices were employed in order to allow for MPR if needed in order to perform measurements, which is a function not capable with sequential slices, and 3 mm slice thickness was selected in order to be able to perform good resolution MPRs.

It was expected that there would be variation of the region of each lung lobe between dogs, depending on anatomical variation between individuals (minimised by selecting dogs of the same breed and similar weight), and some lung movement during respiration or breath-hold technique, but these combinations of visual and physical landmarks were deemed adequate and reasonably consistent between dogs based on findings of a pilot study. Some variation due to breed variation between the pilot studies and the research study was also likely. The initial planning of the location of the boxes, as well as pilot studies, were performed on large breed dogs (>30 kg), but the actual research studies done on Beagles. The visual landmarks as demonstrated in Fig. 1 were superior compared to positioning the boxes at specific vertebral body landmarks. As the scans follow quite rapidly after each other, it was expected that it would not be possible to scroll through all the images in order to define the exact region for scanning to occur and thus this method was used as an alternative attempt to consistently locate the lung lobe region of interest, which should on the whole stay consistent within in each dog.

Scans at the 5 locations were performed at the following time intervals, timed from the time that the dog was placed in lateral recumbency:

- 3-5 minutes
- 8 minutes
- 13 minutes
- 20 minutes
- 30 minutes.

Justification for the selection of these time intervals was based on available human and veterinary literature.[5,11,20]

The first lateral recumbent scans at 3 minutes were attempted as close to 3 minutes as possible, but obtaining a topogram and subsequently selecting the correct 5 regions to scan allowed for a very short time limit with no room for error, thus this value was advanced up to include up to 5 minutes in some cases.

Scanning was performed with a manual breath-hold technique[6] (the same technique for all scans) with pressures maintained at 15 cm water for the entire duration of the survey helical full thoracic scan, or the duration of the helical scans of

the 5 selected regions, which took about 45 seconds to 1 minute (without a break in breath hold, as the CT machine protocol is set to move automatically to the next box). The anaesthetic machine was mounted with a gauge that allowed measurement of pressure. It was expected that the dogs would start involuntary breathing against the breath-hold as the time progressed, but due to the caudo-cranial direction of the scan any respiratory movement would then occur when the machine was scanning the cranial aspect of the thorax, thus the effect of respiratory motion would be minimised. This is the breath-hold technique usually employed for thoracic CT at the Onderstepoort Veterinary Academic Hospital to reduce motion blur due to respiration. The need for personnel to be present in the CT room to perform the breath hold was a concern for radiation safety. Allowance was made for this, and this person stood behind a lead shield and wore protective apparel (lead jacket and thyroid shield), thus adhering to ALARA principles.

After the last scan in lateral recumbency at 30 minutes, the dog was returned to sternal recumbency and a topogram and full helical thoracic scan repeated (using settings as previously described), as atelectasis was expected to be at its most severe and that this scan would provide an overview of regions of the lungs that may have been missed when just scanning certain segments. The time taken to reposition the dog in sternal recumbency and perform the first scan was recorded, in order to ensure time consistency between dogs and studies.

Repeat helical scans at the 5 selected sites were performed again at the following time intervals, timed starting from repositioning in sternal recumbency:

- 5 minutes
- 10 minutes
- 20 minutes.

Justification for selection of these time intervals again was based on available human and veterinary literature.[11,20]

The opposite lateral recumbency was investigated as above, but performed two weeks later.

All scan protocols, as described above, were entered and saved as a specific thoracic scan protocol on the CT machine. The timing of the scans was done using a

cell phone stopwatch (*iPhone 5, Apple, South Africa*). All scans, at each time interval, were manually activated but would run automatically through boxes “a” to “e”.

3.4 Observations and analytical procedures

It would be determined from the data:

1. In what order and with what severity which lung lobes developed atelectasis, when in LLR and RLR.
2. The order in which resolution of atelectasis occurred when replaced in sternal recumbency.
3. Whether indirect indices, such as mediastinal shift, were present concurrently with atelectasis.

It would not be possible to differentiate between passive atelectasis and positional hypostasis, or resorption atelectasis due to oxygen maintenance during anaesthesia.

CT images were assessed and helical scans reconstructed (MPR), with interpretation and measurements made using the primary CT computer and its dedicated software (*Somaris/5 syngo CT 2006A, Siemens©, Berlin and Munchen)*. A single slice, deemed most representative of the lung in lateral recumbency, was selected from each block “a” to “e”, and measurements were done on these images. The slice was selected visually according to the images provided in Table 1 and Fig. 1, and kept as consistent between dogs and within each dog as possible. The slices selected on the lateral scans were visually compared to the full helical sternal scans and similar comparative slices were then selected from these scans. Images were reconstructed into soft tissue windows (WL = 40, WW = 400) for aortic root and tracheal measurements, and additional windowing was manually performed, when deemed necessary to enhance the ability to perform measurements. Lung measurements were all performed in a lung window (WL = -600, WW = 1200). Images were assessed over a 3 week period, on a daily or alternate day basis, and each component of data analysis of the study for each dog was performed in its entirety before progressing to the next dog. Subjective data analysis measurements were not

done at the same time as actual measured data, but were separated by at least 3 days. All data were captured on Microsoft Excel® data sheets, and each data sheet contained information on the date of CT, the dog identification/number, the breed, age, body condition score, total CT dose index and dose length product, and which lateral recumbency was performed first.

3.5 Data measurements

3.5.1 Image symmetry and interpretation

Images were aligned, using MPR, in such a way that the thorax was symmetrically visualised (Fig. 2a and b) and thus consistent between dogs, and measurements taken in specific planes as depicted in the images to follow.

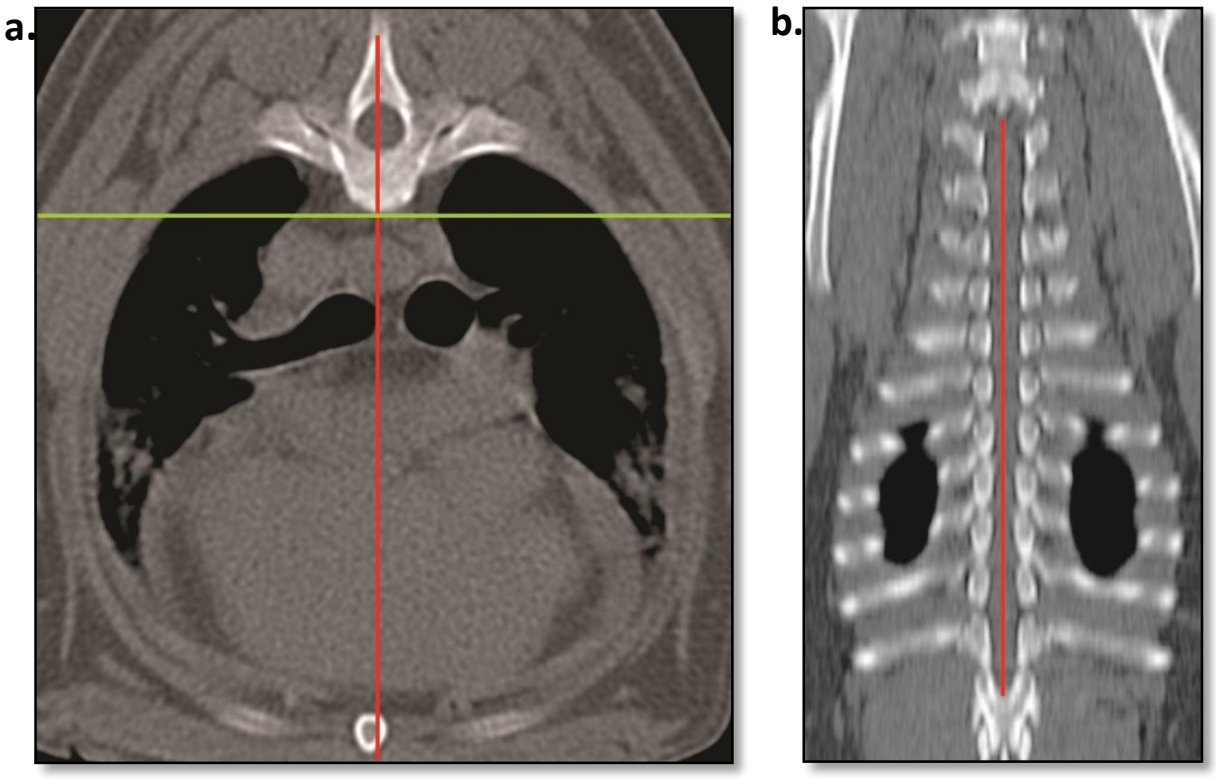

FIG. 2. For all image evaluations and measurements, left to right symmetry was obtained by positioning the CT reference line from dorsal to ventral on the transverse image (red line) (a), bisecting the vertebra into equal halves as accurately as possible. On the dorsal view (b), the reference line bisected the vertebral column in a cranio-caudal direction. Orientation of the other two lines is depicted elsewhere and was dependent on the area of interest. Left of the dog is to the left of the image for the transverse

images, and right of the dog is to the left of the image for the dorsal planes images. Images are shown in a bone window (WL 450, WW 1500) and were acquired in sternal recumbency.

For each dog, the following parameters were measured/determined for the selected 3 mm slice, at each lung lobe location where the structure of interest occurred (aorta, trachea, lung lobes) and compared within each dog (serving as their own control) and between dogs.

3.5.2 Trachea

I. The trachea was initially inspected in both transverse (TRA) and dorsal (DOR) planes, but measurements were only performed on the TRA planes as this was the more intuitive plane.
II. Position of the trachea (done on full helical thorax scan, or slice levels “a”, “b”, and “c”) was determined to detect mediastinal shift as an indirect indicator of pulmonary atelectasis.
III. Images were orientated so that the thorax had a symmetrical appearance (Fig. 2), and measurements were obtained from along planes depicted in Fig. 3.
IV. The tracheal/carina position was measured/determined in a transverse plane (Fig. 4). Measurements (in centimetres) were done at the centre of the trachea/carina and extended towards the left body wall, to terminate at the inner aspect of the pleura/soft tissue margin. A contralateral measurement towards the right body wall was not necessary, as the information gained would be redundant.
V. This measurement was divided by the total thoracic width, taken at the same level, in order to obtain a fractional value to enable quantification of the location of the trachea between dogs of different sizes (i.e. fraction denotes how much thorax is located on either side of the trachea).
VI. Calculated fractions denoted the following:
    - >0.5 indicated a right-sided location
    - =0.5 indicated a midline position
    - <0.5 indicated a left-sided position
VII. Subjectively, the position of the trachea was also recorded as midline, slightly to the right of midline (its normal position), slightly to the left of the midline,

moderately to the right of the midline, moderately to the left of the midline, markedly to the right of the midline, and markedly to the left of the midline. Subjective measurements were done at a different time from the quantitative measurements, to avoid bias.

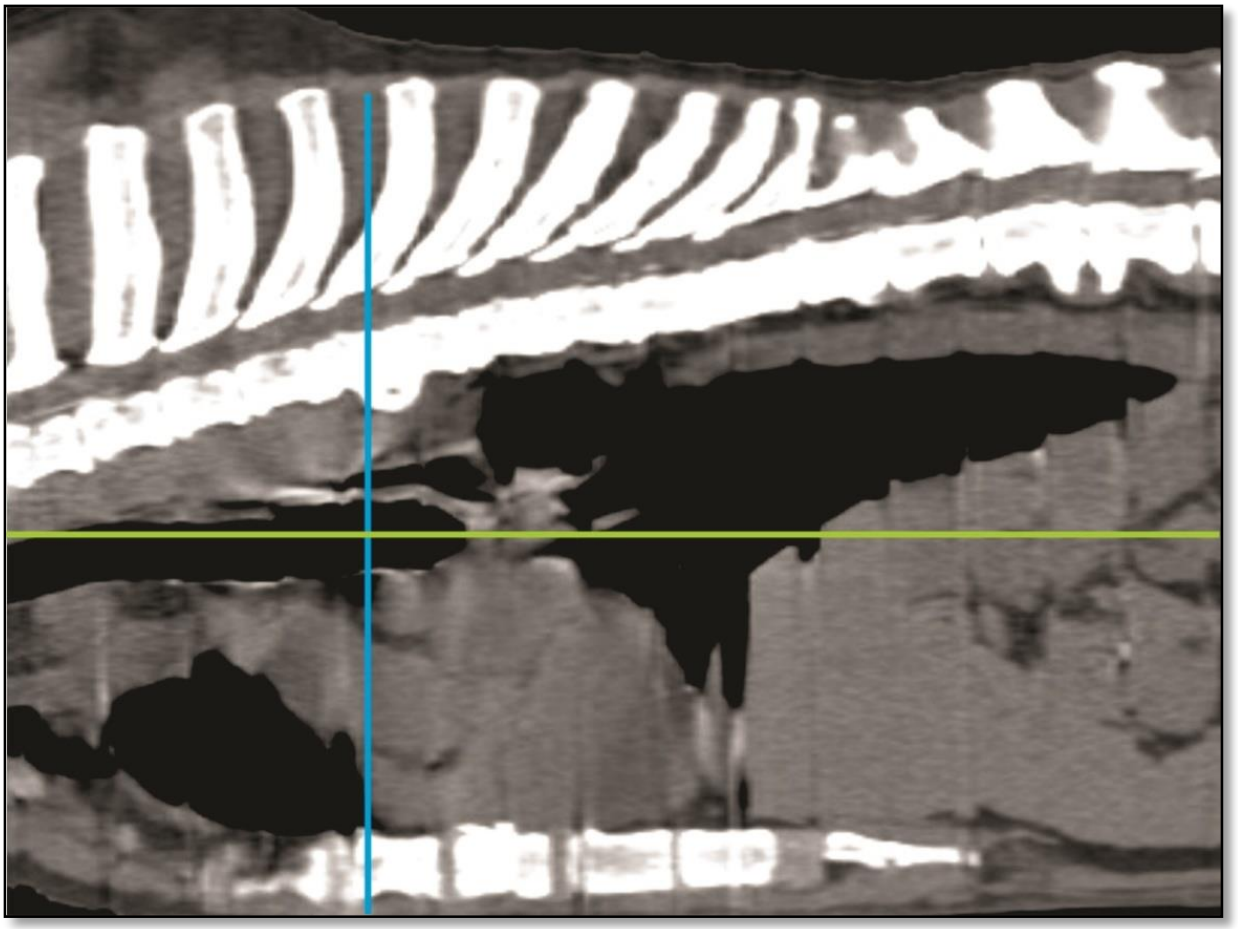

FIG. 3. For the trachea, the dorsal plane measurements were obtained parallel to the terminal trachea (green line), and the transverse plane measurements obtained perpendicular to the dorsal plane (blue line). For the aortic root, the transverse plane measurements (blue line) were perpendicular to the sternum and the dorsal plane measurements parallel to the sternum (similar to the green line in this image). Image is in a soft tissue window (WL 40, WW 400). Image was acquired in sternal recumbency. Note the stair-step artefact in this image, due to some patient motion and use of MPR.

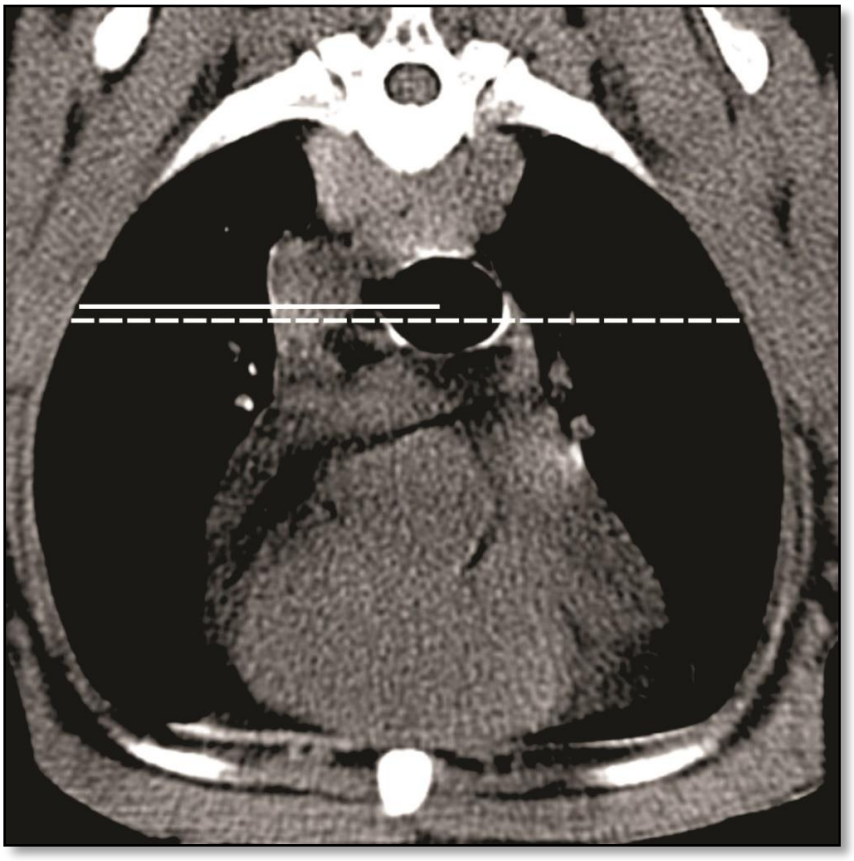

FIG. 4. Transverse plane indicating the measurement technique for tracheal position. The solid line indicates the measured distance from the centre of the trachea (found by measuring its widest section and dividing this by two), to the left parietal pleural margin. The dashed line, measured at the exact same level (demonstrated slightly below the solid line for clearer depiction), indicates the total thoracic width at this level, measured from the left to right parietal pleural margins. Note that the trachea normally is situated slightly to the right of the midline. Image is in a soft tissue window (WL 40, WW 400), and the left of the dog is to the left of the image. Image was acquired in sternal recumbency.

3.5.3 Aortic root

I. The aortic root was initially inspected in both TRA and DOR planes, but measurements only performed on the TRA planes as this was the more intuitive plane and there was difficulty encountered when defining the aortic root margins on the DOR plane.
II. The position of the heart using the aortic root (done on full thorax scans and slice level “c”) was determined to detect mediastinal shift as an indirect indicator of pulmonary atelectasis.

III. Measurements were performed in a similar manner to that of the trachea (ensuring symmetrical positioning of the thoracic images, Fig. 2 and Fig. 3). Measurements were done in a symmetrical image orientation in a transverse plane (Fig. 5). The intra-cardiac aortic root was measured at the level where it was visualised as a nearly round structure within the heart (followed from the descending aorta in a cranial direction to localise it).

IV. Subjectively, the position of the aortic root was recorded as midline, slightly to the right of midline, slightly to the left of the midline, moderately to the right of midline, moderately to the left of the midline, markedly to the right of the midline, and markedly to the left of the midline. Subjective measurements were done at a different time from the quantitative measurements, to avoid bias.

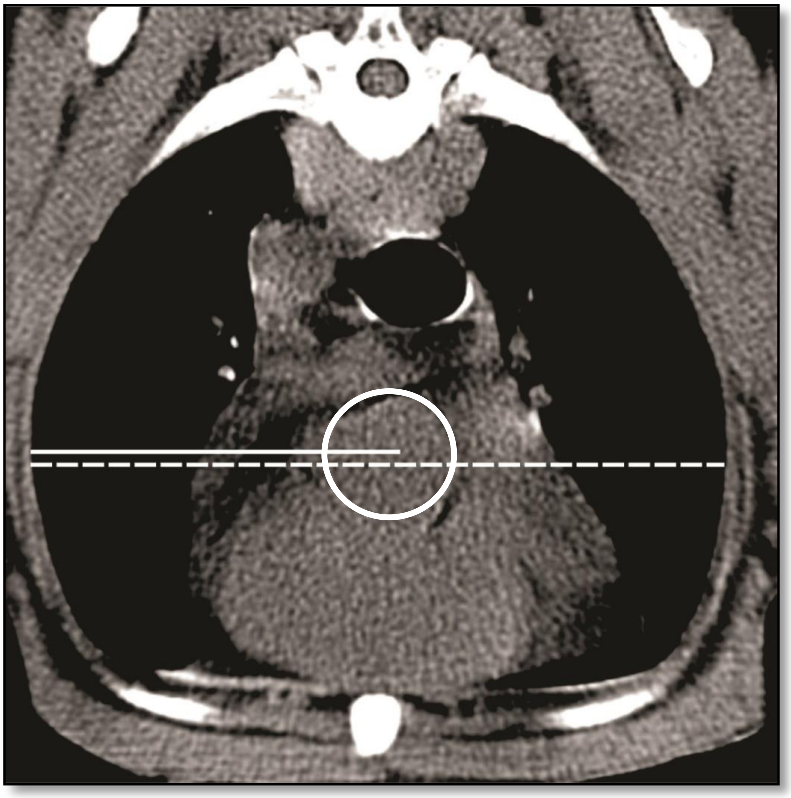

FIG. 5. Transverse plane indicating the measurement technique for aortic root position. The white circle indicates the intra-cardiac aortic root. The solid line indicates the measured distance from the centre of the aortic root to the left parietal pleural margin. The dotted line is measured at the exact same level (demonstrated slightly below the solid line for clearer depiction), and indicates the total thoracic width at this level, measured from the left to right parietal pleural margins. Image is in a soft tissue window (WL 40, WW 400), and the left of the dog is to the left of the image. Image acquired in sternal recumbency.

3.5.4 Diaphragm

I. Symmetry of the diaphragmatic crura/crus (determined only from the two full helical thoracic scans, S_i and S_e, per study) was assessed for evidence of mediastinal shift and to compare degree of inspiration amongst dogs.

II. The level of maximum diaphragmatic excursion was determined from a sagittal plane image (Fig. 6). At this level, in a dorsal plane parallel to the sternum, measurements/analysis were done to determine cupula symmetry and position. Also in the dorsal plane, measurements were obtained at the mid-thorax (trachea level) to assess the crura.

III. Position of the diaphragmatic cupula and crura, in a dorsal plane at the level of maximal cranial excursion and at the mid-thorax respectively, was described subjectively (Figs. 7 and 8) as symmetrical (at equal levels), mild asymmetry (indicating which side left or right was cranially displaced), moderate asymmetry (indicating which side left or right was cranially displaced), or marked asymmetry (indicating which side left or right was cranially displaced). Subjective measurement was done at a different time from the quantitative measurements, to avoid bias.

IV. Positions of the diaphragmatic crura/cupula at the level of maximum excursion and at the level of the mid thorax, were described quantitatively by comparing which side was located more cranially, using the ribs as a reference (Fig. 8). A line was drawn from the level of excursion (using CT measuring tool software) and extended to the left side of the thorax (for measurements of both left and right sides, in order to be able to compare to the same reference points) and the ribs on this side of the body were used as reference. One “rib width” was equal to the distance from the cranial cortex of the more cranial rib to the cranial cortex of the subsequent rib.

V. Degree of inspiration was compared between and within animals by measuring the angle between the sternum and the caudal extent of the lung field on the midline of the dog (lumbophrenic angle), taken from the level of the maximal diaphragmatic excursion (Fig. 9). Originally this method was developed arbitrarily for this study, but retrospectively adapted to a radiological method of measurement of the diaphragmatic angle as used by Grandage.[47]

i) If extrapolated from his study, and the sternum and vertebral bodies at the level of measurement are relatively parallel, using the geometry of corresponding and congruent angles (www.mathplanet.com), the expected measured angles in our study should range from 110 to 170° (180° minus 40 to 70°). This range of angles from his study appeared subjectively quite wide, and a similar wide range of angles was expected in the current study.
ii) Angles were expected to be similar with similar states of inspiration.

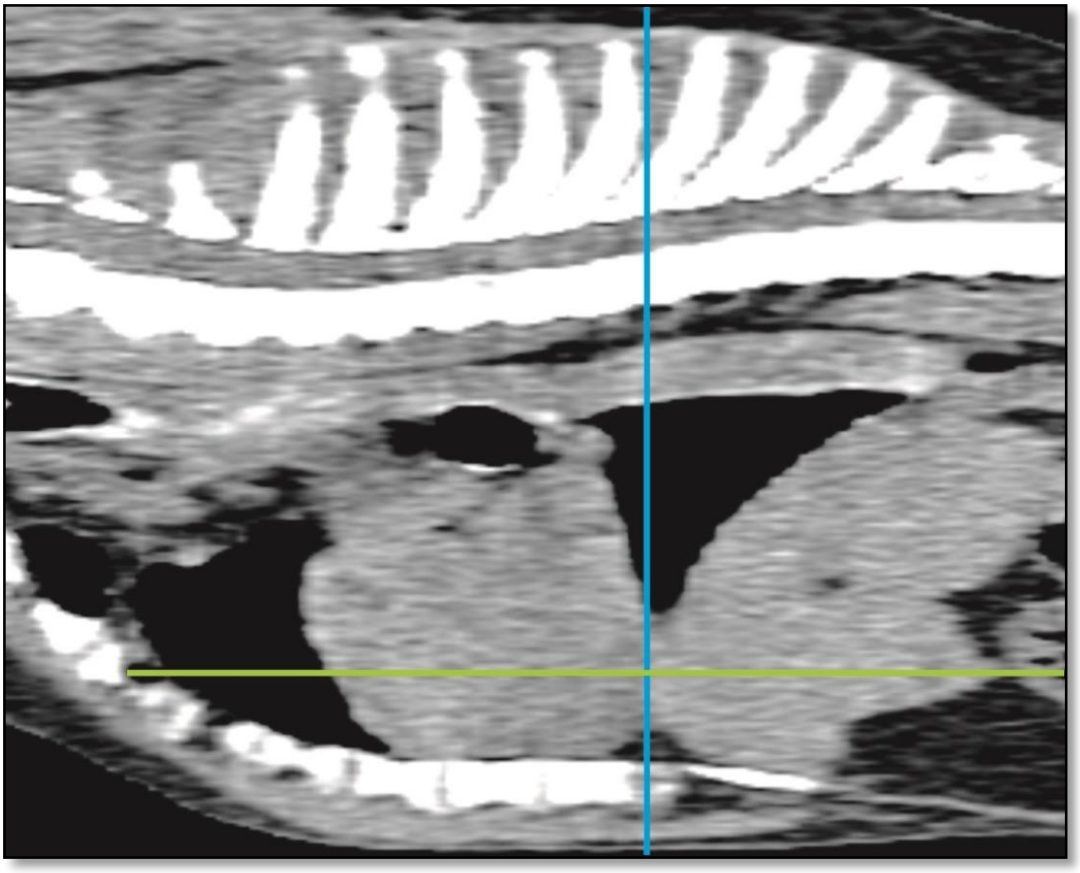

FIG. 6. Point of maximal cranial diaphragmatic excursion is indicated by the blue line (transverse plane, perpendicular to the sternum), and at this level measurements were performed in a dorsal plane (green line). For lung image evaluation, the transverse plane was also perpendicular to the sternum, as indicated by the blue line. Image is in a soft tissue window (WL 40, WW 400). Image acquired in sternal recumbency.

FIG. 7. Dorsal plane of the thorax, at the level of maximal cranial diaphragmatic excursion. The orange line indicates the point of maximal diaphragmatic excursion, which was assessed for symmetry subjectively and quantitatively by comparing left and right sides to the corresponding ribs. In this image the diaphragm was considered symmetrical. Image is in a soft tissue window (WL 40, WW 400), and the left of the dog is to the right of the image. Image acquired in sternal recumbency.

FIG. 8. In the mid-thorax, at the level of the trachea in a dorsal plane, left and right crura were compared subjectively and by using adjacent ribs for comparison. In this case, the left crus was located cranially (which is normal) by approximately ¾ of an intercostal space. The orange lines indicate cranial margins of crura, and are both extended to the right of the thorax. The yellow arrows indicate the distance, measured in intercostal spaces, between the two crura. Image is in a soft tissue window (WL 40, WW 400), and the left of the dog is to the right of the image. Image acquired in sternal recumbency.

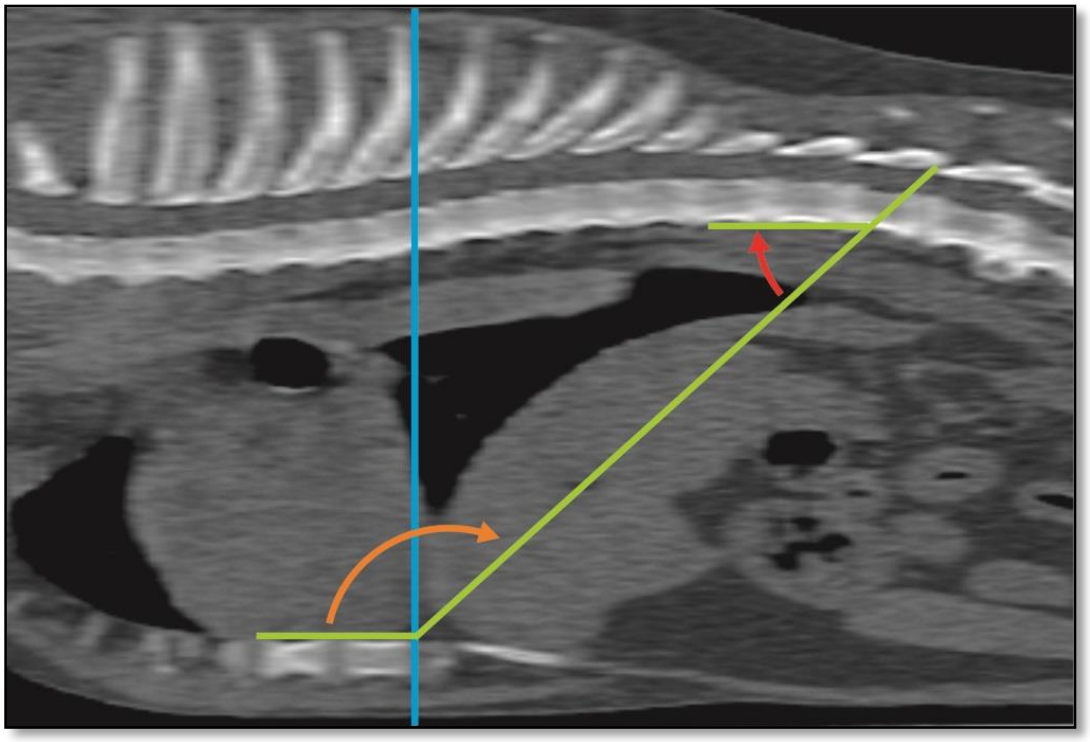

FIG. 9: To determine the degree of inspiration amongst dogs and within dogs on subsequent scans, the angle (orange arrow) between the sternum and the caudodorsal most extent of the diaphragm (lumbophrenic angle), measured from the level of maximal diaphragmatic excursion (indicated by the blue line) was measured. The green lines indicate the extension from the diaphragm at the sternum, caudally to the lumbophrenic angle, as well as from the caudodorsal extent of the diaphragm to a line drawn parallel to the thoracic vertebral bodies at this point. Subsequently the angle indicated by the red arrow was mathematically calculated in order to be able to compare the measured values to existing literature.[47] Image is in a bone window for purposes of illustrating the measurement technique (WL 450, WW 1500); however measurements were done in a soft tissue window. Image acquired in sternal recumbency.

3.5.5 Lungs

I. Lungs were assessed in a lung window (WL -600, WW 1200) transverse plane orientated perpendicular to the sternum (Fig. 6) with images symmetrically orientated (Fig. 2).
   i) The HU scale employed was that used by Staffieri,[32] employed successfully in dogs from human studies. True atelectic lung was defined as lung with a HU of -100 to +100, normally aerated from -900 to –501 HU, and poorly aerated from –500 to –101 HU.

II. Each lung lobe was measured from its dorsal-most to ventral-most aspect (from the para-spinal dorsal limit to its ventral-most tip) and this measurement divided into three equal vertically orientated compartments, in order to represent dorsal, middle and ventral lung fields (Fig. 10).

III. For each total lung lobe, and each of the three compartments, the mean HU, HU standard deviation, and CSA (cm^2) was determined (using Siemens' inherent CT software) using a free-hand region of interest (ROI) drawn by computer mouse by the author around each section. This was performed for every lung lobe on each slice "a" to "e" at each time interval. It was postulated that atelectasis will lead to a decrease in lung volume over time and an increased HU over time, with the reverse occurring with resolution of atelectasis.

IV. Large central blood vessels and bronchi were excluded in each lobe if they could consistently be identified and avoided (e.g. those located on the midline at the mediastinum, particularly at slice "c"), but the smaller more peripheral or larger central vessels (e.g. CVC) were not excluded, as they were not expected to affect findings due to the serial scans being performed (i.e. their presence stays constant between scans in each dog).

V. Hounsfield units between -713 and -846 were considered to be within normal range of expiratory to inspiratory values,[35] and these values were applied to the images to mean that the lungs fell within "normal respiratory range". Due to the breath-hold technique, it was believed there may be some increased inflation of the lung over and above the upper limits of normal "inspiratory" lung, and thus values below -846 were also still considered normal (up to -900, as utilised by Staffieri).[32]

VI. HU ranges that were within 50 to 80 HU of each other (for example, when comparing values between time points) were considered close enough to each other not to be considered as a significant change. These values were arbitrarily decided upon for this study, and were applied whilst evaluating the data. The same was attempted for CSA measurements, but due to the more noticeable variation in CSA it proved to be more difficult to apply a consistent value.

VII. In those lungs with visualized attenuation changes, it was further determined at what time interval the changes could be seen for the first time, which lobes were affected most frequently, as well as at which time interval resolution

commenced or was complete. By assessing the recorded HU and cross-sectional areas for these lobes, it was determined by which time interval the highest HU and smallest cross-sectional area measurements occurred (measured from the baseline value at S_i to the applicable measured value), and which third of the lobe contributed most to changes. These measurements were done for descriptive reasons only.

VIII. In areas that were visually affected by attenuation changes, a small circular ROI of 0.1 to 0.3 cm^2 was placed in the most severely affected region being careful to exclude any peripheral blood vessels.

FIG. 10. Transverse image at slice “b”, demonstrating the technique used to divide the lobes (left cranial *pars cranialis* on this image) into three vertical thirds (dashed white lines around each third), and then drawing a free-hand ROI around the entire lobe (solid white line) in order to obtain mean HU and CSA measurements. Image is in a lung window (WL -600, WW 1200). Left of the dog is to the left of the image. Image acquired in sternal recumbency.

3.6 Data and statistical analysis

Data were assessed for normality by evaluating descriptive statistics, plotting histograms and performing the Anderson-Darling normality test with statistical software (*MINITAB Statistical Software, Release 13.32, Minitab Inc, State College, Pennsylvania, USA*). Data that were not normally distributed were transformed using either the natural logarithm (HU; after adding 920 to all values so that the minimum value was 1) or the square root (CSA) prior to statistical analysis. Mixed-effects linear regression that incorporated a random effect term for the dog was used to determine changes in HU and cross-sectional area over time. Models were fit including fixed effect terms for the phase of the study (phase 1 in lateral recumbency versus phase 2 in sternal recumbency), starting recumbency side, time, and lung location (dorsal, middle, ventral). Independent models were also fit for each slice/lung lobe combination. Post hoc comparisons were adjusted using the Bonferroni correction of *P* values. Comparisons were independently performed for the total time period in lateral recumbency (phase 1 - “development” of atelectasis, S_i to RLR/LLR_{30}) and time in sternal recumbency (phase 2 - “resolution” of atelectasis, S_e to S_{20}). Statistical modelling was performed in commercially available software *(IBM SPSS Statistics Version 21, International Business Machines Corp., Armonk, New York, USA*) and results interpreted at the 5% level of significance.

Statistical analysis was not performed on the small number of visualized attenuation changes.

Chapter 4: Results

4.1 Study population

Six sterilized female Beagles (dog details summarized in Appendix A), were used in the study.

All dogs were eligible to be included in the study based on the findings of each of the clinical examinations, blood smears, full blood counts, biochemistries, urinalyses, abdominal ultrasound and initial thoracic CTs. Dog 6 was found to have a mildly enlarged left adrenal gland (10 mm latero-lateral width and 7 mm dorsoventral height)[56] on ultrasound, however did not demonstrate clinical signs or biochemistry changes indicative of adrenal disease, and thus was not excluded from the study.

Dogs were starved for 12 hours for 9 out of the 12 studies. Unfortunately, due to the dogs being housed in a colony and staff rotation on weekends when the studies were performed, 3 of the dogs (dogs 1, 2 and 6) were not adequately starved (only 6 hours for Dogs 1 and 2, and 3 hours for Dog 6) for the second phase of the study (not known by the examiner until the first thoracic scan had already been performed). It was decided not to abort the study but to be attentive to the potential effects of a partially ingesta-filled stomach on the diaphragm (and indirectly the lungs) and to monitor the dogs carefully clinically to avoid side effects of inadequate starvation.

4.2 Data acquisition

4.2.1 General anaesthesia

Each dog responded well to and recovered uneventfully from the anaesthetic protocol and all monitored values were deemed to be within normal limits. The breath-hold technique employed worked well, but all dogs showed some breathing against the hold towards the end of each scan as was expected (Figs. 11 and 12).

Total general anaesthetic time ranged from 57 to 62 minutes (from time to induction to cessation of isofluorane administration).

FIG. 11. The study setup of the mobile lead shield with the anaesthetic machine partially behind it is demonstrated, in relation to the dog and gantry. The anaesthetist would be positioned fully behind the shield to have access to the re-breathing bag in order to perform breath-hold. The re-breathing bag portion of the anaesthetic machine is positioned behind the lead shield.

FIG. 12. The anaesthetist was positioned behind the lead shield, demonstrating the setup in order to perform the breath-hold technique safely. No body part of the anaesthetist protruded beyond the lead shield.

4.2.2 Computed tomography procedure

The time taken to perform the scans after placing the dogs in the various recumbencies throughout the studies was recorded, to determine whether the time intervals were comparable between and within dogs (summarized in Appendix B).

Variations in time were usually due to the time required to position the dog, connect the dog to the anaesthetic machine and stabilize the anaesthetic plane, adjust the CT table height, or due to unavoidable machine delays. The preloaded protocols for the study worked excellently (Fig. 13).

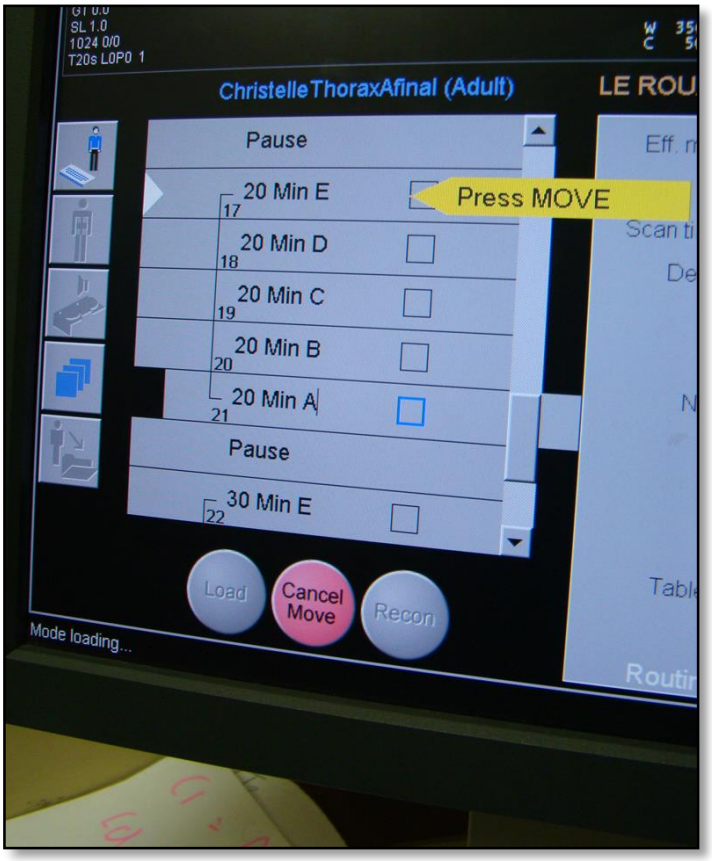

FIG. 13. An example of the tailored CT protocol, indicating the scan procedure for the five blocks scanned starting from caudal (slice e) to cranial (slice a) for the 20 minutes time interval (RLR or LLR_{20}) in lateral recumbency. A pause was inserted before and after each time interval, and the scans were started manually for each interval after which slices “e” to “a” were automatically performed.

The predetermined scan times could generally be followed accurately, with the following consistent exceptions:

- The initial lateral recumbent scan at the start of the study at 3 minutes (RLR_3 or LLR_3) varied between dogs from 3:04 to 4:14 minutes. Only 3 out of the 12 studies were delayed to over 4 minutes (Dog 1 phase 1, Dog 2 phase 2, and Dog 6 phase 1).
- The scan at 5 minutes after repositioning the dog in sternal recumbency (S_5) was delayed in 2 studies (2/12) by 30 seconds and 45 seconds respectively (Dog 1 phase 1 and Dog 3 phase 2).

Overall it was felt that the consistency of the timed scans was good, and thus the study deemed adequate to compare CT images between and within dogs.
All CT studies were diagnostic. Mild motion artifact was seen on a single image/scan time on the first study for dog 1 and the second study in dog 3, and the MPR reconstructions showed mild stair-step artifacts, but this did not interfere with the diagnostic quality of the images.
The approximate landmarks were adapted somewhat as the research progressed; due to unavoidable small variations in the placement of the scan boxes studies and possible variation in degree of inspiration due to the breath-hold.

4.3 Data sets analysed

4.3.1 Image symmetry and interpretation

Images were easily aligned in a symmetrical fashion, as described.
Images were interpreted for all variables (i.e. tracheal and aortic position and movement, and lung CSA and Hounsfield units) with special attention given to changes occurring at the following time intervals:

- Initial sternal scan (S_i) - baseline
- Time between the baseline scan and placement into lateral recumbency (S_i to LLR_3 or RLR_3)
- Time spent in lateral recumbency (LLR_3/RLR_3 to LLR_{30}/RLR_{30})
- Time between the last lateral recumbent scan and repositioning into sternal recumbency (LLR_{30}/RLR_{30} to S_e)
- Time spent in sternal recumbency from S_e to S_{20}
- Comparison between values at S_i and S_e
- Comparison between value at S_e and S_{20}
- Comparison between values at S_i and S_{20}

These time intervals were chosen in order to divide the large amount of data into smaller more manageable comparisons for the descriptive analyses. For statistical analyses, the comparisons were limited to the total time period in lateral recumbency (phase 1, or “development” of atelectasis, S_i to RLR/LLR_{30}) versus that in sternal recumbency (phase 2, or “resolution” of atelectasis, S_e to S_{20}).

A large degree of overlap between the subjective assessment (i.e. position of the trachea or aorta as midline, or to either side of the midline) and the actual measured values was found in many cases. Values <0.47 or >0.53 tended to be identified correctly subjectively as towards the left of towards the right of the midline, respectively. Because none of the subjectively values that were incorrectly identified relative to the measured values were extremes, these findings were considered insignificant. Differences between measured values over time that were less than by 0.05 (5%) were thought unlikely to be significant and thus were called insignificant in the results. This value was arbitrarily decided upon for this study.

Findings that were only present in certain dogs, e.g. oesophageal gas distension, gastric food content, were also assessed for each variable in order to ensure that there was no possible external influence on the measurements done.

Some general subjective thoracic changes that were noted within the study (correlated to the findings of the clinical dogs undergoing CT, as previously) are noted here, and were applied to each variable as necessary:

- When in sternal recumbency, the thorax had a wider rounder conformation (compared to lateral recumbency), and the ventral sternal boundary was flattened by the table. The thorax demonstrated a more oval shape in the more cranial thorax (dorsoventral height larger than width), becoming rounder more caudally and at the most caudal extend (in the region of T9 caudally), the thoracic width was often wider than the dorsoventral height (refer to Fig. 23).
- When in lateral recumbency, the thorax assumed a slightly asymmetrical oval dorsoventrally elongated conformation, due to an increase in dorsoventral height with a corresponding decrease in lateral width. Moving in a caudal direction, the thorax tended to have a rounder appearance again, but not to the same degree as in sternal recumbency. The decreased thoracic width appeared mostly generalised, except at the cranial extend of the thorax (up to thoracic vertebra (T3) where the dependent thoracic limb sometimes created a focal inwards wall deviation (very mild), and caudally at the diaphragm where the caudal most asternal and floating ribs showed some inwards deviation.
- In sternal recumbency, the cardiac silhouette was located on the ventral midline (5:30 to 6:30 location, using a clock face analogy).
- When placed in lateral recumbency, the cardiac silhouette shifted towards the dependent side. It was located towards the left (from 6 to 8 o'clock, if left was the left of the image on TRA) in LLR, and towards the right (4 to 6 o'clock) in RLR.
- In LLR, the cardiac apex/ventral mediastinum made contact with the left ventro-lateral thoracic wall (7 o'clock, using the same clock face analogy, Fig. 14).
- In RLR, the cardiac apex was only mildly displaced towards the right and appeared in a more midline position (6 o'clock). The cardiac silhouette did not make contact with the right ventro-lateral thoracic wall, and often had lung between it and the thoracic wall (Fig. 14).
- The normal position of the cardiac apex in sternal recumbency appeared to be very mildly left of the thoracic midline, at the 6:30 position using a clock-face analogy.

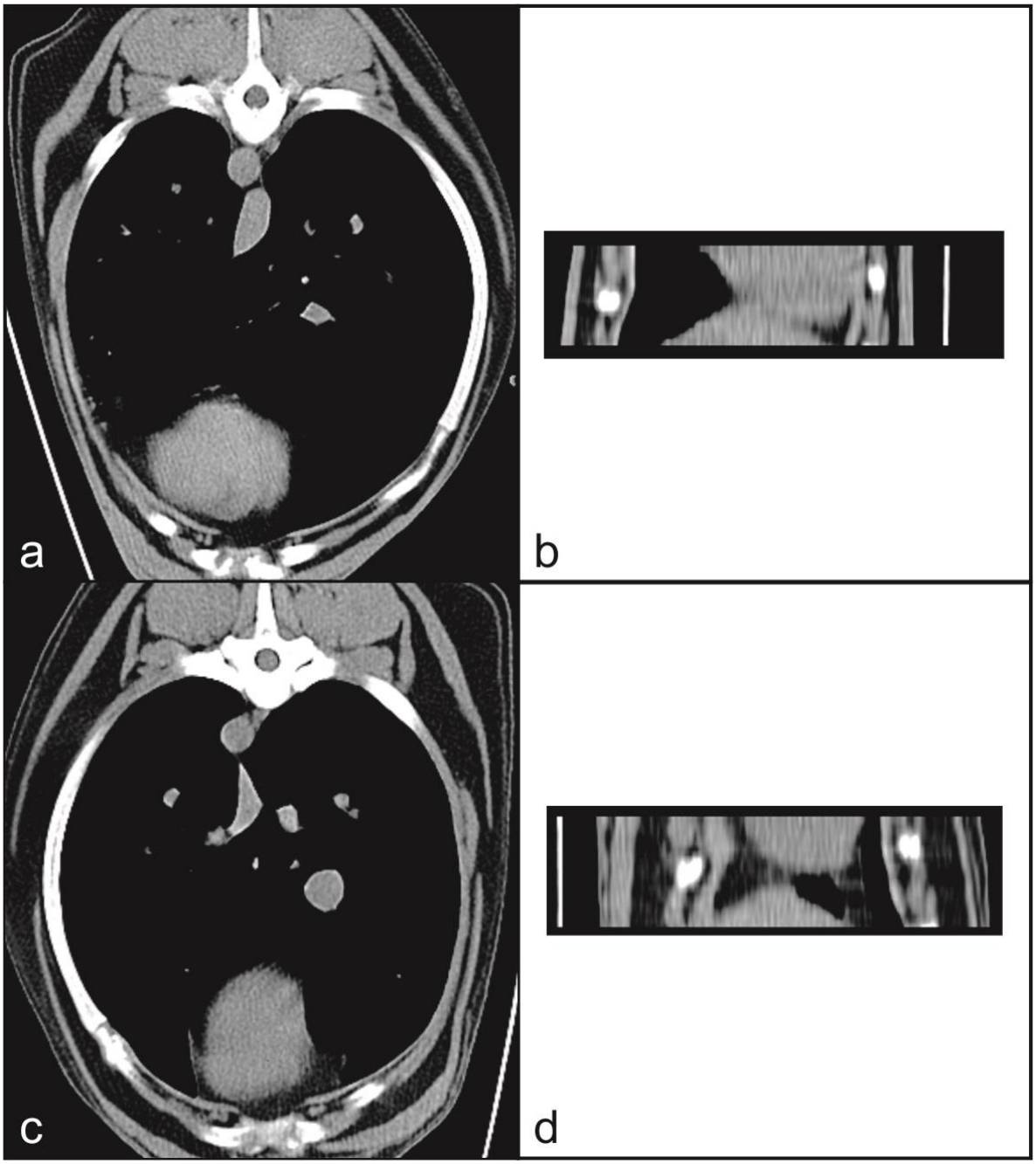

FIG. 14. Transverse (a) and dorsal (b) images of Dog 1 in LLR, demonstrating the more left-sided cardiac apex, see at the 7 o'clock position on the TRA images, and seen nearly against the left body wall on the DOR image. Transverse (c) and dorsal (d) images of Dog 6 in RLR, demonstrating a more midline location of the cardiac apex. The cardiac silhouette also does not contact the right body wall. All images were in a soft tissue window (WL 40, WW 400). Left of the dog is to the left of the transverse images, and left of the dog is to the right of the dorsal images.

- Comparing the cardiac apex position at the same slices revealed a greater shift towards the left when in LLR than to the right in RLR. The heart appeared more mobile when in LLR.
- The pericardiophrenic ligament is believed to have been accurately visualised as a thin soft tissue attenuating band (separable from the fat attenuation of the mediastinum), extending from the caudoventral cardiac silhouette to the mid-ventral diaphragmatic cupula (Fig. 15). No obvious effect of the ligament was noted on brief evaluation.

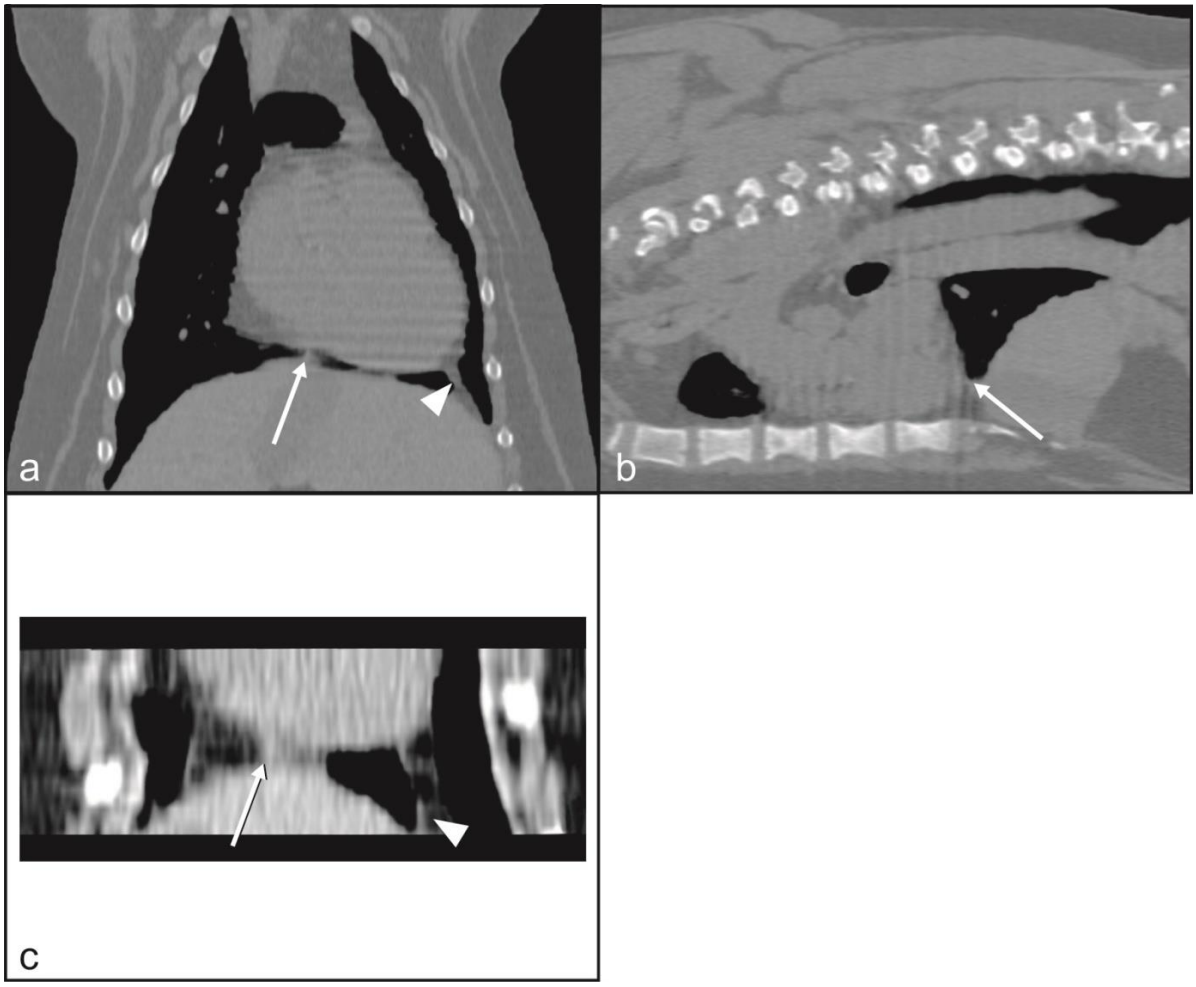

FIG. 15. Images in dorsal (a and c) and sagittal (b) planes, depicting a fine soft tissue attenuating band (arrow), clearly seen as a separate structure from the surrounding mediastinal fat, and which is presumed to be the pericardiophrenic ligament. The caudoventral mediastinal reflection, which has been confused with the pericardiophrenic ligament, is indicated by the arrow head. Figures a) and b) are of an unrelated canine hospital patient, whereas c) is of Dog 6. All images were obtained in sternal recumbency and windowed in order to demonstrate the ligament most optimally (a and b WL=450 and WW=1500, c WL=40 and WW=400). The left of the dog is to the right on the dorsal plane images.

- Despite the cardiac shift, the dorsal mediastinum (descending aorta) remained fixed relative to the ventral vertebral bodies and of similar width despite body position changes.
- The dorsal mediastinum, in the region of the cardiac base, up to the trachea, decreased to a variable degree in width when the dog was placed in lateral recumbency, versus sternal recumbency, ranging from nearly undetectable decreases of 2.5% up to 11%. In one of the additional retrospective CT assessments, this value ranged from 15-18%. This value was obtained by comparing the width of the mediastinum at the same anatomical point (usually mid-trachea) in sternal and in lateral recumbency, which resulted in a smaller width when in lateral recumbency.
- When in lateral recumbency, due to the patient head being unsupported, the trachea entered the thoracic inlet with a gentle curve away from the recumbency the dog was in (e.g. LLR the trachea curved mildly towards the right to enter the thorax). This was more pronounced for LLR, and in RLR the trachea was often only subtly curved.
- The dependent diaphragmatic crus, in addition to cranial displacement, demonstrated a marked dorsal displacement (Fig. 16). This was very pronounced when the dogs were in LLR, with the left dependent crus often being up to 50-65% higher than the right one. This was determined by measuring the distance from the highest point of the dorsal costal arch to the diaphragmatic border ventral to it, and comparing left and right crura. When in RLR, the right crus was often only mildly more dorsal than the left one, by up to 14%. In Dog 6, which was inadequately starved for the RLR study, both crura were nearly symmetrical.

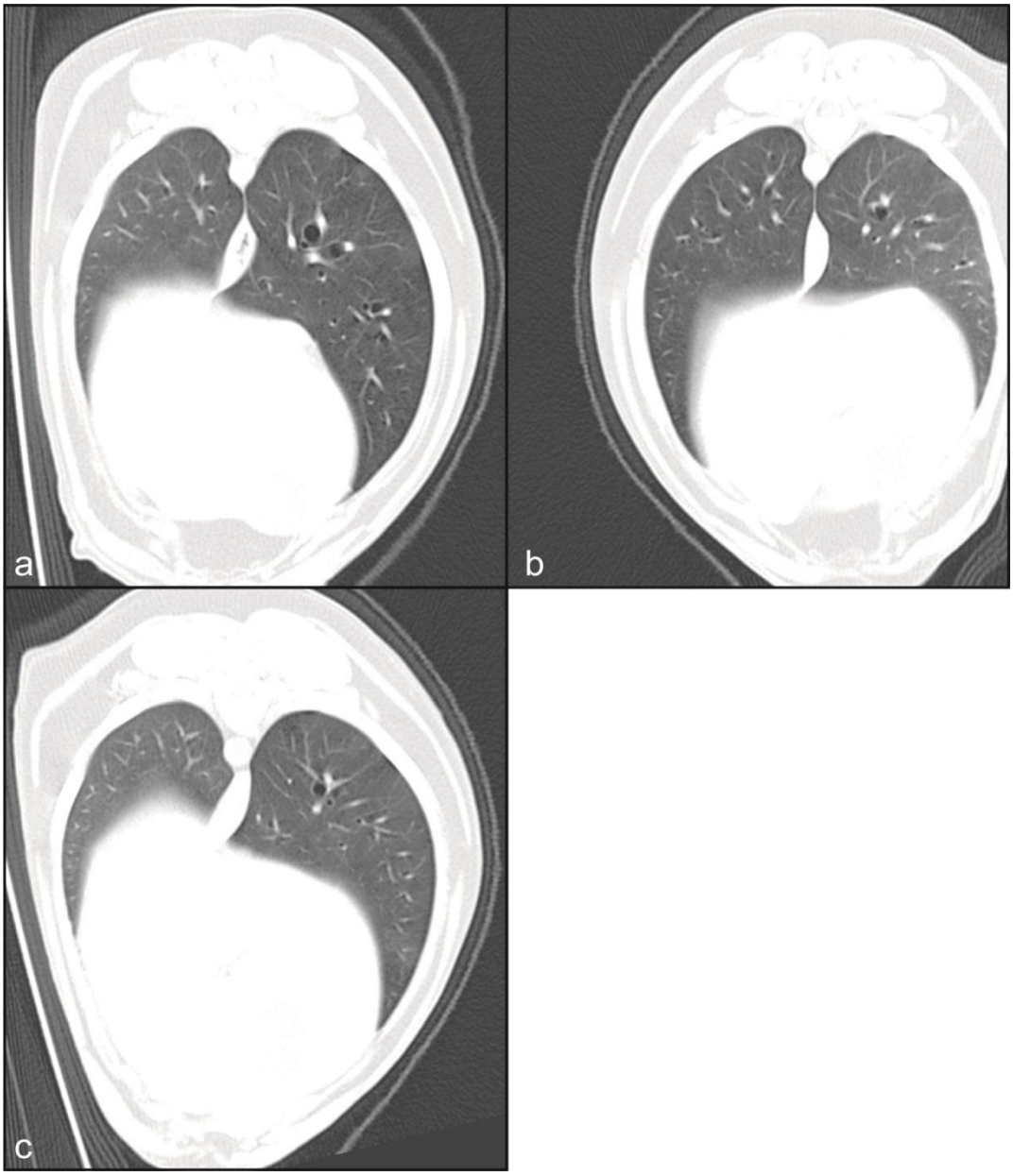

FIG. 16. Dog 6 in LLR (a) and in RLR (b) – note that when in LLR, the left crus was relatively more dorsally displaced, compared to when RLR, where the right crus was relatively less dorsally displaced. Dog 1 in LLR (c), demonstrating even more dorsal displacement of the left crus in LLR. All images are in a lung window (WL -600, WW 1200), and left of the dog is to the left of the image.

- Certain observations were made when dogs were placed in RLR, which were not noted when in LLR:
    - When placed in RLR, the total thoracic width decreased mildly as expected (by approximately 5%).

  - The distance from the left lateral body wall to the centre of the trachea (as done in all measurements) also decreased, but to a greater degree than the total thoracic width (approximately up to 15-20% decrease).
  - Thus the ratio of the distance from the left thoracic wall to the total thoracic width would decrease, giving a fractional value that would indicate a leftwards shift (in RLR).
- The findings above could not be consistently found for measurements done in LLR. The distance from the left lateral body wall to the centre of the trachea was more inconsistent and was increased, decreased or unchanged to variable degrees compared to the change in thoracic width.

4.3.2 Trachea

The trachea was assessed on slices “a”, “b” and “c”. Measurements were performed in a soft tissue window (WL 40, WW 400).

It was straightforward to measure the tracheal location on transverse planes. There were 360 tracheal measurements for the entire study of 6 dogs (2 studies each, and 3 slices where the trachea was measured on transverse planes, at ten time intervals). The effect of oesophageal gas distension on tracheal position was assessed subjectively for the dogs in which it occurred, but no effect was noted.

There was no significant statistical difference in tracheal position between the three slices (“a”, “b” and “c”), for RLR (P=0.714) and LLR (P=0.456), nor for sternal recumbency after RLR or LLR (P=0.888 and P=0.933, respectively). Therefore, for each RLR and LLR, all three slices were combined into a single analysis for statistical assessment.

Tracheal measurements were plotted on a graph using the median fractional location on the y-axis and time interval on the x-axis. Six dogs were plotted on one graph per study (LLR or RLR), and this was done for each of the 3 slices (“a”, “b” and “c”). This resulted in 6 separate graphs. Due to the lack of statistical significance between the three slices, the median values at each time point was combined for all 6 dogs for all 3 slices, and demonstrated on a single graph (Fig. 17).

Statistically there was a significant effect of time on measured tracheal shift during RLR (P<0.001), but the effect of time was not significant during sternal recumbency (P=0.535).

Statistically there was a significant effect of time on measured tracheal shift during LLR (*P*=0.019), but the effect of time was not significant during sternal recumbency (*P*=0.232).

These findings indicated that whilst there was significant tracheal shift away from the baseline position during lateral recumbency, there was no significant tracheal shift during sternal recumbency.

The statistical findings correlated with the descriptive findings.

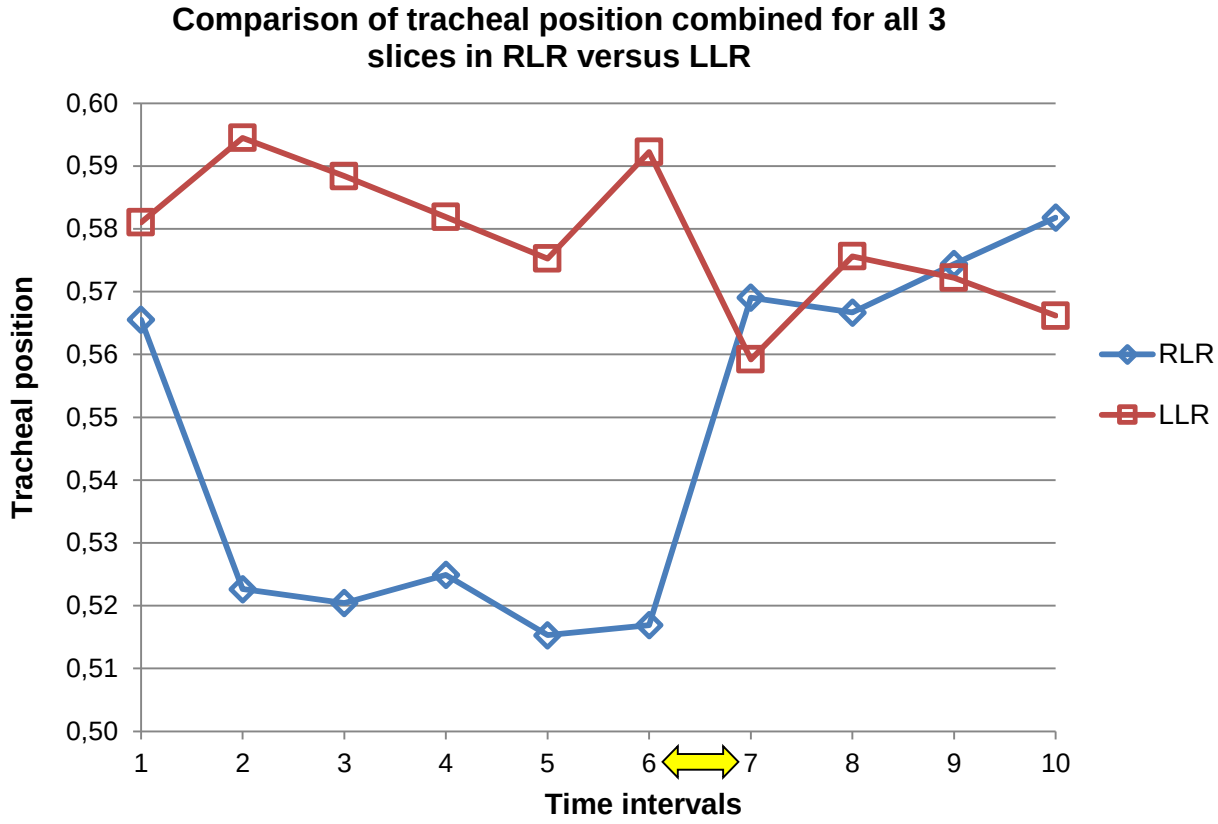

FIG. 17. Line graph of the median fractional positional values (y-axis) of the trachea of the 6 dogs combined for slices “a”, “b” and “c” when in RLR versus LLR. When placed in and during RLR, the trachea demonstrated a prominent leftwards shift towards the midline, with a subsequent right-wards shift towards its baseline values after repositioning in sternal recumbency. When placed in LLR, the trachea demonstrated a mild rightwards shift with a gradual return towards the left over time. With repositioning in sternal recumbency however, it maintained a more left-sided position compared to its baseline position. Tracheal position is explained as follows: values <0.5 indicate a left-sided position, values of 0.5 indicate a midline position and values of >0.5 indicate a right-sided position within the thorax. Time intervals are depicted on the x-axis, as follows: 1, S_i; 2, RLR/LLR_3; 3, RLR/LLR_8; 4, RLR/LLR_{13}; 5, RLR/LLR_{20}; 6, RLR/LLR_{30}; 7, S_e; 8, S_5; 9, S_{10}; 10, S_{20}. The letter “S” indicates sternal recumbency and “RLR” and “LLR” indicate right and left lateral recumbencies, respectively. The subscript “i” indicates the first initial baseline scan and “e” indicates the sternal scan done upon

immediate repositioning in sternal recumbency. The numerical subscripts indicate time elapsed since placement in lateral or sternal recumbency. Time intervals 1 to 6 (S_i to RLR/LLR_{30}) indicate the time to develop atelectasis in lateral recumbency, while intervals 7 to 10 (S_e to S_{10}) indicate the time to resolve any attenuation or atelectic changes. The double yellow arrow between time intervals 6 and 7 indicates the change in body position from lateral to sternal recumbency.

The graphs of the trachea in RLR demonstrated the most consistency and the clearest recognisable pattern for all 3 slices, compared to the graphs of LLR.

The trachea was always located to the right of the midline on baseline scans, and always remained in a consistent position (mildly right ventrolaterally) if compared to the ventral aspect of the vertebral bodies and the *M. longus colli*. Only dog 4's trachea, on slice c, was measured as immediately to the left of the midline (0.49).

Despite the graphs indicating a shift of the trachea with body position and with time, this movement was not identified on subjective evaluation of the images. The largest shift between time intervals occurred with Dog 1 on slice "a", which showed a difference of 0.13 between S_i and RLR_3 but this was only noted on careful retrospective reassessment of the images, after plotting the graphs.

When the dogs were placed in RLR, there was an unexpected resultant shift of the trachea towards the left. When the dogs were placed in LLR, similar findings occurred as there was a shift of the trachea towards the right instead of towards the left – however, the shift was much milder than when in RLR.

With time spent in lateral recumbency, the trachea did tend to shift mildly towards the dependent side, as would be expected – however, only for dogs in LLR. The tracheas of dogs that were in RLR tended to remain more towards the midline rather than shifting dependently to the right.

With return to sternal recumbency in all studies the trachea moved back to its pre-lateral recumbent position to varying degrees – the trachea tended to be more right-sided compared to baseline values after being in RLR, and after LLR tended to more towards the midline than the original baseline values.

There was an overlap between the measured values and the subjective assessment of midline, slightly to the right and moderately to the right, so that the subjective values only agreed broadly with the measured values.

No correlation could be made with the lung changes recorded.

4.3.3 Aortic root

The aortic root was assessed on slice “c” only, and all measurements were done in a soft tissue window (WL 40, WW 400). It was straightforward to measure the aortic root position on transverse planes.

There were 120 aortic root measurements in total – one transverse measurement per recumbency, per time interval (ten per study) per dog. Aortic root measurements were plotted on a graph as for the tracheal measurements.

Statistically there was a significant effect of time on measured aortic shift when in RLR (*P*=0.009), but when repositioned in sternal recumbency was not significant (*P*=0.085). Statistically there was a significant effect of time on measured aortic shift when in LLR (*P*=0.008), but when repositioned in sternal recumbency was not significant (*P*=0.639). The explanation for the statistical findings was as for the trachea, and the findings were in accordance with the descriptive findings.

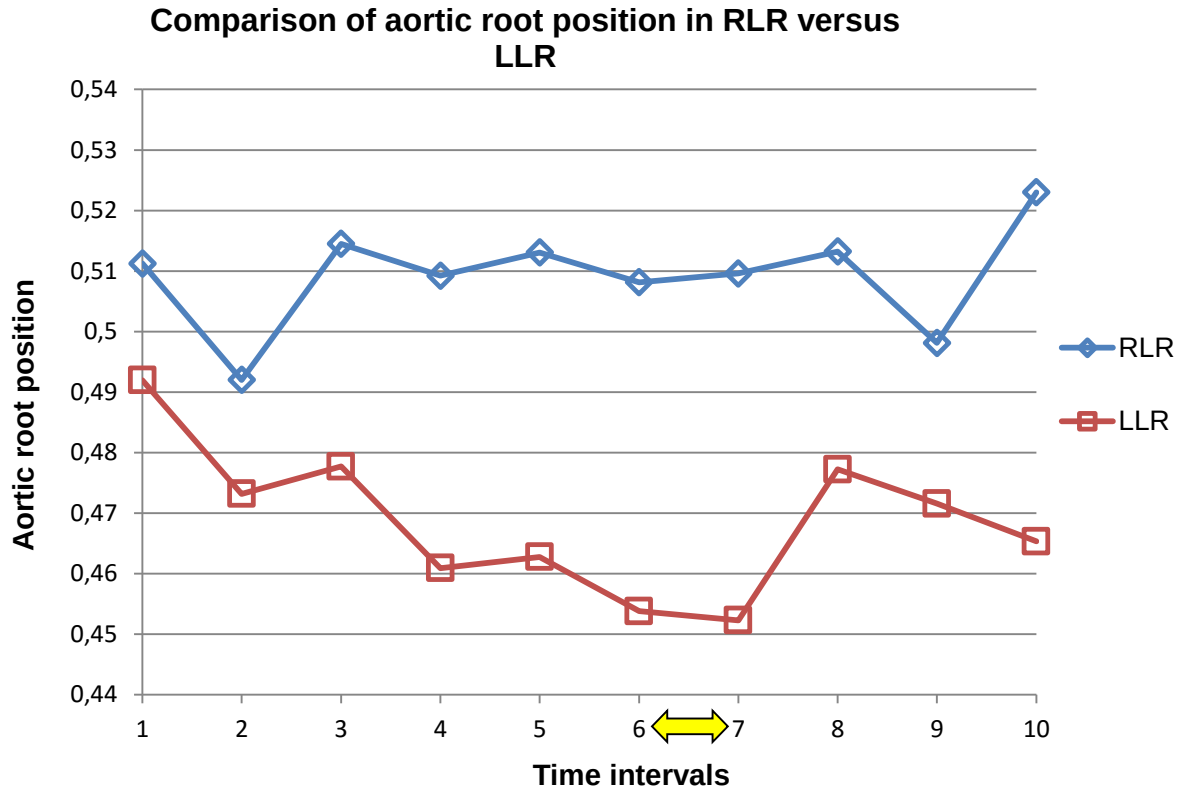

FIG. 18. Line graph of the median fractional positional values (y-axis) of the aortic root of the 6 dogs combined for slices “c”, when in RLR versus LLR. With placement in RLR, the aortic root shifted counter-intuitively towards the midline, however with time spent in RLR it did shift back mildly towards the right, at approximately its baseline position. During sternal recumbency, the aortic root showed no obvious

pattern. In LLR, the aortic root shifted towards the left and remained in that position. With repositioning in sternal recumbency, the aortic root shift towards the midline but did not return to its baseline position. The time intervals and aortic position are explained as for the trachea in Fig. 17.

The aortic root's baseline sternal position was frequently to the right of the midline (6/12 measurements, or 50%), almost equally to the left (5/12, or 41.6%) and rarely on the midline (1/12, or 8.3%).
With placement in RLR, the aortic root shifted counter-intuitively towards the midline, rather than towards the right (mirroring the tracheal movement). With time spent in RLR, the aortic root did shift back mildly towards the right, at approximately its baseline position. During sternal recumbency, the aortic root showed no obvious pattern.
In LLR, the aortic root shifted towards the left (which is opposite to the trachea) and stayed towards the left (which mirrored the tracheal movement during LLR). With repositioning in sternal recumbency, the aortic root did shift towards the midline but did not return to its baseline position.
No correlation with the measured lung values was established when aortic measurements were compared to HU and CSA. Subjective measurements were quite variable in their correlation with actual measured values.

4.3.4 Diaphragm

The diaphragm was assessed in a soft tissue window (WL 40, WW 400) for all dogs to most accurately define its borders. Assessment was only performed on full helical studies (i.e. S_i and S_e).
It was difficult to maintain the same image plane for measurement of the angle between sternum and caudal extent of the lung field in dogs (lumbophrenic angle), because lining the vertebral bodies up to the sternum was not always possible to the same degree between dogs, due to mild positional differences.
Assessing the cupula was challenging at times due to mild undulation of the curved cranial borders, which may affect where the measurements were taken from as well as subjective evaluation.
No statistical analyses were performed on the few diaphragmatic measurements.

RLR

The diaphragm angle (sternum to lumbophrenic angle) varied between 132 to 140° (see Fig. 9), and 5 out of the 6 dogs showed a decreased angle from the initial (S_i) to the middle sternal (Se) study (consistent with a decreased degree of inspiration).

LLR

Angles ranged between 130 and 141°, and only 2 dogs showed a decreased angle from the initial sternal to mid-sternal study. This was consistent with the predicted values of 110-140°.

There was no correlation of degree of inspiration (diaphragmatic angle) with the degree of gastric filling for the dogs that were not starved to the same degree as the rest of the studies.

The point where the crura intersected the ventral vertebral bodies ranged from caudal T12 to cranial L1.

The diaphragmatic cupula was symmetrical (11/24 measurements, or 45.8%, Fig.19) or the right part of the cupula was displaced slightly cranially (13/24, 52.2%, Fig. 20) by up to 0.5 intercostal spaces (ICS).

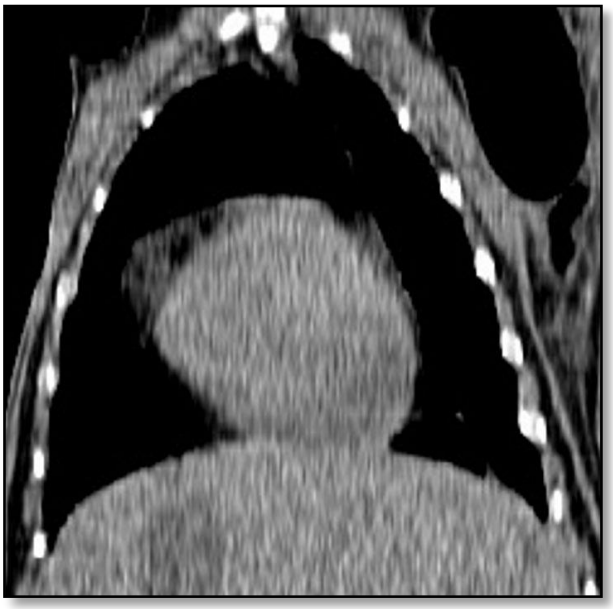

FIG. 19. Dorsal plane image of Dog 1 at S_i, at the level of the ventral third of the thorax and most cranial excursion of the diaphragm, demonstrating a symmetrical (on subjective evaluation as well as measured values) cupular margin. Image is in a soft tissue window (WL 40, WW 400) and left of the dog is to the right of the image.

Fig. 20: Dorsal plane image of Dog 1 at S_i, at the level of the ventral third of the thorax and most cranial excursion of the diaphragm, demonstrating a slightly asymmetrical (on subjective evaluation as well as measured values) cupular margin. The right half of the cupula is mildly more cranially located. Image is in a soft tissue window (WL 40, WW 400) and left of the dog is to the right of the image.

The left diaphragmatic crus was always located in a more cranial position compared to the right crus (24/24, or 100% - see Fig. 21) by between 0.25 to 1.5 ICS's (2 dogs by 0.25, 4 dogs by 0.5, 1 dog by 0.66, 5 dogs by 0.75, 8 dogs by 1, 2 dogs by 1.25, and 2 dogs by 1.5).

FIG. 21. Dorsal plane image of Dog 1 at S_i, at the level of the trachea, demonstrating crural asymmetry (on subjective evaluation as well as measured values). The left crus is mildly but obviously more cranially located. Image is in a soft tissue window (WL 40, WW 400) and left of the dog is to the right of the image.

There was no correlation between the cranial locations of the cupula, nor the crura, with gastric filling in the dogs that were starved for a shorter time period than the rest, when in sternal recumbency (full helical scans at S_i and S_e).

The position of the diaphragm during lateral recumbency was only cursorily assessed in this study. Only scan box “e” included a sufficient representation of the diaphragmatic cupula to evaluate adequately. In all the slices evaluated (in a dorsal plane), the diaphragmatic cupular dome’s left half protruded markedly cranially when in LLR, and the right half protruded cranially when in RLR.

The subjective measurement of cupula and crura excursion correlated well with the measured values. The measured values up to 1 ICS correlated with a subjective measurement of “mild asymmetry”, and from 1 ICS to 1.5 ICS correlated well with “moderate asymmetry”. There was minor overlap at 1 ICS between the two subjective measurements for the crura, where two dogs were identified as “moderate asymmetry” and 6 were identified as “mild asymmetry”. For the cupula measurements, there was no overlap.

4.3.5 Lungs

4.3.5.1 General overview

Measured median HU and CSA values were plotted separately on two graphs, with HU and CSA on the y-axis and the time intervals on the x-axis. These graphs were initially done for each lung lobe at each slice, and for the six dogs displayed individually, with separate graphs for RLR and LLR. However, these graphs could be condensed into a graph for each lobe at each slice, with the six dogs’ values combined and RLR and LLR displayed on one graph. The accessory lung lobe, despite being considered as part of the right lung,[57] was not included in this initial graph due to its midline location and its unique behaviour in recumbency (in that it behaved similarly irrespective of recumbency).

The location where measurements were performed within each study was determined to be most consistent at two intervals:

- Between the slices and time intervals in RLR or LLR from 3 to 30 minutes (dogs remained in lateral recumbency and were not moved).

- During the last set of sternal scans (S_e to S_{20}), as again the dogs were not moved between intervals.

The full helical scans (S_i and S_e) were easily matched anatomically to the scans at “a” to “e”. The largest discrepancy within studies occurred between the lateral and sternal slices, due to the fact that during this time the dog was repositioned, a topogram performed again, and slices “a” to “e” plotted anew. This lead to some variation in measured values.

Slices evaluated at point “a” were the most problematic to assess. This was due to the small size of the lungs in this region, less distinct differentiation of soft tissue/fat/lung margins in this region, and the partial intrusion of the left cranial *pars caudalis* lobe dorsolaterally to the *pars cranialis* lobe in some of the studies (Fig. 22).

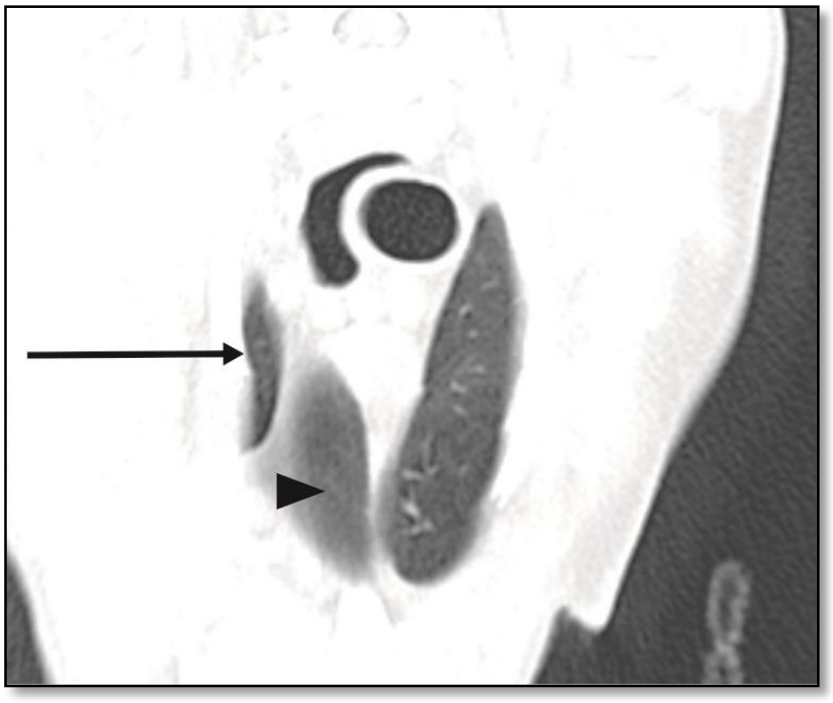

FIG. 22: Transverse image at slice “a” in Dog 4. The black arrow indicates the intruding left cranial *pars caudalis* lobe, which hampered measurement of the *pars cranialis* lobe (black arrow head) in this dog. The image is in a lung window (WL -600 WW 1200) and the left of the dog is to the left of the image. Scan acquired in LLR. Note the asymmetrical thoracic shape due to lateral recumbency.

Slice “b” contained a moderate amount of larger blood vessels and bronchi which were located centrally within the lungs, and thus these could not be excluded from measurements.

On slice “c”, the large blood vessels and bronchi (appearing in cross-section) at the lung-mediastinum border were easily and consistently excluded from the measurements performed.

On slice “d”, the accessory lung lobe proved to be difficult to measure consistently between dogs and studies, as well as between recumbencies. This was due to partial volume averaging affecting the mid- to ventral aspects of the lobe, due to the closely associated caudal cardiac margin and cranial diaphragmatic cupula margin. This resulted in an indistinct poorly defined margin of intermediate HU. The accessory lobe also showed the largest degree of shape variation of the lobes between sternal and lateral recumbencies, and became mildly dorsoventrally elongated (“tall”) and narrow in width when in either lateral recumbency (Fig. 23). The CVC was included in all measurements of the accessory lung lobe.

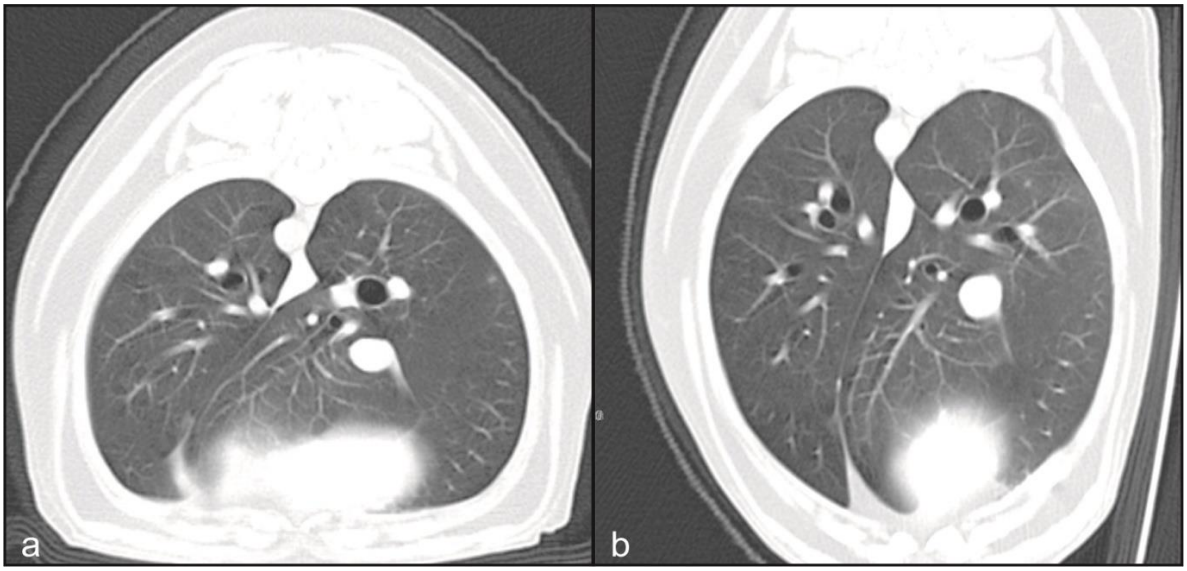

FIG. 23: Dog 6 in sternal recumbency (a) and RLR (b) at slice “d”, demonstrating the shape change in the accessory lobe shape from wide to narrow, as well as its often poorly delineated ventral borders. The general shape in thoracic conformation can also be seen as a narrowed latero-lateral width and an increase in dorsoventral height. The dog’s left is to the left of the images, and the images were acquired in a lung window (WL -600 WW 1200).

Slice “e” consistently included some of the caudal aspect of the accessory lobe located medial to the right caudal lobe at the diaphragm. This portion of the accessory lobe was not included in measurements at this level and was successfully differentiated from the right lobe when measurements were performed.

The HU and CSA graphs were evaluated together and whether they correlated with each other (i.e. an increase in HU should occur with a decrease in CSA, and vice versa).

Standard deviation measurements (automatically given by the CT software) for each lung HU measurement were considered while recording the measured values to ensure that neither excessive soft tissue nor bone was included in the free-hand ROI. SD values across all slices except for slice "d" were within close range of each other, and were between 6 and 258 (average in the range of 105 to 132). The values for slice "d" ranged from 12 to 330 (average 161), with all values greater than 300 due to the accessory lobe, which had poorly defined lung borders and included the CVC.

Statistical evaluation was carried out slightly differently compared to the general descriptive findings, and should be borne in mind when evaluating the findings and graphs. Statistical evaluation, as previously mentioned, evaluated the two main time divisions of each study – time in lateral recumbency (phase 1, or time to "develop" atelectasis, from S_i to RLR/LLR_{30}) and the subsequent time in sternal recumbency (phase 2, or time to "resolve" atelectasis, from S_e to S_{20}). The assessment of "lung lobe portion" refers to the dorsal, middle or ventral third of the lobe assessed.

The statistical analysis showed agreement with the descriptive findings, and each lobe and slice's findings are expressed under the relevant section when needed.

4.3.5.2 Subjective visual assessment of lung lobes

During the initial subjective assessment of the lungs, obvious visualised HU changes were seen on Dog 1, 2, 4, 5 and 6. These findings were noted as patchy increased regions of attenuation within the lungs, as follows (described more in depth in the lung analysis to follow):

In LLR:

- Left cranial *pars cranialis* on slice "b" (Dog 1, 2)
- Left cranial *pars caudalis* on slice "c" (Dog 1, 2, 4, 5)
- Left caudal lobe on slice "d" (Dog 1)

In RLR:

- Right caudal lobe on slice "e" (Dog 5)

4.3.5.3 Overall assessment of combined left and right lung lobes in RLR versus LLR

An overall combined assessment of all the left lobes and all the right lobes (excluding the accessory lobe), for each LLR and RLR, was performed (Figs. 24 and 25).

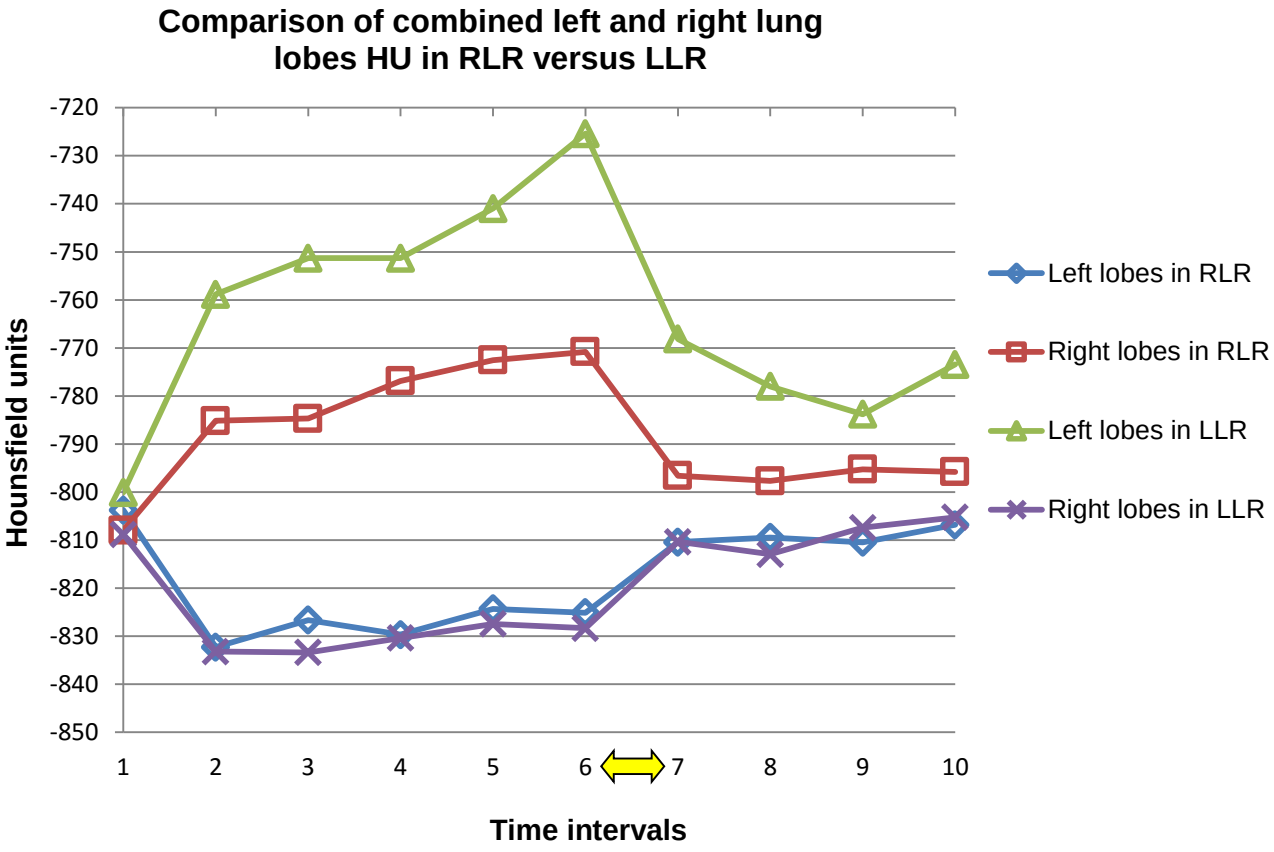

FIG. 24. Line graph depicting the median HU values (y-axis) for the combined left and right lung lobes for all 6 dogs, in LLR and RLR. The graph demonstrates improved aeration for the lobes when they are non-dependent (decreased measured HU) and decreased aeration when they are dependent (increased measured HU), as expected, with a degree return towards the initial HU values after repositioning in sternal recumbency. The shapes of the plots depicted are fairly typical for what was expected to occur with body position changes. Time intervals are depicted on the x-axis, as follows: 1, S_i; 2, RLR/LLR_3; 3, RLR/LLR_8; 4, RLR/LLR_{13}; 5, RLR/LLR_{20}; 6, RLR/LLR_{30}; 7, S_e; 8, S_5; 9, S_{10}; 10, S_{20}. The letter "S" indicates sternal recumbency and "RLR" and "LLR" indicate right and left lateral recumbencies, respectively. The subscript "i" indicates the first initial baseline scan and "e" indicates the sternal scan done upon immediate repositioning in sternal recumbency. The numerical subscripts indicate time elapsed since placement in lateral or sternal recumbency. Time intervals 1 to 6 (S_i to

RLR/LLR$_{30}$) indicate the time to decrease inflation or develop atelectasis in lateral recumbency, while intervals 7 to 10 (S_e to S_{10}) indicate the time to resolve any attenuation or atelectic changes. The double yellow arrow between time intervals 6 and 7 indicates the change in body position from lateral to sternal recumbency.

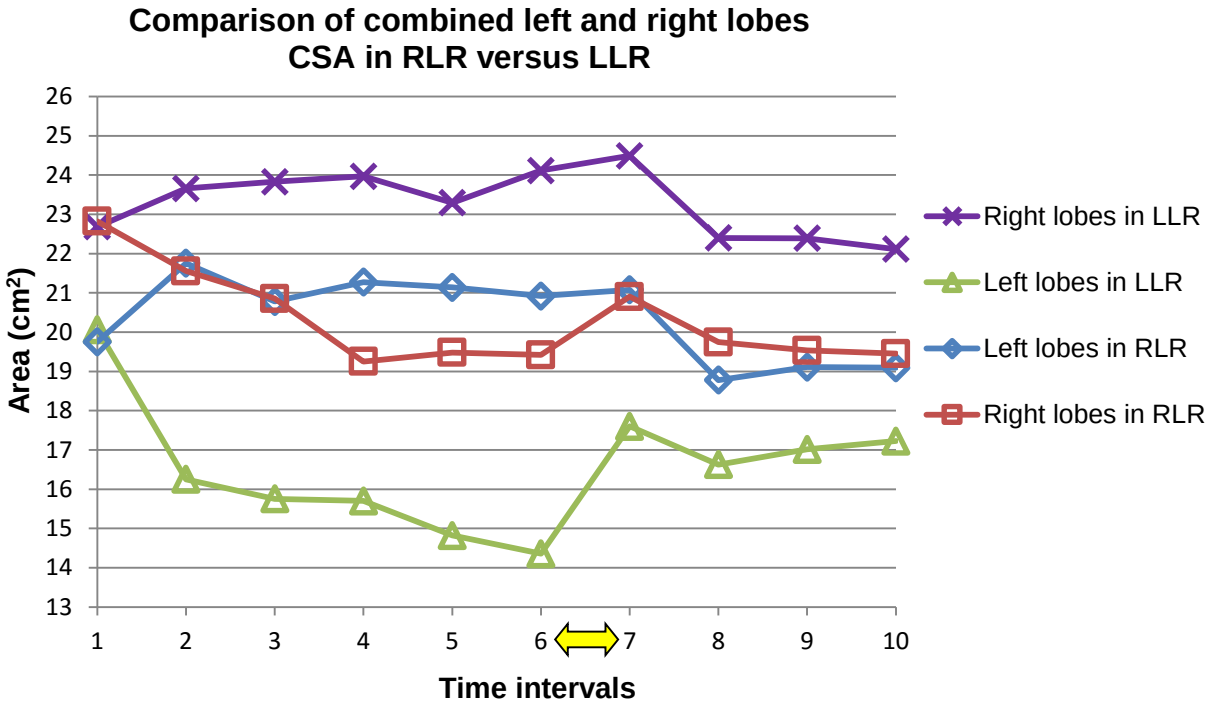

FIG. 25. Line graph depicting the median CSA values (y-axis) for the combined left and right lung lobes for all 6 dogs, in LLR and RLR. The graph demonstrates an increase in CSA for the lobes when they are non-dependent and decrease in CSA when they are dependent, as expected, with a variable return (but not obtaining a full return) towards the initial CSA values after repositioning in sternal recumbency. The plots are fairly typical of expected behaviour of CSA values for lungs with body position changes. The graph should be assessed in conjunction with the associated HU measurements in Fig.24, and HU and CSA plots are expected to show opposite trends. Time intervals are depicted on the x-axis, see Fig. 24 for explanation.

Hounsfield units varied over time, recumbency, slice, lung lobe and lung portion (all P<0.001; **Table 2**). However, starting recumbency side did not have a significant effect (P=0.143). Similar significant associations were identified for cross–sectional area (**Table 3**).

Table 2 -The Effects of Study Variables on Hounsfield Units Measured in the Six Dogs over the Entire Duration of the Study

Variable	Level	Estimate	95% CI	P value*
Time				<0.001
	Baseline	-0.092	-0.143, -0.041	<0.001
	Lateral 3 min	-0.105	-0.177, -0.032	0.005
	Lateral 8 min	-0.093	-0.166, -0.021	0.012
	Lateral 13 min	-0.075	-0.148, -0.003	0.042
	Lateral 20 min	-0.036	-0.109, 0.036	0.327
	Lateral 30 min	-0.030	-0.081, 0.021	0.249
	Sternal 5 min	-0.013	-0.064, 0.038	0.617
	Sternal 10 min	-0.019	-0.070, 0.033	0.479
	Sternal 20 min	Referent		
Recumbency				<0.001
	Left	0.037	-0.017, 0.091	0.179
	Right	-0.050	-0.104, 0.004	0.068
	Sternal	Referent		
Starting recumbency				
	Left	-0.192	-0.485, 0.101	0.143
	Right	Referent		
Slice				<0.001
	a	-0.224	-0.271, -0.177	<0.001
	b	0.058	0.012, 0.105	0.014
	c	-0.204	-0.254, -0.154	<0.001
	d	-0.042	-0.080, -0.004	0.031
	e	Referent		
Lung lobe†				<0.001
	Accessory	0.482	0.431, 0.532	<0.001
	Left caudal	0.006	-0.032, 0.044	0.769
	Left *pars caudalis*	0.317	0.263, 0.370	<0.001
	Left *pars cranialis*	0.073	0.035, 0.111	<0.001
	Right caudal	Referent		
	Right cranial	Referent		
	Right middle	Referent		
Lung portion				<0.001
	Dorsal	-0.029	-0.057, -0.001	0.044
	Middle	0.045	0.017, 0.073	0.002
	Ventral	Referent		

CI = confidence interval.

*Based on mixed-effects linear regression including dog as a random effect. The first P value for each categorical predictor is for the overall test and subsequent P values are for each level of the variable. HU was transformed by adding 920 so that the minimum value was 1 and then taking the natural logarithm prior to statistical analysis.

†More than a single referent lobe was required since all lobes were not present in all slices and redundant parameters were removed from the model.

Table 3 - The Effects of Study Variables on Cross-Sectional Area Measured in the Six Dogs over the Entire Duration of the Study

Variable	Level	Estimate	95% CI	P value*
Time				0.025
	Baseline	0.110	0.041, 0.178	0.002
	Lateral 3 min	0.125	0.028, 0.221	0.011
	Lateral 8 min	0.111	0.015, 0.208	0.024
	Lateral 13 min	0.091	-0.005, 0.187	0.065
	Lateral 20 min	0.080	-0.017, 0.176	0.105
	Lateral 30 min	0.079	0.010, 0.147	0.024
	Sternal 5 min	0.011	-0.057, 0.080	0.742
	Sternal 10 min	0.022	-0.046, 0.090	0.530
	Sternal 20 min	Referent		
Recumbency				0.005
	Left	-0.100	-0.172, -0.029	0.006
	Right	-0.046	-0.118, 0.025	0.207
	Sternal	Referent		
Starting recumbency				
	Left	0.063	-0.075, 0.201	0.276
	Right	Referent		
Slice				<0.001
	a	-1.252	-1.314, -1.190	<0.001
	b	-0.606	-0.668, -0.544	<0.001
	c	-0.254	-0.321, -0.187	<0.001
	d	0.477	0.426, 0.527	<0.001
	e	Referent		
Lung lobe†				<0.001
	Accessory	-0.720	-0.787, -0.653	<0.001
	Left caudal	-0.189	-0.240, -0.139	<0.001
	Left *pars caudalis*	-0.244	-0.315, -0.172	<0.001
	Left *pars cranialis*	-0.366	-0.416, -0.315	<0.001
	Right caudal	Referent		
	Right cranial	Referent		
	Right middle	Referent		
Lung portion				<0.001
	Dorsal	0.314	0.277, 0.352	<0.001
	Middle	0.625	0.587, 0.662	<0.001
	Ventral	Referent		

CI = confidence interval.

*Based on mixed-effects linear regression including dog as a random effect. The first P value for each categorical predictor is for the overall test and subsequent P values are for each level of the variable. Cross-sectional area was transformed by taking the square root prior to statistical analysis.

†More than a single referent lobe was required since all lobes were not present in all slices and redundant parameters were removed from the model.

When broken down into time spent in either lateral recumbency (phase 1), for all lung lobes, the following was found:

- With placement in and during RLR, the left lobes demonstrated a decrease in HU and concomitant increase in CSA. The right lobes demonstrated an increase in HU and concomitant decrease in CSA.
- With placement in and during LLR, the left lobes showed an expected increase in HU and concomitant decrease in CSA. The right lobes demonstrated a decrease in HU and concomitant increase in CSA.
- The HU and CSA graphs correlated well with each other (indicating that they behaved as described above in relation to each other).

For all lung lobes during lateral recumbency, there was a statistically significant association between measured HU values and each of the following:

- time (P=0.034)
- recumbency (P<0.001)
- slice (P<0.001)
- lung lobe (P<0.001)
- lung lobe portion (P=0.001).

There was no significant association between measured HU and starting lateral recumbency (P=0.112).

For measured CSA values during lateral recumbency, there was a statistically significant association with each of the following:

- recumbency (P=0.014)
- slice (P<0.001)
- lung lobe (P<0.001)
- lung lobe portion (P<0.001)

There was no significant association of time (P=0.614) nor starting lateral recumbency (P=0.099) on CSA.

During sternal recumbency (phase 2), the following was found:

- During sternal recumbency, the measured HU and CSA values tended to return towards but never fully attain their initial baseline values, and usually demonstrated a notable degree of fluctuation.

For all lung lobes when replaced in and during sternal recumbency, there was a statistically significant association of measured HU values with each of the following:

- slice (P<0.001)
- lung lobe (P<0.001)
- lung lobe portion (P<0.001).

There was not a significant association of time (P=0.479) and starting lateral recumbency (P=0.245) during sternal recumbency.

For measured CSA values, there was a statistically significant association of:

- slice (P<0.001)
- lung lobe (P<0.001)
- lung lobe portion (P<0.001).

There was not a significant effect of time (P=0.095) or starting lateral recumbency (P=0.636) during sternal recumbency.

Whether a dog started the study in LLR or RLR (starting recumbency) had no effect on measured HU or CSA when looking for development of atelectasis.

When assessing lung lobe portion, for both lateral and sternal recumbency, the ventral lung lobe third had the highest HU values, the dorsal lung lobe third had the most negative value, and the middle lobe third was intermediate between dorsal and ventral. However, for the sternal part of the study, the middle and ventral lobes had very similar HU values. For both lateral and sternal recumbency, the middle lobe third had the largest CSA, followed but the dorsal and lastly the ventral lobe thirds.

HU demonstrated a change over time during lateral recumbency, but did not change over time when replaced into sternal recumbency (i.e. no appreciable change in HU from being replaced in sternal recumbency (from S_e to S_{20})). The effect of time on CSA was the same as for HU.

The effects of lung lobe and slice were not investigated further.

4.3.5.4 Findings on slice “a”

Left cranial *pars cranialis* lobe (Figs. 26 and 27)

Assessment of this lobe for Dog 4 in LLR proved somewhat problematic as the left *pars caudalis* intruded dorsolaterally to this lobe, making the measured CSA very small.

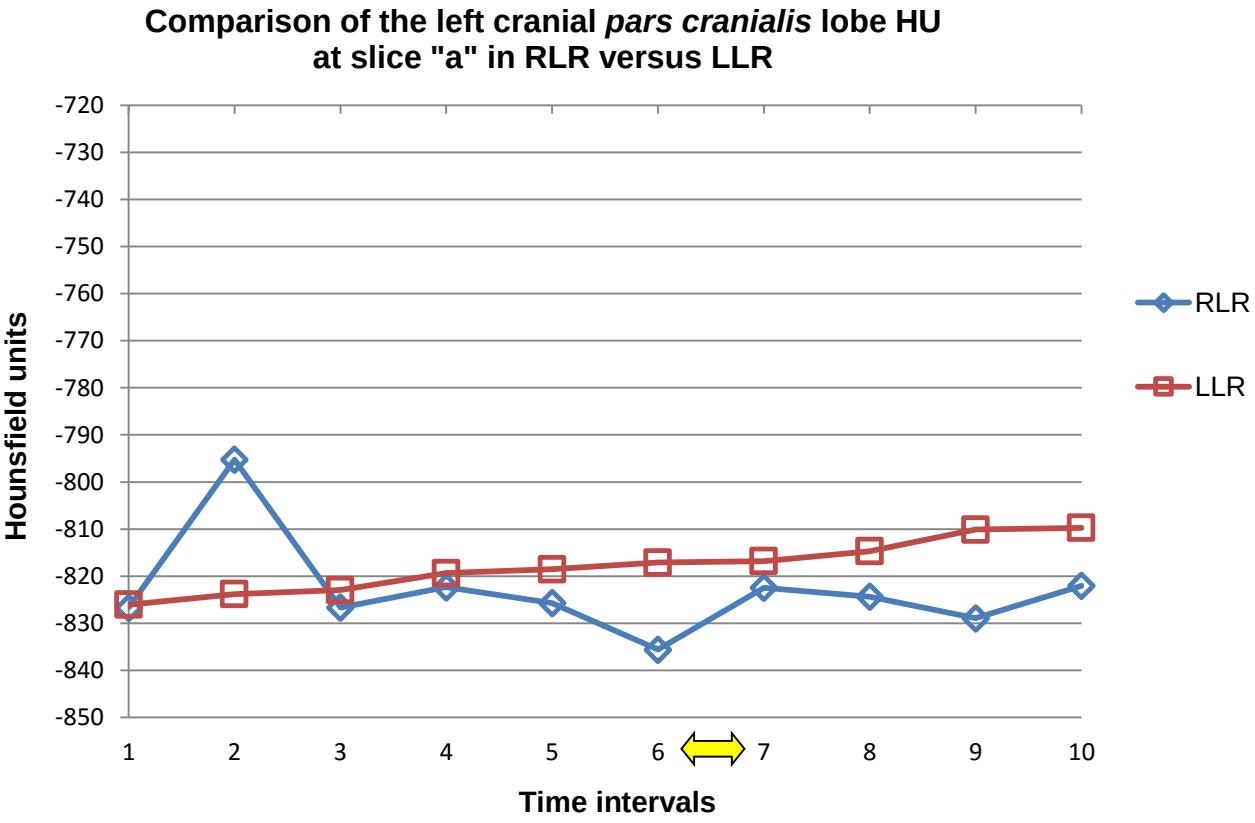

FIG. 26. Line graph depicting the median HU values (y-axis) for the left cranial *pars cranialis* lobe at slice “a”, in LLR and RLR for all 6 dogs. When placed in RLR, there was a sudden marked increase in HU, however this value immediately returned to approximately its baseline value, with fluctuation towards a more negative HU with time in RLR, but no clear pattern throughout the study. After placement in LLR, and throughout the entire study, there was a mild gradual increase in HU. The HU plots for this lobe were inconsistent with what was expected for normal lungs with body position changes. Time intervals are depicted on the x-axis, see Fig. 24 for explanation.

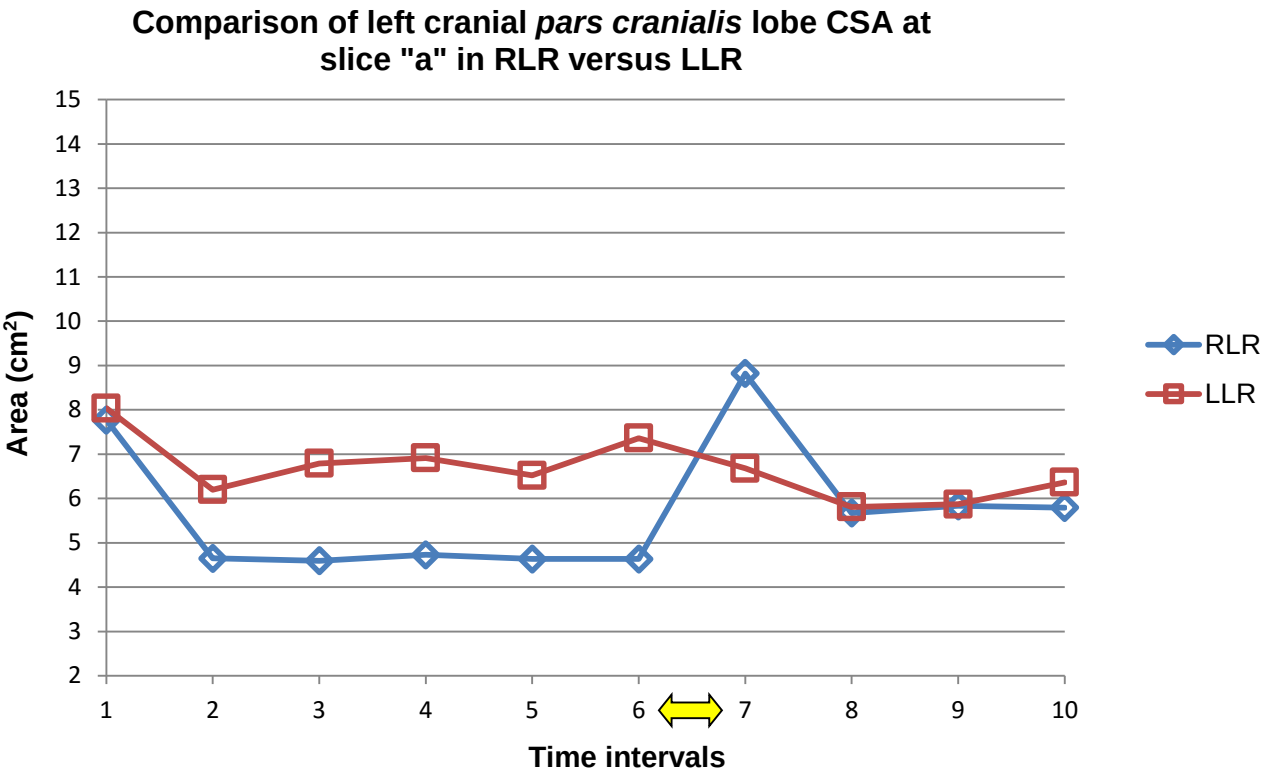

FIG. 27. Line graph depicting the median CSA values in cm^2 (y-axis) for the left cranial *pars cranialis* lobe at slice "a", in LLR and RLR for all 6 dogs. When compared to Fig. 26, it is clear that there was very little correlation between HU and CSA with RLR and LLR. The lobe demonstrated a smaller CSA in RLR despite being non-dependent with no obvious pattern when replaced in sternal recumbency. With placement in and time spent in LLR, there was a decrease in CSA as would be expected, however during sternal recumbency there also was no obvious pattern. Time intervals are depicted on the x-axis, see Fig. 24 for explanation.

RLR:

The baseline HU range of all six dogs fell within normal respiratory range.

The left *pars cranialis* lobe demonstrated a decrease in CSA and concomitant increase HU when placed in RLR (at S_i to RLR_3), despite being non-dependent.

Whilst in RLR, there was an immediate return to a more negative HU near comparable to that at S_i, with fluctuation in HU over time in RLR. CSA measurements remained lower than baseline values. HU and CSA plots did not appear to be correlated.

With repositioning in sternal recumbency, there was a mild increase in HU that fluctuated variably but never returned to baseline values. The CSA values increased when repositioned in sternal recumbency however dropped again. The CSA values also did not return to baseline values by the end of the study.

When plotted individually, the six dogs demonstrated a wider range of HU than that appreciable on the combined median graph, but the CSA graphs correlated excellently.

Statistically, there was not a significant effect of time (*P*=0.835) on measured HU values during RLR. The effect of time was still non-significant (*P*=0.477) after repositioning in sternal recumbency.

For CSA, there was a significant effect of time (*P*<0.001) during RLR, and after repositioning in sternal recumbency (*P*=0.002).

LLR:

The baseline HU range of all six dogs was within normal respiratory range.

For CSA measurements, Dog 4 consistently had outlying values due to notably smaller measurements for most of the study (for example, S_i was 2.8 cm^2 for Dog 4 and 7.14 cm^2 for Dog 2, which had the next smallest value). This was attributed to the intrusion of the left *pars caudalis*.

Recumbency did not appear to influence HU measurements and rather showed a steady increase over time. However, the measured CSA decreased initially as expected for a dependent lobe but the pattern over time was less clear after repositioning in sternal recumbency.

When plotted individually, the six dogs again demonstrated a wider range of HU without obvious pattern, than that appreciable on the combined median graph. The six individual CSA plots showed less marked variation than the HU.

There was not a significant effect of time (*P*=0.110) on HU during LLR. After being positioned in sternal recumbency there was still no significant time effect (*P*=0.531).

For CSA, there was not a significant effect of time (*P*=0.363) during LLR. During sternal recumbency, the effect of time (*P*=0.284) was similar.

Right cranial lobe (Figs. 28 and 29)

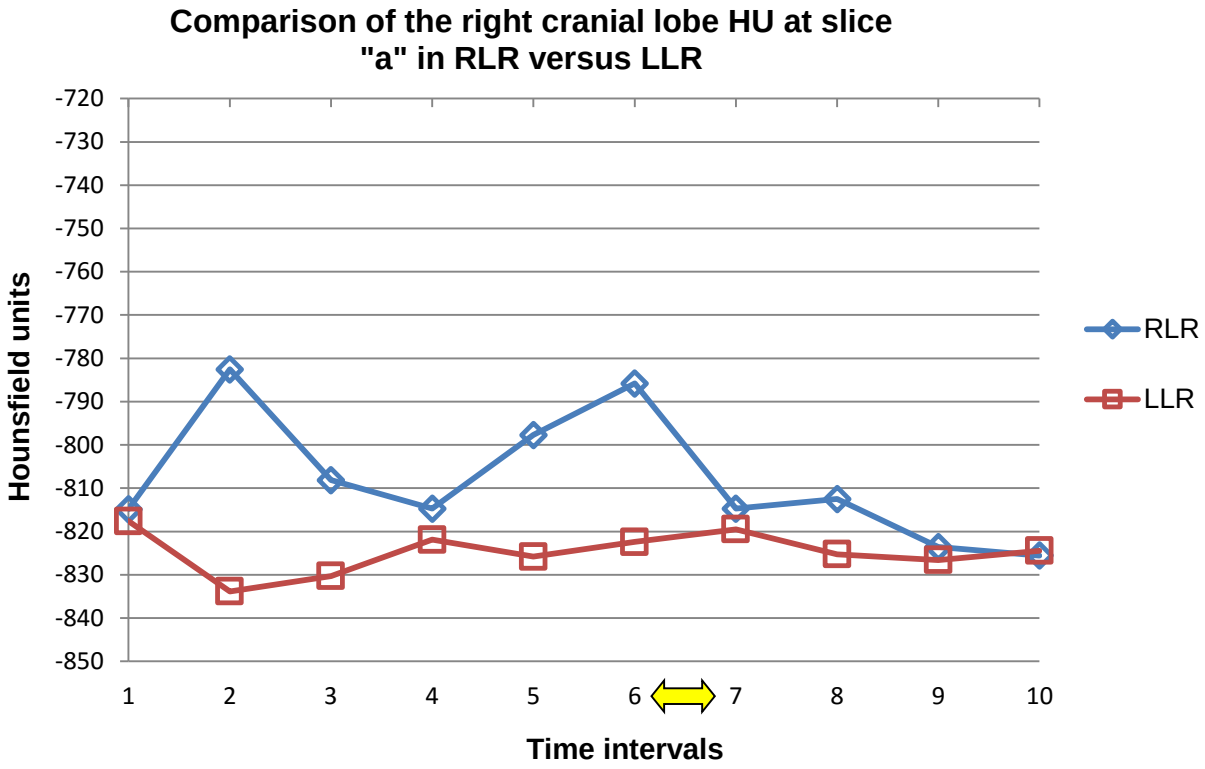

FIG. 28. Line graph depicting the median HU values (y-axis) for the right cranial lobe at slice “a”, in LLR and RLR for all 6 dogs. There was an increase in HU when placed in RLR, but obvious variation in HU whilst in RLR with no appreciable pattern. With repositioning in sternal recumbency, the HU values returned to approximately baseline values. In LLR, there was a decrease in HU with mild fluctuations and increase to near baseline values during LLR. There was a mild decrease in HU with repositioning in sternal recumbency. Mild HU fluctuation persisted with repositioning in sternal recumbency. The plots demonstrated some of the features that are expected for normal lungs with changes in body position. Time intervals are depicted on the x-axis, see Fig. 24 for explanation.

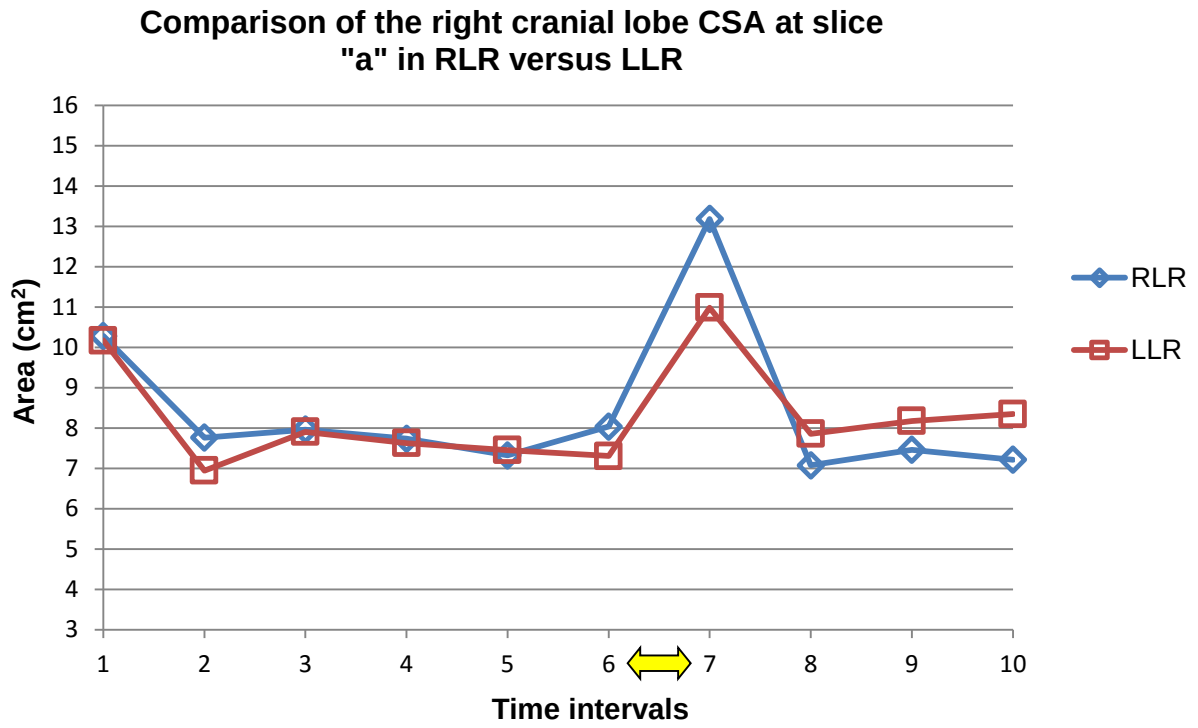

FIG. 29. Line graph depicting the median CSA values in cm^2 (y-axis) for the right cranial lobe at slice "a", in LLR and RLR for all 6 dogs. When in RLR, the graph was fairly typical for what is expected of a dependent lobe, with a decreased CSA in RLR and an increase CSA in sternal recumbency. It correlated somewhat with the HU findings. However the sudden decrease in CSA during sternal recumbency is atypical. The LLR graph mirrored that for RLR, and was inconsistent with its HU graph. Time intervals are depicted on the x-axis, see Fig. 24 for explanation.

RLR:

The baseline HU range of all six dogs was within normal respiratory range.

The right cranial lobe showed an increase in HU and concomitant decrease in CSA to some when placed in RLR, which is consistent with a dependent location.

There was noticable variation in HU whilst in RLR with no appreciable pattern, however the CSA measurements remained decreased compared to the baseline values.

With repositioning in sternal recumbency there was a concomitant decrease in HU and increase in CSA. However the CSA measurements sharply decreased again within sternal recumbency.

When plotted individually, the six dogs demonstrated a wider range of HU than that appreciable on the combined median graph, but the CSA graphs correlated excellently.

Statistically, there was not a significant effect of time (*P*=0.080) on measured HU during RLR, and nor after being repositioned in sternal recumbency (*P*=0.115).
For CSA, there was a significant effect of time in lateral (*P*<0.001) and sternal (*P*<0.001) recumbency.

LLR:

The baseline HU range of all six dogs was within normal respiratory range.
The right cranial lobe generally showed a decrease in HU when placed in LLR, as expected, but the CSA also decreased which was unexpected, resulting in contradictory findings.
With time in LLR, there were mild HU and CSA fluctuations without any pattern.
The mild HU fluctuations persisted with repositioning in sternal recumbency, and there was a sharp unexpected increase and decrease in CSA (similar to findings in RLR).
When plotted individually, the six dogs demonstrated a wider range of HU and CSA values than that appreciable on the combined median graph.
Statistically, there was not a significant effect of time (*P*=0.407) on measured HU during LLR nor for repositioning in sternal recumbency (*P*=0.803).
For CSA, there was a significant effect of time (*P*=0.023) during lateral recumbency but nor after repositioning in sternal recumbency (*P*=0.096).

4.3.5.5 Findings on slice “b”

Left cranial *pars cranialis* lobe (Figs. 30 and 31)

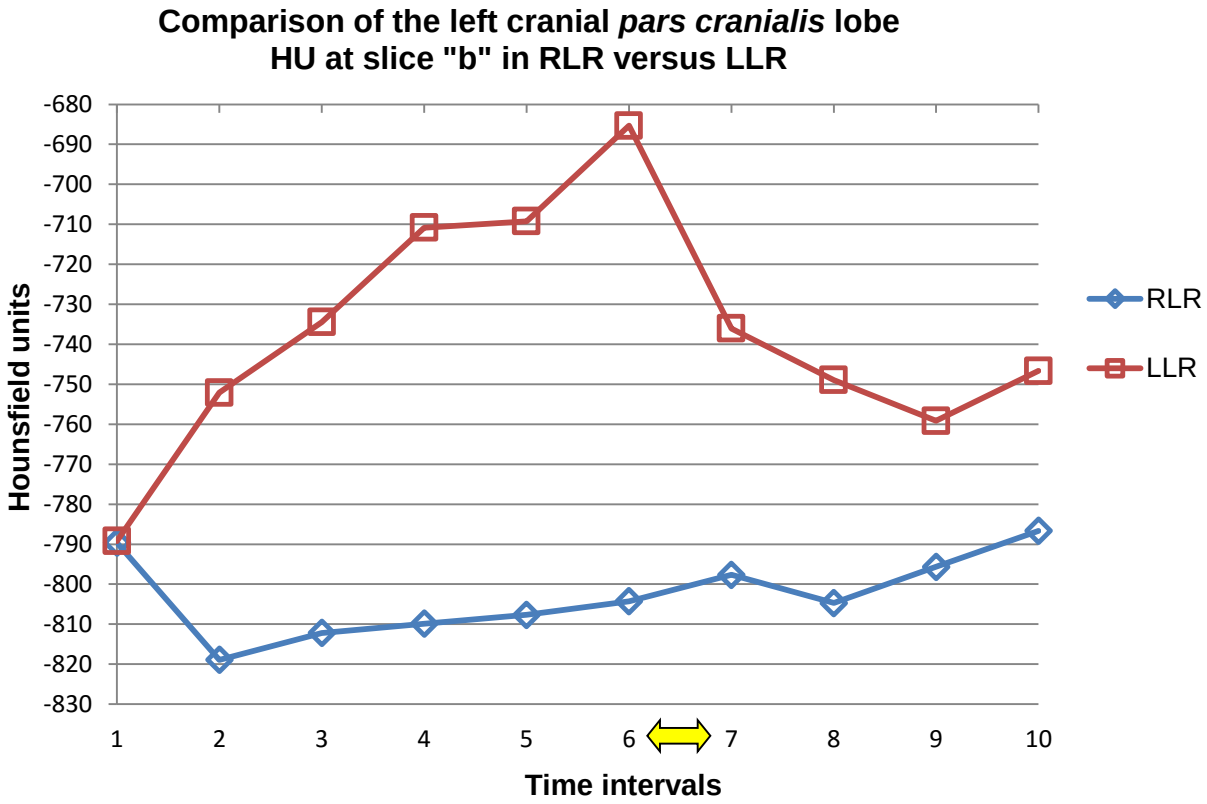

FIG. 30. Line graph depicting the median HU values (y-axis) for the left cranial *pars cranialis* lobe at slice “b”, in LLR and RLR for all 6 dogs. With placement in RLR, there was a mild decrease in HU, but with time in RLR there was a mild unexpected continuous increase in HU with minimal change in time over all. There was an increase in HU with placement in LLR, which continued to increase during LLR and then decrease again with repositioning in sternal recumbency – the LLR plot is fairly typical of what is expected in a lobe with body position changes. Time intervals are depicted on the x-axis, see Fig. 24 for explanation.

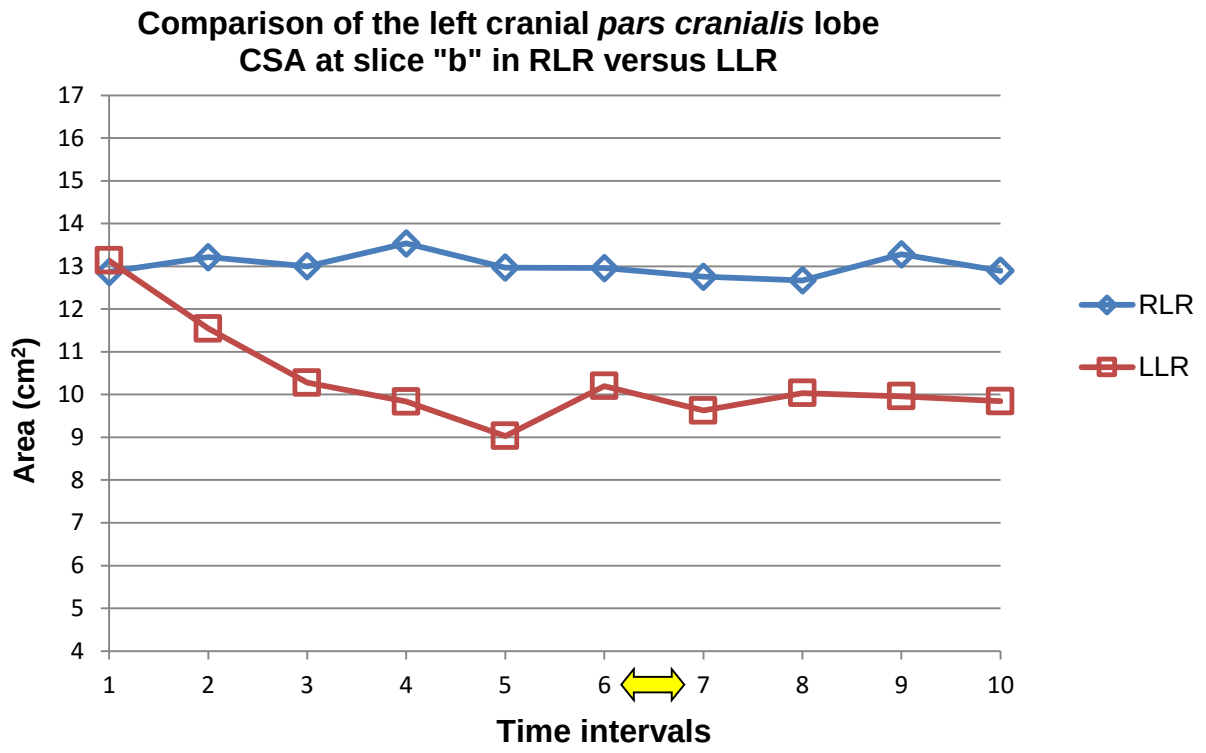

FIG. 31. Line graph depicting the median CSA values in cm^2 (y-axis) for the left cranial *pars cranialis* lobe at slice "b", in LLR and RLR for all 6 dogs. There was minimal change in CSA over time in RLR for the duration of the study, without any obvious pattern. However for LLR, there was good correlation of the CSA plot with the HU, with a decrease in CSA when dependent in LLR and an increase with repositioning in sternal recumbency. The CSA fluctuated in sternal recumbency but did not return to near its baseline values. Time intervals are depicted on the x-axis, see Fig. 24 for explanation.

RLR:

The baseline HU range of all six dogs was within normal respiratory range.

With placement in RLR, there was a decrease in HU and mild increase in CSA, as expected for the non-dependent lobe.

With time in RLR there was a mild unexpected continuous increase in HU, with CSA measurement fluctuation without any appreciable pattern.

The subtle increasing trend in HU continued with repositioning in sternal recumbency with no discernible CSA pattern.

When plotted individually, the six dogs demonstrated a good correlation with the combined median graph.

Statistically, there was a significant effect of time (*P*=0.001) on measured HU during RLR, not after repositioning in sternal recumbency (*P*=0.874).

For CSA, there was not a significant effect of time in lateral (*P*=0.632) nor sternal recumbency (*P*=0.326).

LLR:

The baseline HU range of all six dogs was within normal respiratory range.

The lobe showed an expected increase in HU and decrease in CSA with placement in LLR, and both continued to decrease and increase, respectively, with time spent in LLR.

With repositioning in sternal recumbency, there was a decrease in HU and mild fluctuation in CSA measurements.

When plotted individually, the six dogs demonstrated a mildly wider range of HU and CSA values than that appreciable on the combined median graph.

Dog 1 showed a visible increased patchy attenuation from LLR_8 onwards, which started mildly at the middle of the middle third of the left *pars cranialis*. It only progressed visually mildly to LLR_{30}, but Dog 1 showed a steady increase in HU throughout the whole study (see Fig. 32).

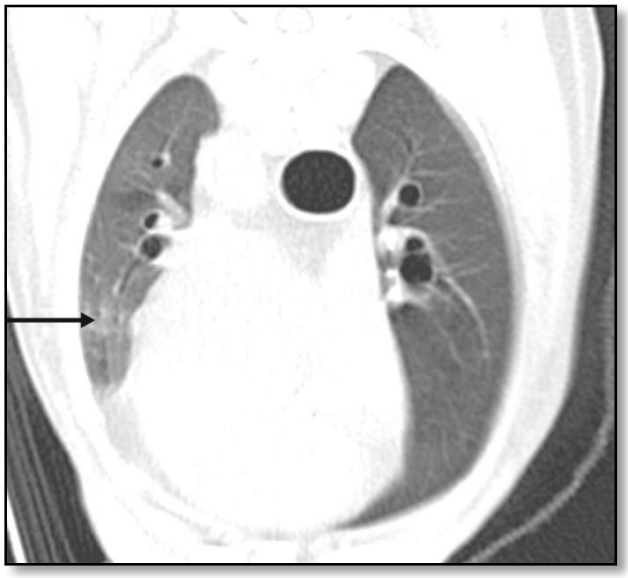

FIG. 32. Transverse plane image of Dog 1 at slice “b” at LLR_{30}. Note the patchy increased soft tissue attenuation of the left cranial *pars cranialis*, especially in the ventral third of the lobe (black arrow). The dorsal third is spared. Image is in a lung window (WL -600 WW 1200) and the dog’s left is to the left of the image.

Dog 2 had the highest HU at LLR_{13} and LLR_{20}, of -560 and -577 respectively (see Fig. 33 a and b). These changes were clearly noted on initial image evaluation as a diffuse patchy increased soft tissue attenuation of the entire lobe. The most dorsal aspect of the lobe was relatively less affected, and the middle third of the lung appeared most severely affected. These changes were absent at S_i, and appeared at LLR_3 and showed moderate progression throughout LLR. The changes were still visible at S_e, at which point they subjectively appeared mildly decreased in severity. By S_{20}, they had not resolved but were improved to some extent subjectively compared to S_e (measured values showed less than 50 HU between the two points). The CSA measurements correlated well with the HU changes, and demonstrated a decrease to by up to 5.85 cm^2 between S_i to LLR_{13}, where the CSA was the smallest.
Dog 1 and 2's HU values remained below normal respiratory values (-669 and -642 respectively) at the end of the study.

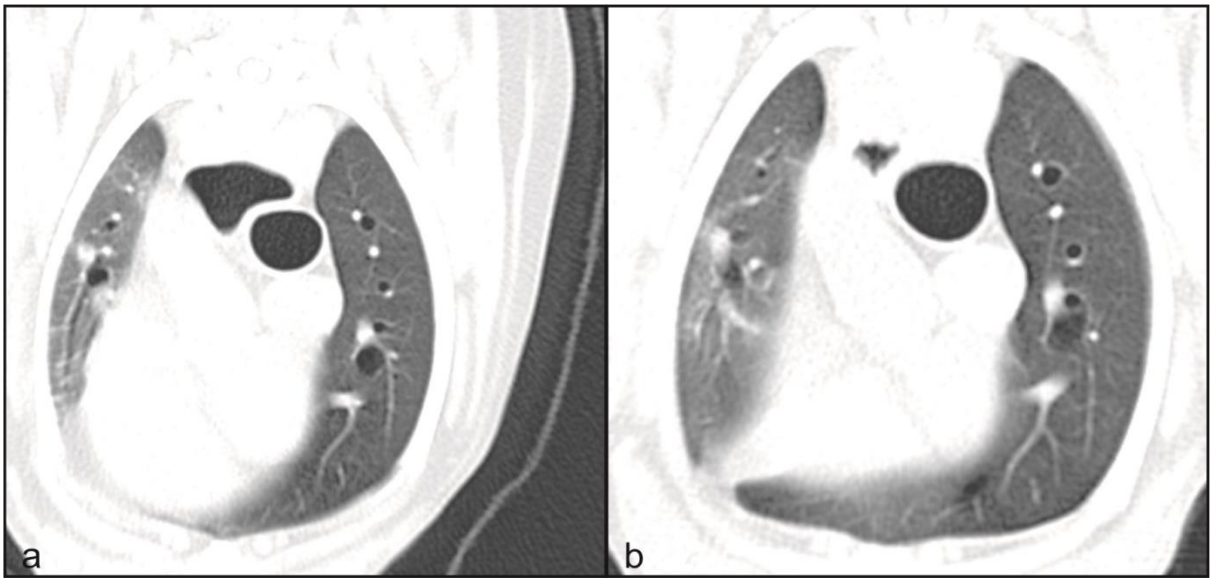

FIG. 33. Transverse plane images at LLR_{30} (a) and S_{20} (b) of Dog 2, at slice "b" for the study in LLR, demonstrating a lack of resolution of the patchy increased attenuation of the left cranial *pars cranialis* after repositioning into and time spent in sternal recumbency. Whilst not at exactly the same location, the images are representative of this lobe. Images are in a lung window (WL -600 WW 1200) and the dog's left is to the left of the image.

Statistically, there was a significant effect of time (P<0.001) on measured HU change during in LLR not after repositioning in sternal recumbency (P=0.189)

For CSA, there was a significant effect of time during lateral recumbency (P<0.001) but not during sternal recumbency (P=0.401).

Right cranial lobe (Figs. 34 and 35)

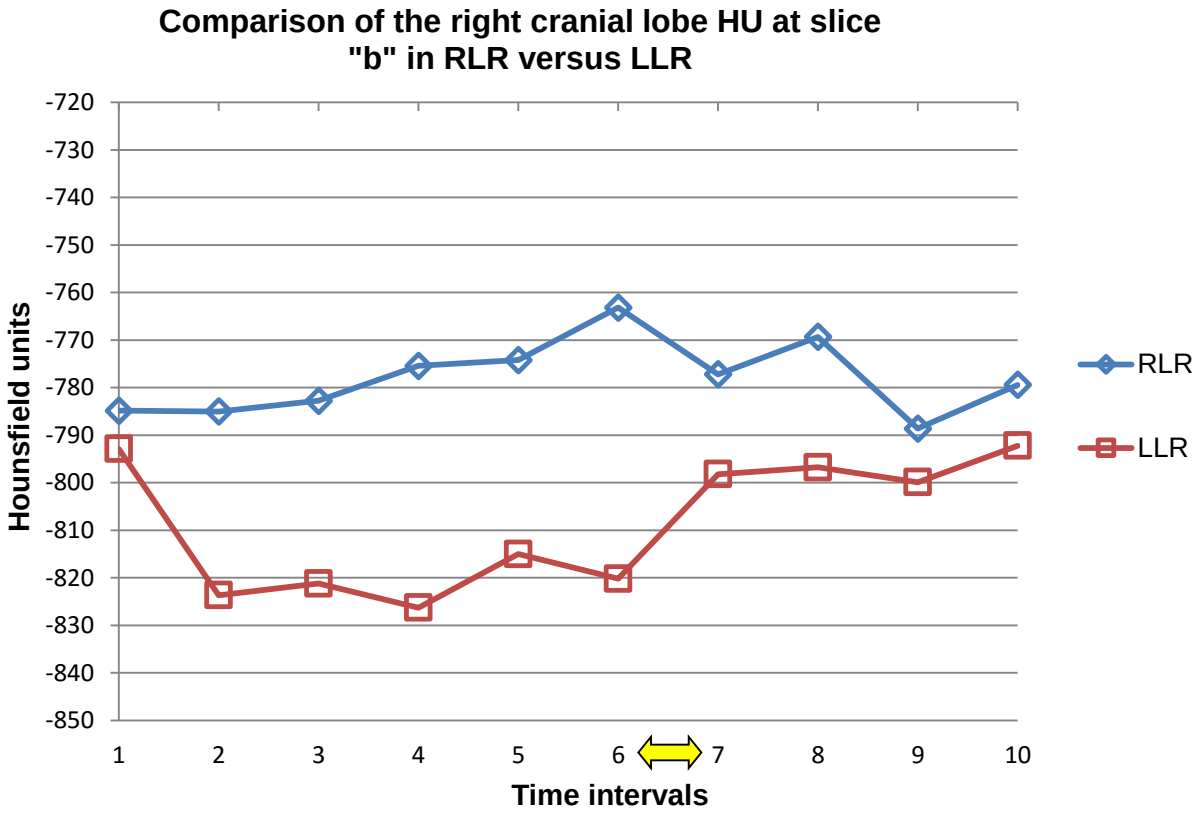

FIG. 34. Line graph depicting the median HU values (y-axis) for the right cranial lobe at slice “b”, in LLR and RLR for all 6 dogs. There was minimal HU change with placement in RLR, but a steady increase with time in RLR. With repositioning in sternal recumbency, there was a decrease in HU, but fluctuation during sternal recumbency. The plot for LLR was typical for a non-dependent lung lobe, with decrease HU with positioning in LLR and a subsequent increase with repositioning in sternal recumbency. Time intervals are depicted on the x-axis, see Fig. 24 for explanation.

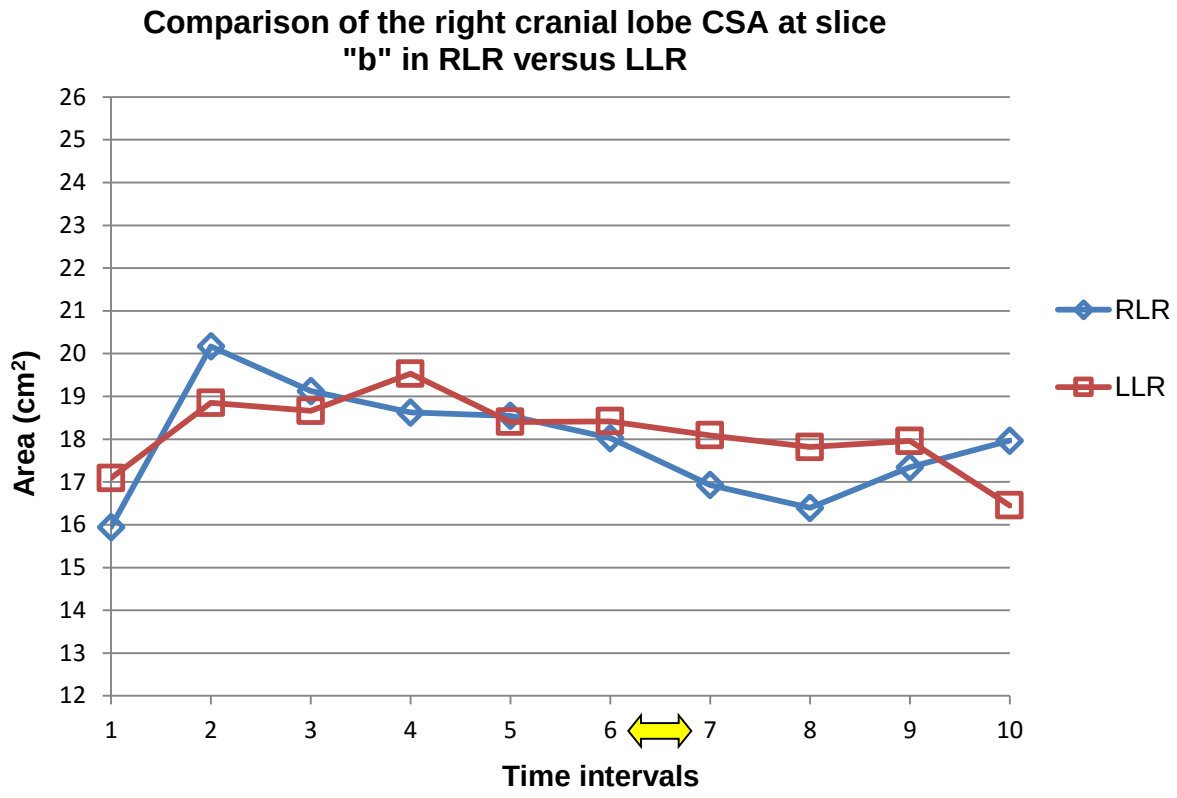

FIG. 35. . Line graph depicting the median CSA values in cm^2 (y-axis) for the right cranial lobe at slice "b", in LLR and RLR for all 6 dogs. In RLR, and unexpected increase in CSA occurred. However with time in RLR, there was a steady decrease in CSA which continued to decrease into early sternal recumbency before increasing again – the CSA plot did not correspond to the HU plot in RLR. The LLR CSA plot correlated well with the HU plot, and was considered a fairly typical representation of changes in the lung when non-dependent. Time intervals are depicted on the x-axis, see Fig. 24 for explanation.

RLR:

The baseline HU range of all six dogs was within normal respiratory range.

There was minimal HU change but a prominent unexpected increase in CSA values when placed in RLR, which was unexpected for the dependent lobe.

With time in RLR, there was a steady decrease in CSA and concomitant increase in HU as would be expected for the dependent lobe.

With repositioning in sternal recumbency, there was a decrease in HU which fluctuated also during sternal recumbency in a more negative direction, however the CSA measurements did no correlate well and continued to decrease into early sternal recumbency before increasing again.

When plotted individually, a single dog demonstrated very variably haphazard HU values; however the other five dogs' plots correlated well with the combined median graph. The CSA graphs had similar findings.

Statistically, there was a significant effect of time (*P*=0.009) on measured HU during in RLR, but not during in sternal recumbency (*P*=0.510).

For CSA, there was a significant effect of time (*P*=0.029) in lateral recumbency but not during sternal recumbency (*P*=0.597).

LLR:

The baseline HU range of all six dogs was within normal respiratory range.

With placement in LLR, the right cranial lobe demonstrated an expected decrease in HU and concomitant increase in CSA values. Both values showed similar but fluctuating values throughout time in LLR, as expected.

With repositioning in sternal recumbency, there was an increase in HU values and concomitant decrease in CSA.

When plotted individually for the six dogs, the HU plots corresponded well to the median plot, but the CSA values tended to have a wide range of individual values but overall a similar shape.

Statistically, there was a significant effect of time (*P*=0.002) on measured HU during LLR, but not after being repositioned in sternal recumbency (*P*=0.052).

For CSA, there was not a significant effect of time (*P*=0.290) in lateral recumbency, nor in sternal recumbency (*P*=0.554).

4.3.5.6 Findings on slice “c”

Left cranial *pars caudalis* lobe (Figs. 36 and 37)

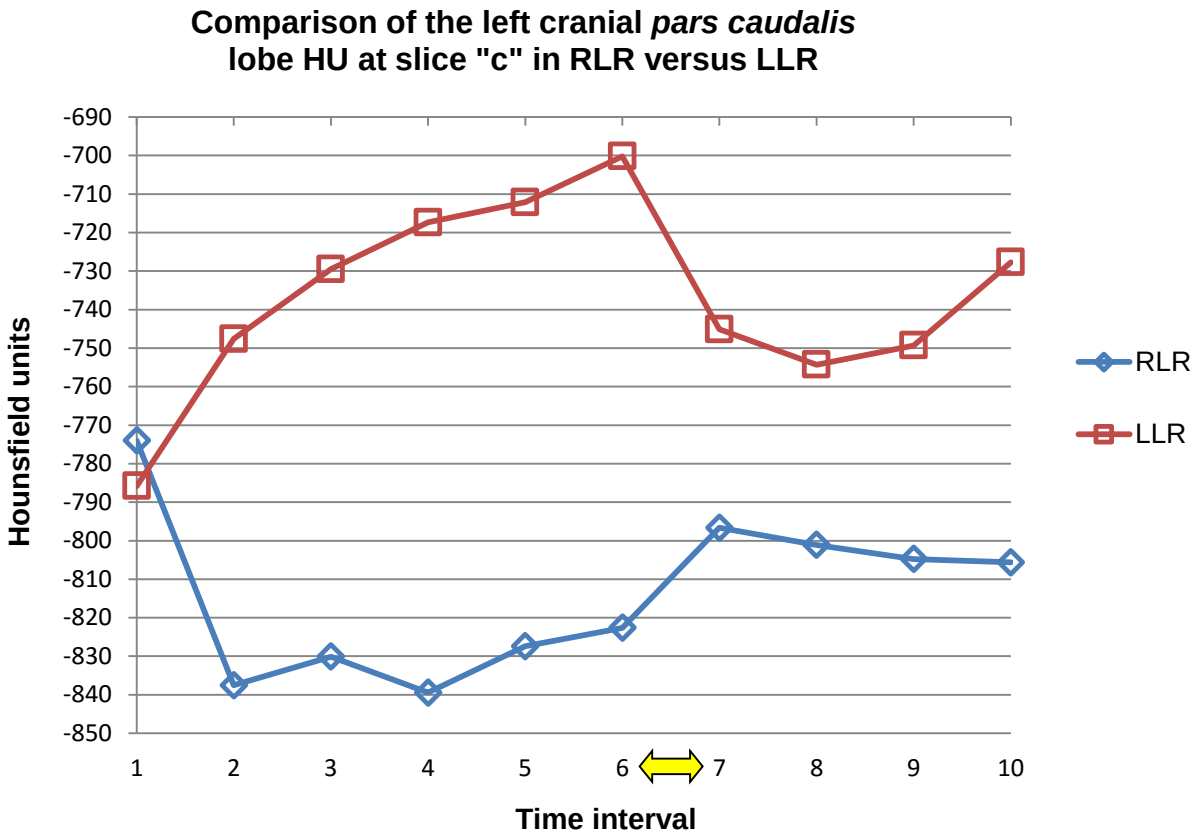

FIG. 36. Line graph depicting the median HU values (y-axis) for the left cranial *pars cranialis* lobe at slice “c”, in LLR and RLR for all 6 dogs. This was the first graph to demonstrate the typical opposing plots for a lobe when dependent versus non-dependent. In RLR, there is a decrease in HU, indicative of increased aeration, which remains this way for the duration in RLR, with a subsequent increase in HU, indicative of decreased aeration, when repositioned in sternal recumbency. Baseline values were not regained. In LLR, the expected opposite findings were present as the lung was dependent, but again a full return to baseline values was not seen and there was variation in sternal recumbency. Time intervals are depicted on the x-axis, see Fig. 24 for explanation.

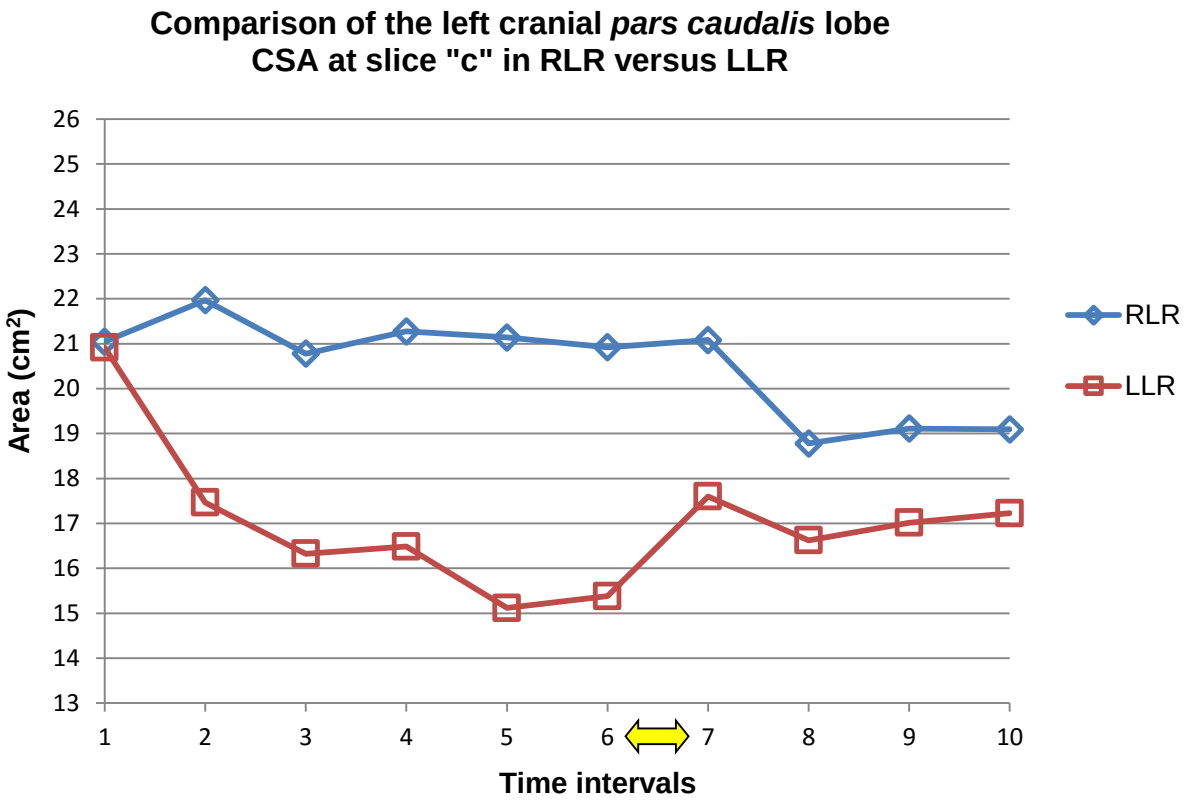

FIG. 37. Line graph depicting the median CSA values in cm^2 (y-axis) for the left cranial *pars caudalis* lobe at slice "c", in LLR and RLR for all 6 dogs. The CSA plots demonstrate the fairly typical opposing appearance in RLR versus LLR, and correspond well with the associated HU plots. Thus typically, for RLR there is a decrease HU and concomitant increased CSA as expected when the lobe is non-dependent, and for LLR there is an increase HU and decreased are as expected when the lobe is dependent. When repositioned in sternal recumbency, the changes are reversed to some degree. Time intervals are depicted on the x-axis, see Fig. 24 for explanation.

RLR:

The baseline HU range of all six dogs was within normal respiratory range.

With placement in RLR, there was a decrease in HU and concomitant increase in CSA, as expected.

During RLR, HU remained more negative than baseline values, however the CSA decreased again to baseline levels.

With repositioning in sternal recumbency, the HU values increased again and fluctuated mildly during sternal recumbency, but the CSA values continued to decrease and remained below baseline values.

The HU graph correlated very well to the individual plots of the six dogs, and while the CSA graphs shared the same shape, there was a wider range of values between dogs compared to the combined median graph.

Statistically, there was a significant effect of time (P<0.001) on measured HU during RLR. However, after being positioned in sternal recumbency time became non-significant (P=0.968).

For CSA, there was not a significant effect of time (P=0.632) during RLR, however time became significant during sternal recumbency (P=0.035).

LLR:

The baseline HU range of all six dogs was within normal respiratory range.

With placement in LLR, there was an expected increase in HU and concomitant decrease in CSA. HU continued to increase and CSA decrease during LLR.

Dog 1 and 2 showed the greatest increase in HU, at LLR_{13} to LLR_{30}, and LLR_{13} respectively. In both dogs, these HU increases were visualised at initial image assessment.

Dog 1 showed mild patchy increased soft tissue attenuation of the ventral tips of the lobe at LLR_8, which increased mildly in severity to involve the ventral third of the lobe, and was still visible at S_e (Fig. 38).

FIG. 38: Transverse plane image of Dog 1, LLR_{30} at slice “c”. Note the patchy increased soft tissue attenuation of the ventral third of the left cranial *pars caudalis* lobe. These changes were still visible at S_e. Image is in a lung window (WL -600 WW 1200) and the dog’s left is to the left of the image.

Dog 2 started with a mild similar diffuse increased HU at LLR_8, and progressed mildly only in the ventral third of the lobe up to LLR_{30}. At S_e the changes were less severe.

On visual assessment, Dog 4 showed a patchy ventrally located increase soft tissue attenuation which was present form LLR_{13} to LLR_{30}, and appeared similar on these time intervals.

On visual assessment, Dog 5 demonstrated mild patchy increased soft tissue opacity of the most ventral aspects of the lobe at LLR_8, and this stayed similar up to LLR_{30}. This was correlated as a mild increased HU during lateral recumbency on the graph, but appeared mild compared to the changes for Dog 1 and 2. Using the smallest focal ROI, the HU went up to -320 in the most severely affected regions.

With repositioning in sternal recumbency, the CSA increased and HU concomitantly decrease again, but both values did not return to baseline values and fluctuated mildly throughout sternal recumbency.

Dog 1 showed a marked increase in HU from S_e to S_{20} (-698, -659, -605 respectively). These changes were noted on initial image evaluation as patchy increased soft tissue attenuation of the ventral half of the lobe, which appeared increased in severity compared to S_e. CSA measurements showed an expected correlated decrease in measured values.

Dog 4 still had unchanged patchy soft tissue attenuation at S_e, which improved at S_{10} to S_{20} but was still faintly visible as a diffuse mild increased opacity. This correlated to the findings on the dog's individual graph.

Dog 5 at S_e still had visible patchy soft tissue attenuation of the ventral tip, which demonstrated mild decrease in severity up to S_{20} but did not resolve completely. These findings did not correlate with the graph at S_{20} where HU appeared to increase.

The individual plots for HU and CSA for the six dogs corresponded well to the combined median graphs.

Statistically, there was a significant effect of time (P<0.001) on measured HU during LLR. With repositioning in sternal recumbency, the effect of time was no longer significant (P=0.329).

For CSA, there was a significant effect of time (P<0.001) during lateral recumbency, but not of time in sternal recumbency (P=0.117).

Right middle lobe (Figs. 39 and 40)

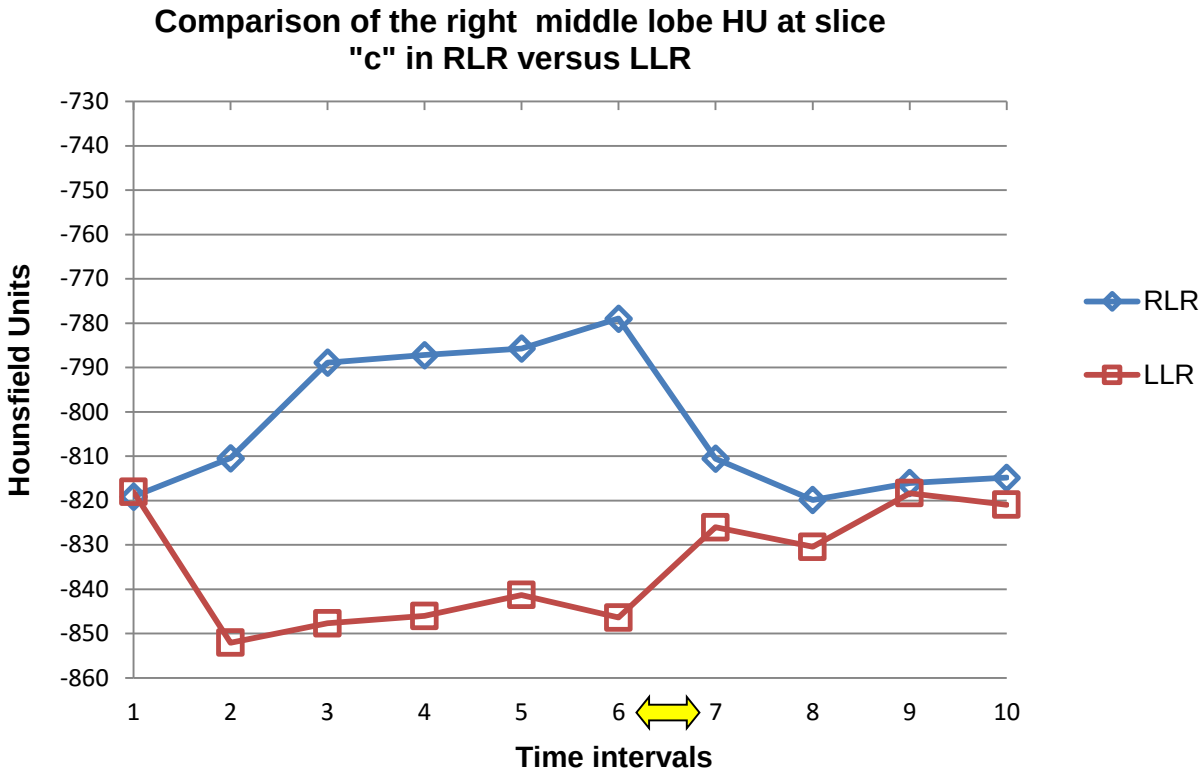

FIG. 39: Line graph depicting the median HU values (y-axis) for the right middle lobe at slice “c”, in LLR and RLR for all 6 dogs. Note the typical expected appearance of the plots, as explained in Fig. 36. Time intervals are depicted on the x-axis, see Fig. 24 for explanation.

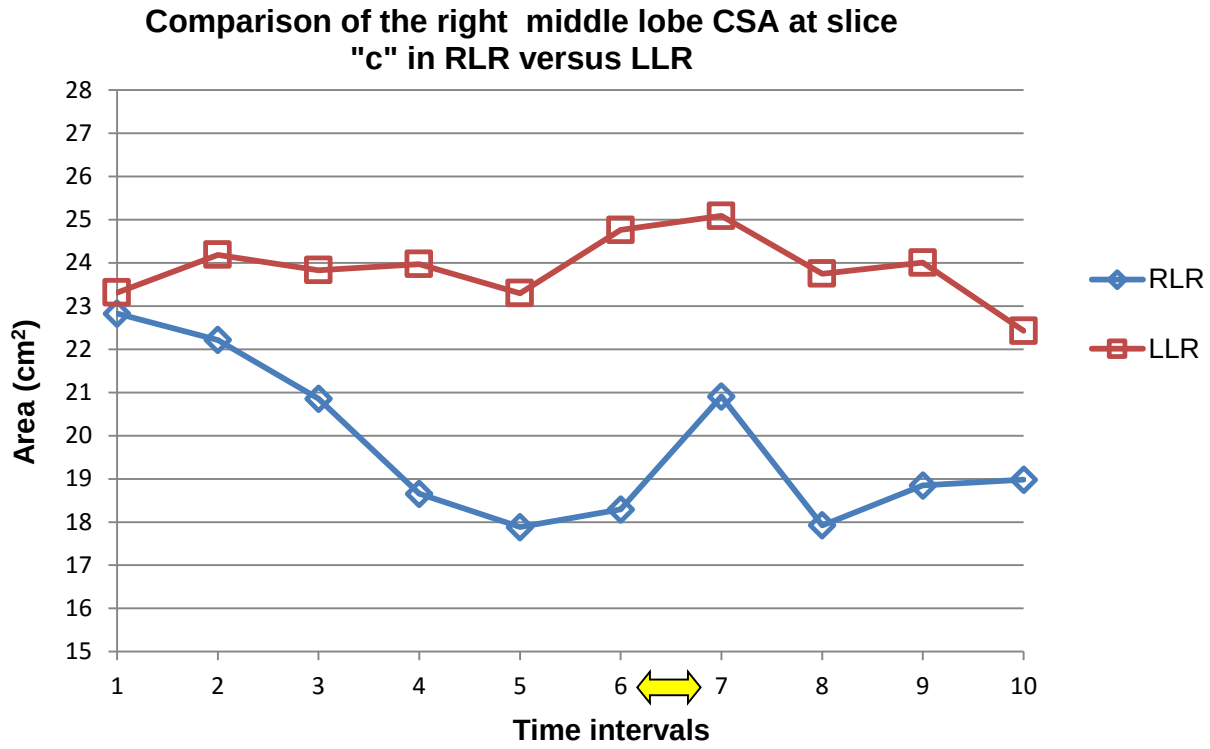

FIG. 40. Line graph depicting the median CSA values in cm^2 (y-axis) for the right middle lobe at slice "c", in LLR and RLR for all 6 dogs. The RLR CSA plots demonstrate the fairly typical opposing appearance in RLR versus LLR (as explained in Fig. 37); however in this case the LLR CSA plot did not correlate well with the HU plot. Time intervals are depicted on the x-axis, see Fig. 24 for explanation.

RLR:

The baseline HU range of all six dogs was within normal respiratory range.

An increase in HU and concomitant decrease in CSA occurred as expected with placement in RLR and during RLR.

With repositioning in sternal recumbency a decrease in HU and concomitant increase in CSA was seen. During sternal recumbency, there was minimal fluctuation in measured HU but the CSA measurement varied with no clear discernible pattern.

The combined median graphs correlated well with the six dogs' individual plots for HU and CSA.

Statistically, there was a significant effect of time (P<0.001) on measured HU during RLR, however not during sternal recumbency (P=0.981).

For CSA, there was a significant effect of time during lateral recumbency (P<0.001) as well as sternal recumbency (P=0.026).

LLR:

The baseline HU range of all six dogs was within normal respiratory range.

There was little correlation between the HU and CSA graphs towards the end of LLR and onwards, as the CSA graph showed no obvious pattern here.

However, the HU graph behaved as expected and demonstrated a decrease in HU with placement in LLR and during LLR, with an increase with repositioning in sternal recumbency and during sternal recumbency.

When the HU were plotted individually for all 6 dogs, the graph corresponded well with the combined median graph. However for CSA, there was a haphazard appearance to the individual graphs.

Statistically, there was a significant effect of time on measured HU during LLR (P<0.001), as well as during sternal recumbency (P=0.005).

For CSA, there was not a significant effect of time in lateral recumbency (P=0.950) nor during sternal recumbency (P=0.181).

4.3.5.7 Findings on slice “d”

Accessory lobe (Figs. 41 and 42)

This lobe consistently had increased HU values compared to the other lung lobes – this is to some extent due to the inclusion of the CVC in all measurements, as well partial volume artefact of the heart and diaphragm.

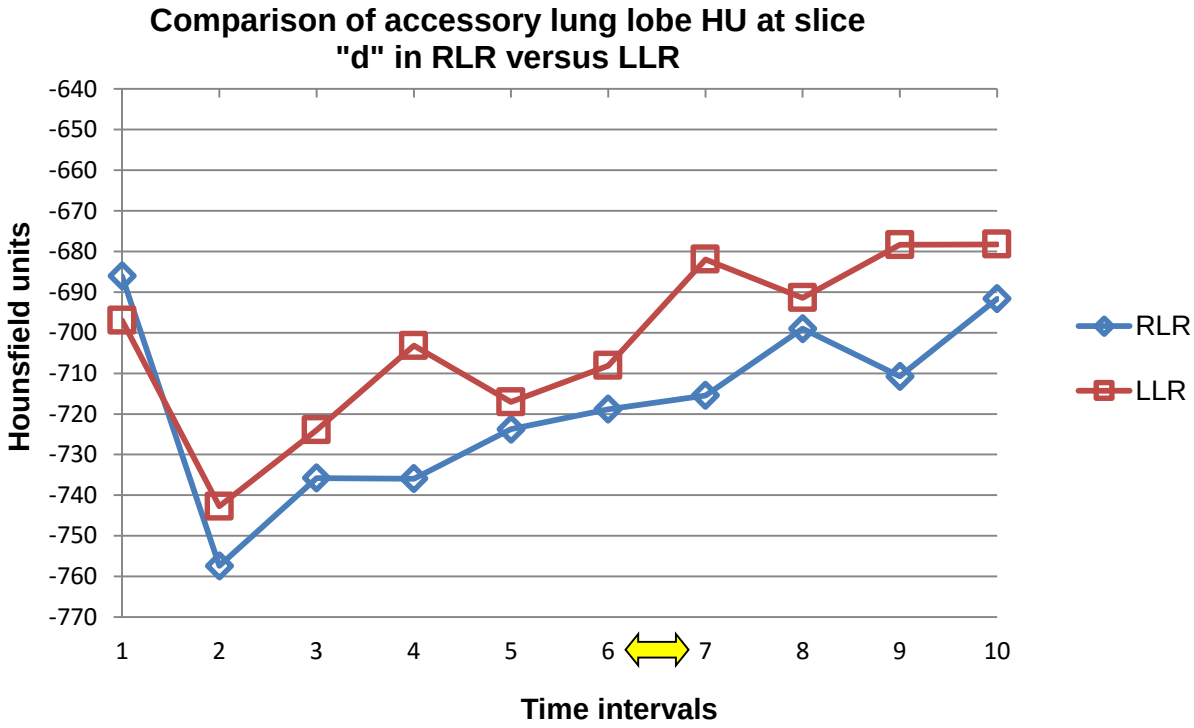

FIG. 41: Line graph depicting the median HU values (y-axis) for the accessory lobe at slice “d”, in LLR and RLR for all 6 dogs. Note the corresponding parallel appearance of the plots, indicating that recumbent side did not affect HU values. In both recumbencies, there was a decrease in HU with placement in lateral recumbency, which subsequently gradually increased over the remainder of the study. Time intervals are depicted on the x-axis, see Fig. 24 for explanation.

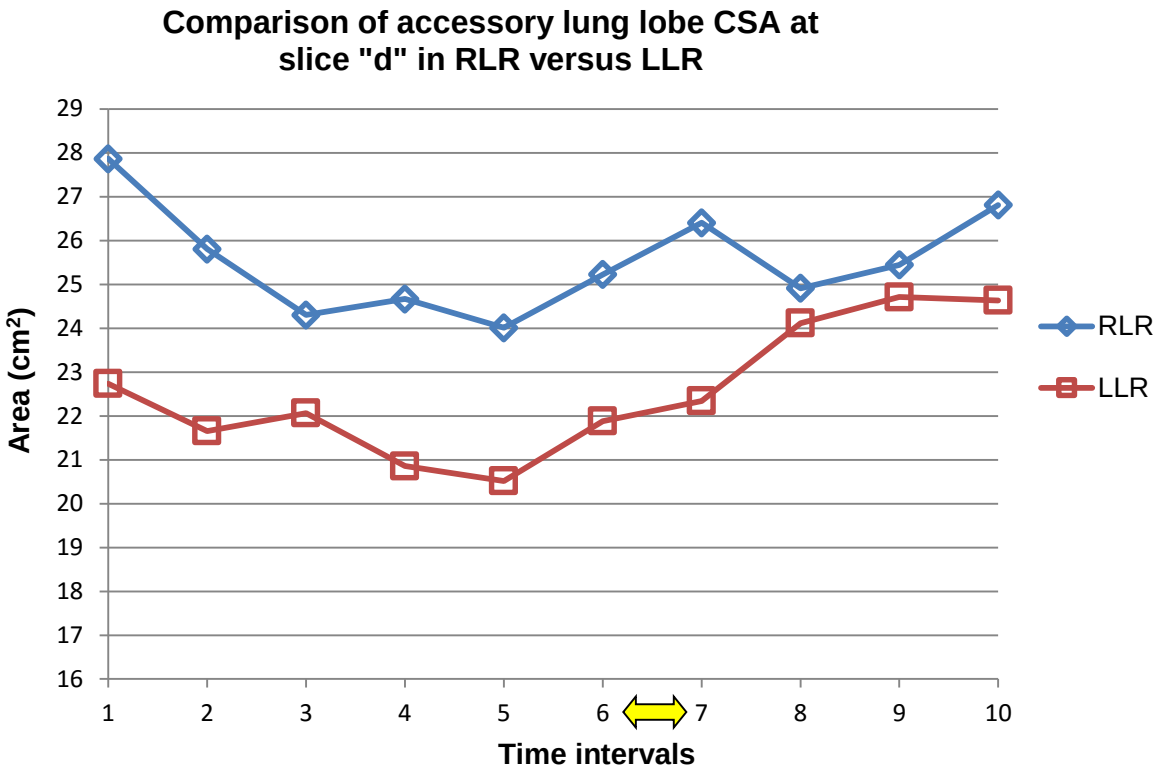

FIG. 42. Line graph depicting the median CSA values in cm^2 (y-axis) for the right middle lobe at slice "c", in LLR and RLR for all 6 dogs. Again, both RLR and LLR plots are parallel, and do not correlate with the HU plots. With placement in lateral recumbency the accessory lobe CSA decreased up to approximately RLR_{20}/LLR_{20}, before gradually increasing again over the rest of the study. Time intervals are depicted on the x-axis, see Fig. 24 for explanation.

RLR:

The baseline measured HU range of all six dogs was often below normal respiratory range (-651 to -753).

There was a decrease in HU with placement in RLR as expected, and during RLR this value steadily increased, similarly when replaced and sternal recumbency and during sternal recumbency.

The CSA values showed an unrelated decrease with placement in RLR, however during RLR and after repositioning in sternal recumbency demonstrated no obvious pattern despite the CSA moderately increasing again. When the CSA measurements were plotted initially for the 6 dogs individually, the graphs had a haphazard appearance.

The HU and CSA graphs correlated poorly, but the HU graph correlated very well with the individual plots of the six dogs, however for CSA there was a wide range of values between the six individual dogs.

Statistically, there was a significant effect of time on measured HU during RLR (P<0.001), however not during sternal recumbency (P=0.528).

For CSA, there was not a significant effect of time in lateral recumbency (P=0.166) nor in sternal recumbency (P=0.753).

LLR:

The baseline measured HU range of all six dogs was often below normal respiratory range (-676 to -742).

The HU measurements paralleled the findings in RLR, however were moderately increased at each time interval.

The CSA measurements behaved similarly to when in RLR, however the actual values in cm^2 were mild to moderately smaller at each time interval. Also as for the findings in RLR, when the CSA measurements were plotted initially for the 6 dogs individually, the graph had a haphazard appearance. As for RLR, the six individual HU plots in LLR correlated well with the combined median plot.

Statistically, there was a significant effect of time (P=0.022) measured HU during LLR, however time was not significant during sternal recumbency (P=0.231).

For CSA, there was not a significant effect of time in lateral recumbency (P=0.174) nor during sternal recumbency (P=0.791).

Left caudal lobe (Figs. 43 and 44)

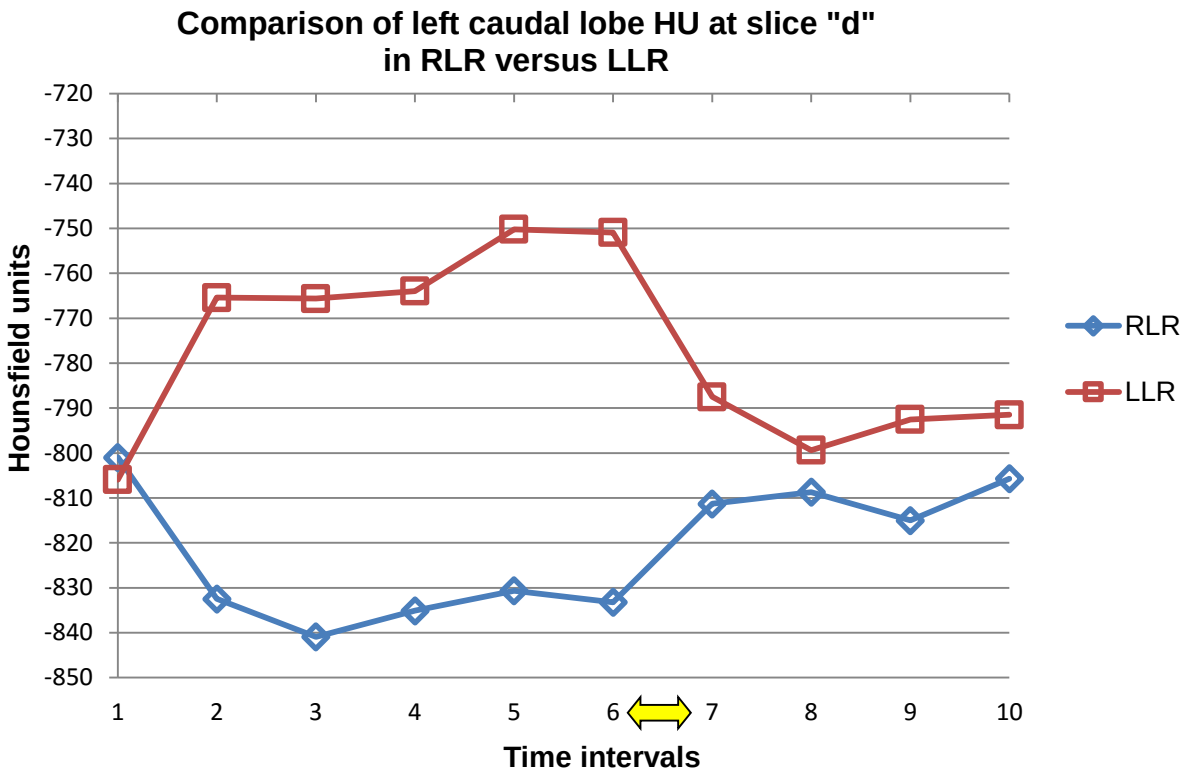

FIG. 43. Line graph depicting the median HU values (y-axis) for the left caudal lobe at slice “d”, in LLR and RLR for all 6 dogs. Note the typical expected appearance of the plots, as explained in Fig. 36. Time intervals are depicted on the x-axis, see Fig. 24 for explanation.

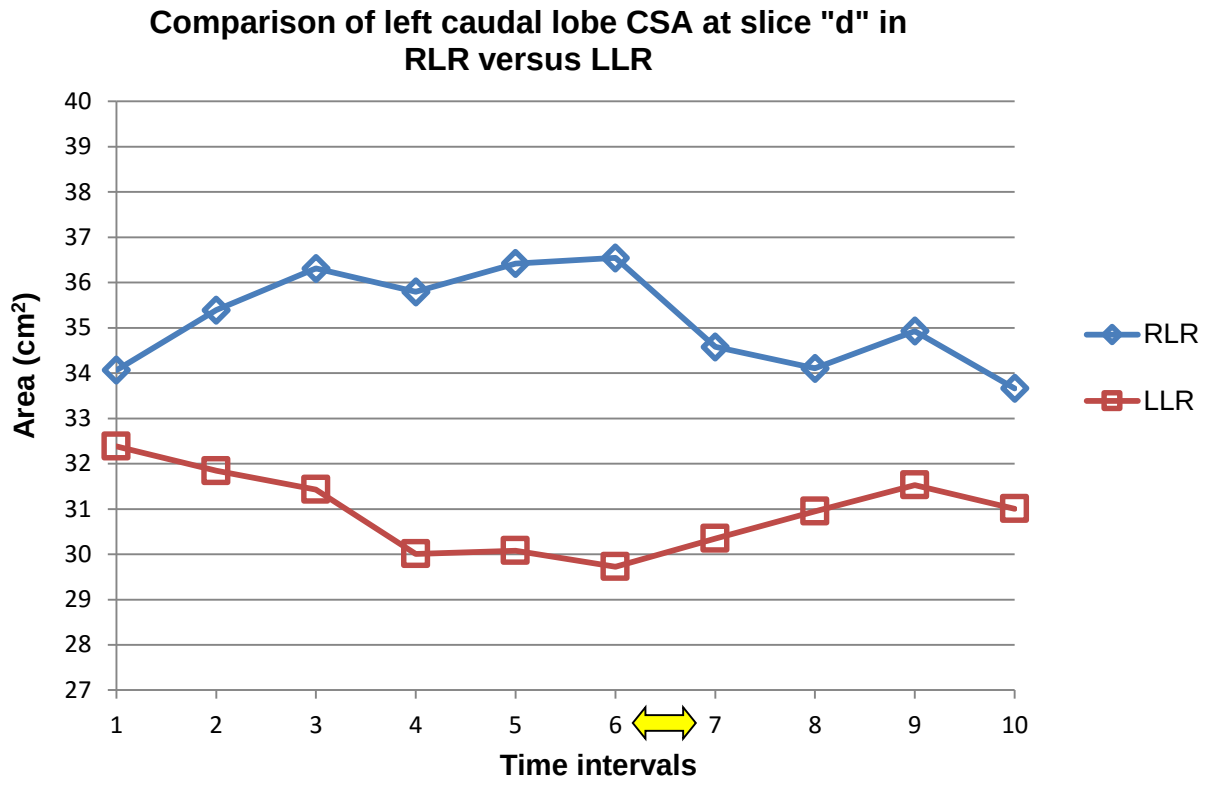

FIG. 44. Line graph depicting the median CSA values in cm^2 (y-axis) for the left caudal lobe at slice "d", in LLR and RLR for all 6 dogs. Note the typical expected appearance of the plots, as explained in Fig. 37. Time intervals are depicted on the x-axis, see Fig. 24 for explanation.

RLR:

The baseline HU range of all six dogs was within normal respiratory limits.

The lung demonstrated behavior as expected, with a decrease in HU and concomitant increased CSA when placed in RLR and during RLR, and an increase in HU and decrease in CSA and when replaced in sternal recumbency and during sternal recumbency.

The HU and CSA graphs correlated well, and correlated well if compared to the six individual dogs' plots.

Statistically, there was a significant effect of time on measured HU during RLR (P<0.001), but not during sternal recumbency (P=0.134).

For CSA, there was a significant effect of lung lobe portion (P<0.001) and time (P=0.001) in lateral recumbency. For sternal recumbency, there was an effect of lung portion (P<0.001) but not for time (P=0.911).

LLR:

The baseline HU range of all six dogs was within normal respiratory limits.

There was an increase in HU and concomitant decrease in CSA with placement in LLR, which continued to mildly increase and decrease respectively during LLR.

Return to sternal recumbency saw an expected decrease in HU and increase in CSA. During sternal recumbency there was mild fluctuation of both values.

The HU and CSA graphs correlated well, and correlated well if compared to the six individual dogs' plots.

Dog 1 at time S_{10} had an outlying value of -644 (single increased value) with a corresponding decrease in CSA to 22.2 cm^2 (at S_i this value was approximately 30.5 cm^2). There were also consistently increased HU values from LLR_{13} onwards (as noted above), with correspondingly decreased CSA values, compared with the other dogs. These changes were noted on the initial image assessments as mild patchy peripheral increased attenuation of the middle (mild) and ventral thirds of the lung (see Fig. 45). A change in CSA was not easily visualised.

Statistically, there was a significant effect of time (P<0.001) on measured HU during LLR. Time during sternal recumbency however was not significant (P=0.484).

For CSA, there was a significant effect of time (P=0.003) during lateral recumbency, but during sternal recumbency it was not significant (P=0.892).

FIG. 45. Transverse plane image of Dog 1, at LLR_{30}, slice "d", demonstrating patchy increased soft tissue attenuation of the ventral third of the left caudal lobe. The middle third is also mildly affected. Image is in a lung window (WL -600, WW 1200), and the dog's left is to the left of the image.

Right caudal lobe (Figs. 46 and 47)

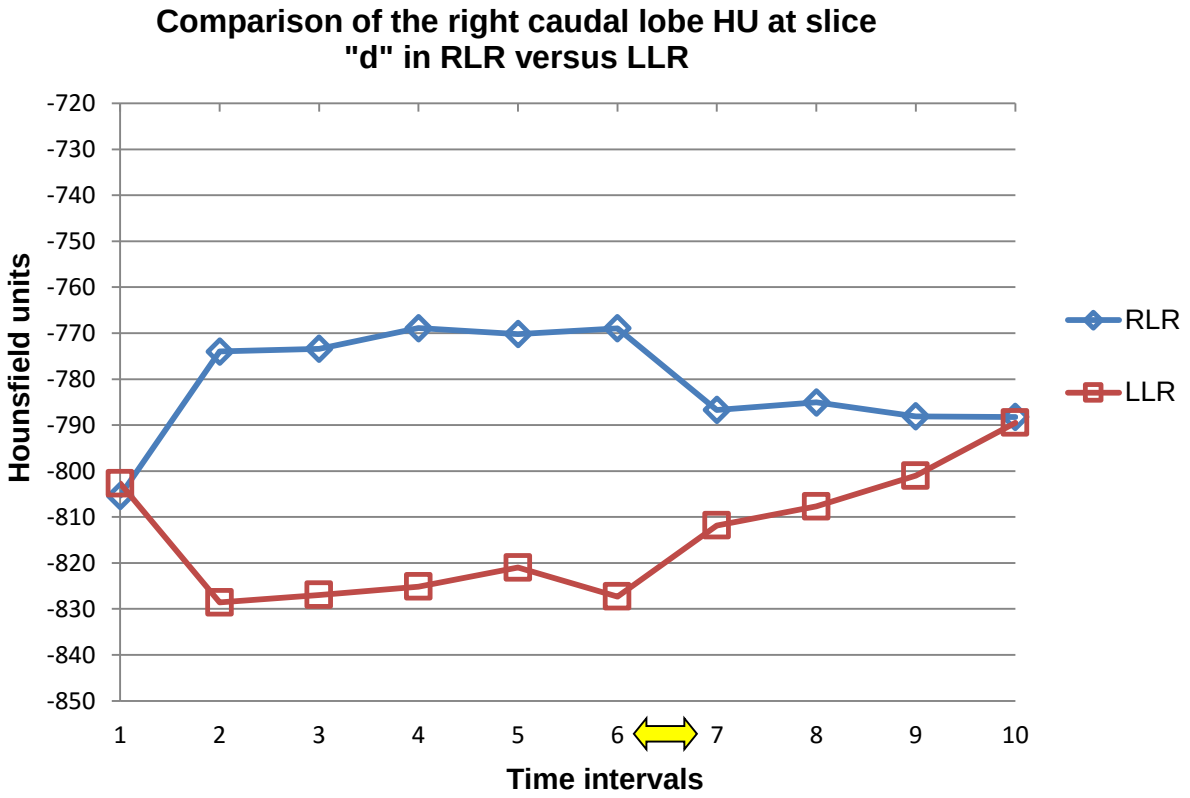

FIG. 46. Line graph depicting the median HU values (y-axis) for the right caudal lobe at slice “d”, in LLR and RLR for all 6 dogs. Note the typical expected appearance of the plots, as explained in Fig. 36. Time intervals are depicted on the x-axis, see Fig. 24 for explanation.

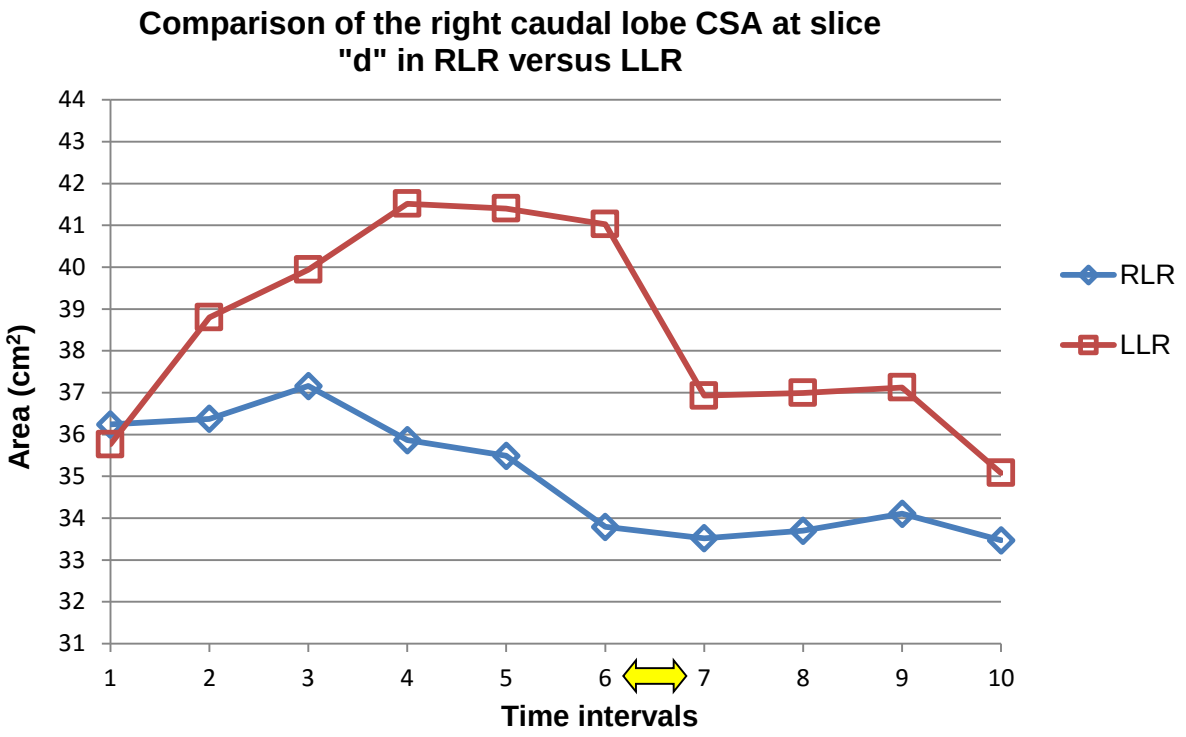

FIG. 47. Line graph depicting the median CSA values in cm^2 (y-axis) for the right caudal lobe at slice "d", in LLR and RLR for all 6 dogs. Note the typical expected appearance of the LLR plot, as explained in Fig. 37. The RLR plot had an increase in CSA initially with values only decreasing from RLR_8 onwards, which did not correspond to the HU findings. Subsequent to this there was good correlation between the graphs. Time intervals are depicted on the x-axis, see Fig. 24 for explanation.

RLR:

The baseline HU range of all six dogs was within normal respiratory limits.

When placed in RLR, there was an expected increase in HU however the CSA values demonstrated an unrelated mild increase.

During RLR, the HU values behaved as expected for a dependent lobe, and the CSA values continued to increase slightly and demonstrated an expected decrease with repositioning in sternal recumbency, with little variation during sternal recumbency. With time in RLR and sternal recumbency, the CSA values continued to decrease as expected however did not increase again in sternal recumbency.

The CSA graph showed a wide range in values when the individual dogs were plotted separately, compared to the combined median graph.

Statistically, there was a significant effect of time on measured HU during RLR (P<0.001), however time became non-significant during sternal recumbency (P=0.715).

For CSA, there was a not a significant effect of time (*P*=0.585) during lateral recumbency, which was similar during sternal recumbency (*P*=0.785).

LLR:

The baseline HU range of all six dogs was within normal respiratory limits.

With placement in LLR, the HU showed a decrease and the CSA values a concomitant increase, as expected.

During LLR, the HU values remained decreased and the CSA values continued to increase mildly.

With repositioning in sternal recumbency, there was a concomitant increase in HU and decrease in CSA values.

The CSA graph again showed a wide range in values when the individual dogs were plotted separately, however the individual HU plots and the combined median HU correlated well.

Statistically, there was a significant effect of time on measured HU during left lateral (*P*<0.001) and sternal recumbency (*P*=0.012).

For CSA, there was a significant effect of time during LLR (*P*<0.001), but not during sternal recumbency (*P*=0.645).

4.3.5.8 Findings on slice “e”

Left caudal lobe (Figs. 48 and 49)

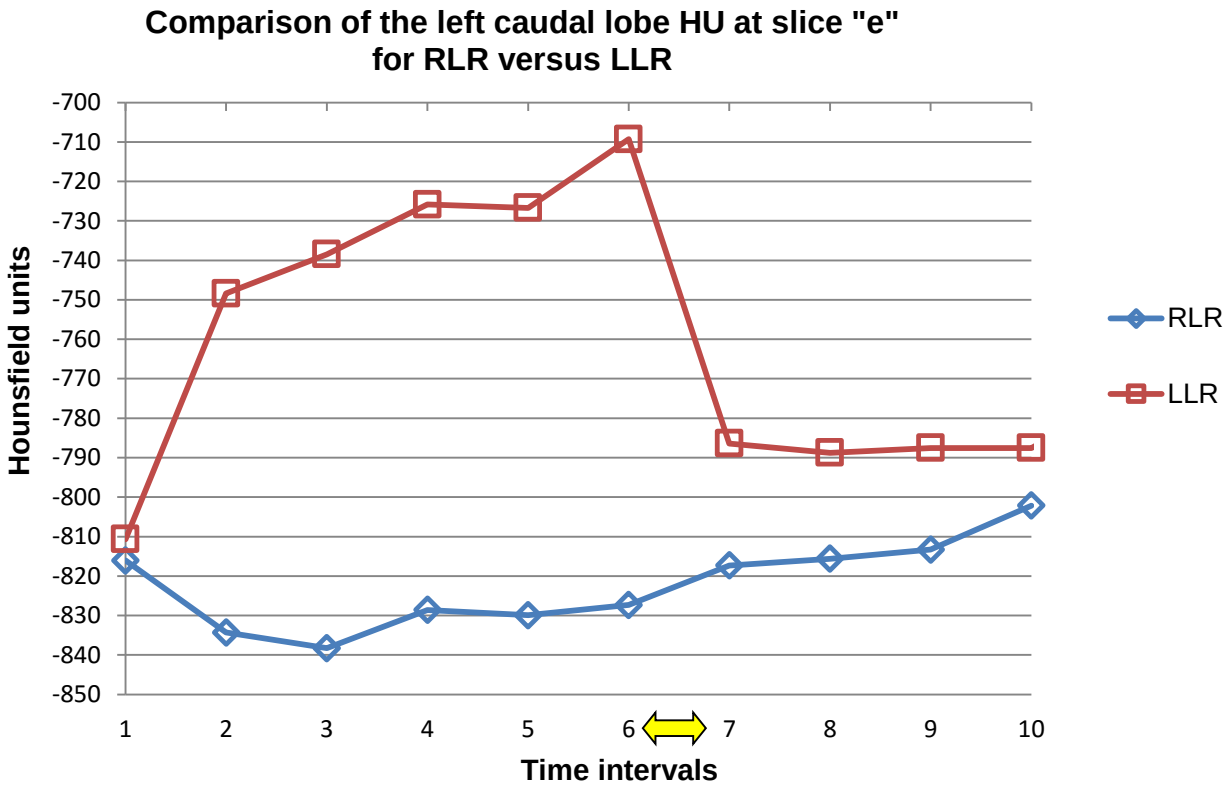

FIG. 48. Line graph depicting the median HU values (y-axis) for the left caudal lobe at slice “e”, in LLR and RLR for all 6 dogs. Note the typical expected appearance of the plots (LLR more so than RLR), as explained in Fig. 36. Time intervals are depicted on the x-axis, see Fig. 24 for explanation.

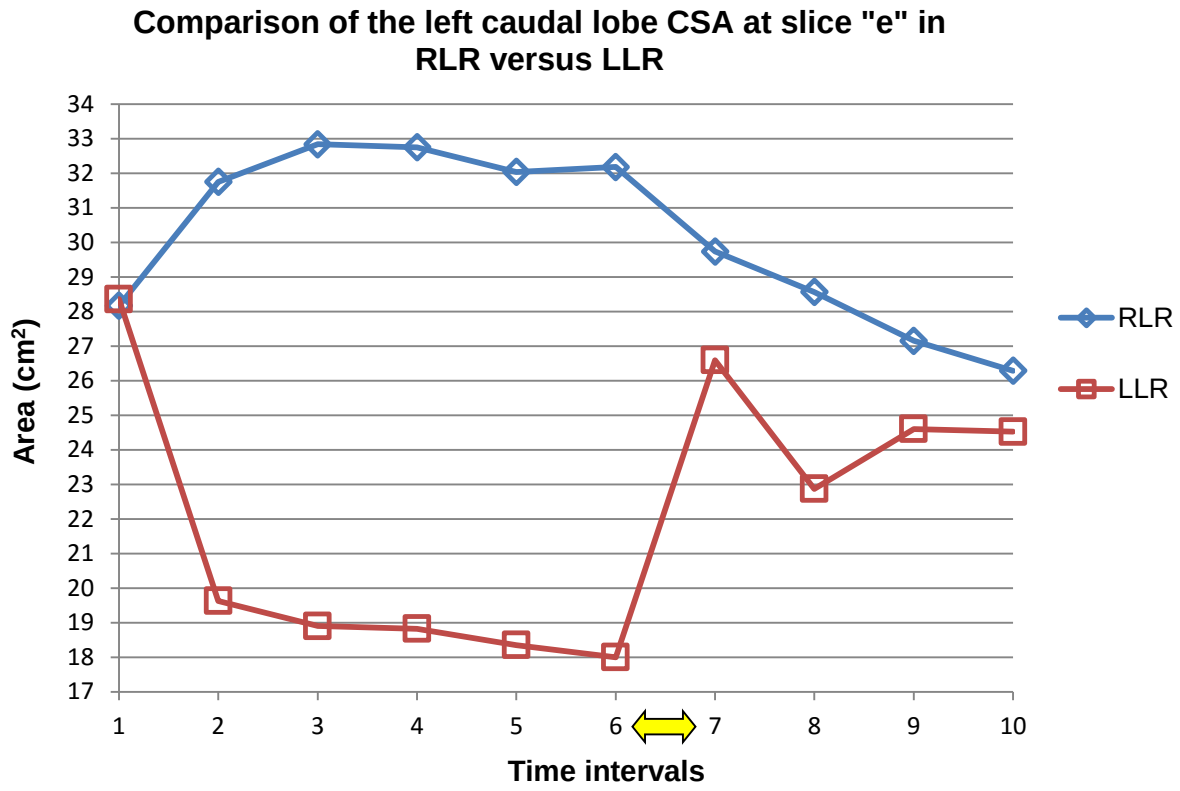

FIG. 49. Line graph depicting the median CSA values in cm^2 (y-axis) for the left caudal lobe at slice "e", in LLR and RLR for all 6 dogs. Note the typical expected appearance of the plots, as explained in Fig. 37. Time intervals are depicted on the x-axis, see Fig. 24 for explanation.

RLR:

The baseline HU range of all six dogs was within normal respiratory limits.

There was minimal HU fluctuation across the study; however mild decrease in HU did occur when placed in RLR. The CSA measurements showed a more marked concomitant increase with placement in and during RLR.

With repositioning in sternal recumbency, there was a subtle increase in HU and mode obvious concomitant decrease in CSA, which continued to decrease mildly during sternal recumbency.

There was a wide range of CSA measurements for this lobe between the 6 dogs, however the individual plots behaved similarly over time and had the same shape. The individual HU and combined median HU plots correlated well.

Statistically, there was a significant effect of time on measured HU during RLR (P<0.001), and during sternal recumbency (P=0.013).

For CSA, there was a significant effect of time in lateral recumbency (P<0.001) and during sternal recumbency (P<0.001).

LLR:

The baseline HU range of all six dogs was within normal respiratory limits.

With placement in LLR, there was an expected increase in HU and concomitant decrease in CSA, which persisted during LLR.

When repositioned in sternal recumbency, the HU again decreased with a concomitant increase in CSA.

When compared to the six individual plots on the HU and CSA graphs, there was good correlation with the median graphs but there was a reasonably wide range of CSA values between dogs.

Statistically, there was a significant effect of time on measured HU during LLR (P<0.001), however not when replaced in and during sternal recumbency (P=0.427).

For CSA, there was a significant effect of time in lateral recumbency (P<0.001) however not during sternal recumbency (P=0.986).

Right caudal lobe (Figs. 50 and 51)

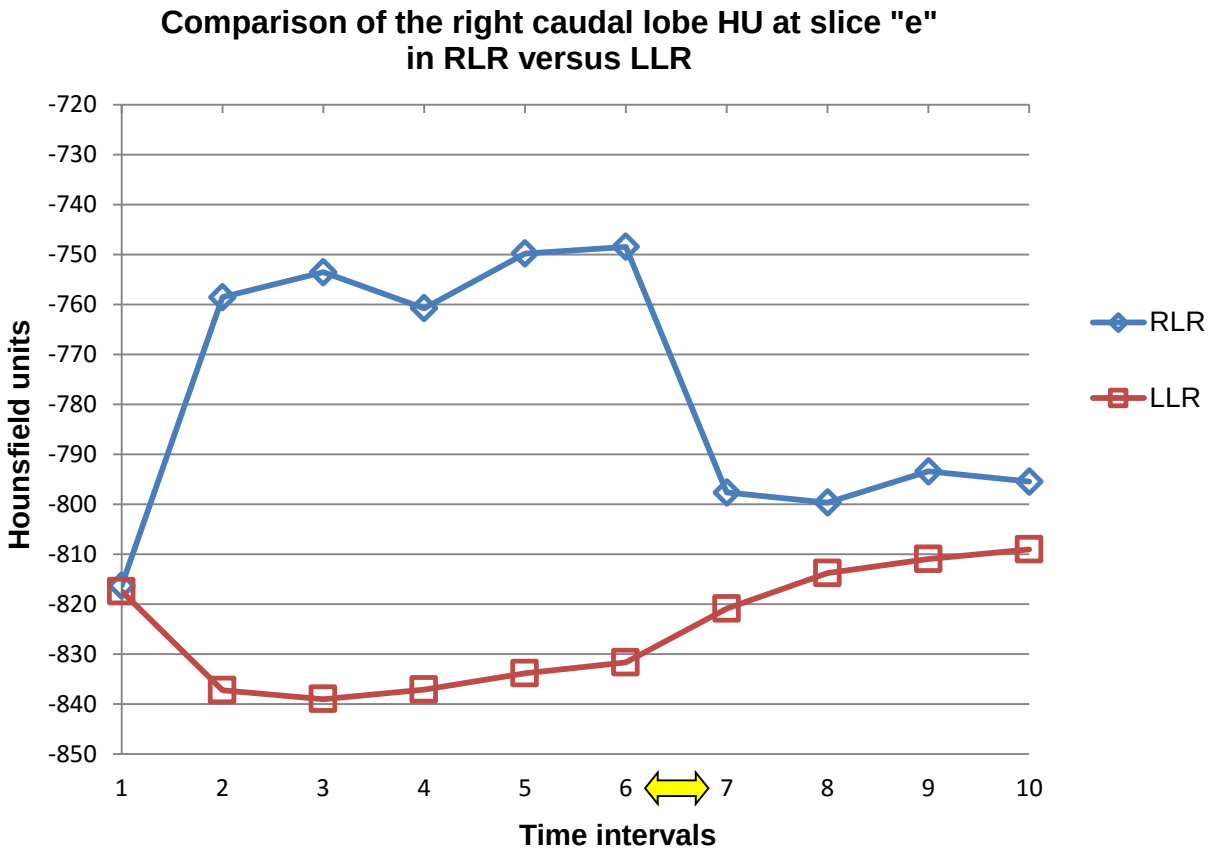

FIG. 50. Line graph depicting the median HU values (y-axis) for the right caudal lobe at slice “e”, in LLR and RLR for all 6 dogs. Note the typical expected appearance of the plots, as explained in Fig. 36. Time intervals are depicted on the x-axis, see Fig. 24 for explanation.

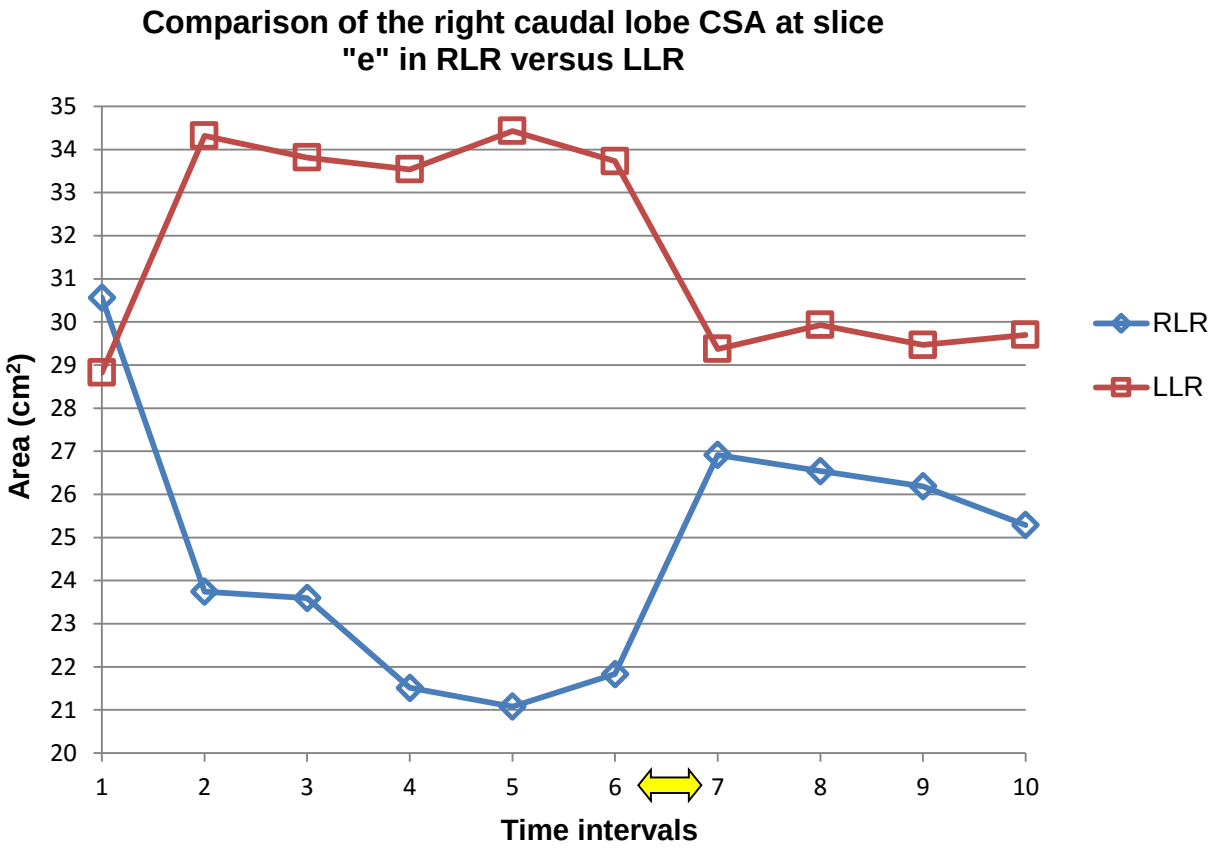

FIG. 51. Line graph depicting the median CSA values in cm^2 (y-axis) for the right caudal lobe at slice "e", in LLR and RLR for all 6 dogs. Note the typical expected appearance of the plots, as explained in Fig. 37. Time intervals are depicted on the x-axis, see Fig. 24 for explanation.

RLR:

The baseline HU range of all six dogs was within normal respiratory limits.

With placement in RLR and during RLR, there was an expected increase in HU and concomitant decrease in CSA.

With repositioning in sternal recumbency, the HU decreased and the CSA increased again, as expected, both with little fluctuation during sternal recumbency.

Dog 6 showed the highest HU value at RLR_{30}, of -688. This was noted on initial image evaluation as patchy soft tissue attenuation within the periphery of the lobe at RLR_{30} (and not present at S_i), along the ventral and middle thirds of the lobe (see Fig. 52). The CSA value was correspondingly small. The soft tissue attenuation was mild at LLR_{20} (not noted initially) and by S_e had mildly improved, but not resolved by S_{20}. However, this was the dog which was starved for the shortest amount of time and thus deemed inadequately starved. The possible/speculative significance of this is discussed later.

FIG. 52**.** Transverse image of Dog 6, $RLR_{20,}$ at slice “e”, demonstrating mild patchy increased soft tissue attenuating of the right caudal lobe along its middle and ventral third subpleural margins. Image is in a soft tissue window (WL -600, WW 1200). The dog’s left is to the left of the image and the image acquired with the dog in RLR.

There was good correlation with the median HU graph when compared to the six individual HU plots, however there was a wider range of CSA values between the dogs when individually assessed, compared the median CSA graph.

Statistically, there was a significant effect of time on measured HU during RLR (P<0.001), however not during sternal recumbency (P=0.799).

For CSA, there was a significant effect of time during lateral recumbency (P<0.001) however not during sternal recumbency (P=0.252).

LLR:

The baseline HU range of all six dogs was within normal respiratory limits.

With placement in LLR, there was an expected decrease in HU and concomitant increase in CSA, which persisted during LLR.

With repositioning in sternal recumbency, there was an increase in HU and decrease in CSA as expected, with little fluctuation of either during sternal recumbency.

The median HU and CSA graphs correlated well with the individual dogs' plots.
Statistically, there was a significant effect of time on measured HU during LLR (P<0.001), however not during sternal recumbency (P=0.251).
For CSA, there was a significant effect of time during lateral recumbency (P=0.002), however not during sternal recumbency (P=0.298).

4.3.5.9 Summary of findings in dogs with visual attenuation changes

Below are additional more detailed descriptions of the lobes that were visually detected to be affected, with assessment of the whole lobe done initially, and subsequently assessment of the dorsal, middle and ventral thirds.

Dog 1, left cranial *pars cranialis* (slice b), in LLR (refer to Fig. 32)
The largest decrease in CSA for the whole lung (50%) occurred at $LLR_{30,}$ with a corresponding HU of -624 at this time, which was also the lowest HU for the whole lobe over the study.
The ventral lobe contributed the most to the decrease in CSA (67% - implies the ventral lobe itself decreased by 67%, not that it contributed 67% to the overall decrease) and had a corresponding HU of -525; both also occurred at LLR_{30}.
The highest HU measured during the entire study was of the ventral lobe (-411) at S_5.
The highest measured HU (circular ROI) within the ventral lobe, drawn in the most severe (visually) affected region, was -432.

Dog 1, left cranial *pars caudalis* (slice c), in LLR (refer to Fig. 38)
The largest decrease in CSA for the whole lung (39%) occurred at LLR_{30}, which had one of the highest HU (–656).
The ventral lobe was the largest contributor (56%) to the CSA decrease, and had the corresponding lowest HU (-391) for the whole study; both also occurred at LLR_{30}. The highest measured HU (circular ROI) in the ventral lobe, drawn in the most severe (visually) affected region, was -289.

Dog 1, left caudal lobe (slice d) in LLR (refer to Fig. 45)

The largest decrease in CSA for the whole lung (24%) occurred at LLR_{13}, and the second lowest HU occurred concurrently (-696 versus -690 at LLR_{30}, which is an insignificant difference).

The largest contributor to the decreased CSA was the dorsal lobe, however the ventral lobe still demonstrated the highest HU.

The highest measured HU (circular ROI) in the ventral lobe, drawn in the most severe (visually) affected region, was -449.

Dog 2, left cranial *pars cranialis* (slice b), in LLR (refer to Fig. 33)

The largest decrease in CSA for the whole lung (48%) and concomitant highest HU measurement (-560), occurred at LLR_{13}.

The highest HU (-510) for the study was in the ventral third of the lobe at LLR_{30}. At LLR_{30}, the ventral lobe also contributed the most to the decrease in overall CSA (65%).

The highest measured HU (circular ROI) in the ventral lobe, drawn in the most severe (visually) affected region, was -439.

Dog 2, left cranial lobe *pars caudalis* (slice c), in LLR

The largest decrease in CSA for the whole lung (53%) and concomitant highest HU (-632) occurred at LLR_{13}.

The dorsal third of the lobe contributed the most to the decrease in CSA (60%) also at LLR_{13}. However, the highest HU recorded in this lobe at this slice was for the ventral third at LLR_{13} (-529).

The highest measured HU (circular ROI) in the ventral lobe, drawn in the most severe (visually) affected region, was -470.

Dog 4, left cranial lobe *pars caudalis* (slice c), in LLR

The largest decrease in CSA for the whole lung (20%) and concomitant highest HU (-695) occurred at LLR_{30}.

The ventral third of the lobe contributed the most to the decrease in CSA (42%) at LLR_{30}, and also had the highest HU (-502).

The highest measured HU (circular ROI) in the ventral lobe, drawn in the most severe (visually) affected region, was -449.

Dog 5, left cranial lobe *pars caudalis*, (slice c) in LLR (Fig. 53)

The largest decrease in CSA for the whole lung (32%) occurred at LLR_{20}, but the CSA at LLR_{30} was very similar. At LLR_{20}, the highest concomitant HU also occurred (-713). The ventral third of the lobe showed the largest decrease in CSA (41%) at LLR_{30}, and highest HU of -654.

The highest measured HU (circular ROI) in the ventral lobe, drawn in the most severe (visually) affected region was -300.

FIG. 53. Transverse plane image of Dog 5, LLR_{20}, at slice "c", demonstrating a very mild diffuse increased attenuation of the ventral left cranial *pars caudalis* lobe. The changes are more noticeable when compared to the right middle lobe. The image is in a lung window (WL -600, WW 1200) and the dog's left is to the left of the image.

Dog 6, Right caudal lobe (slice e), in LLR (Fig. 52)

This dog was the only one that showed right lobe involvement. This was also the dog that was starved for the shortest length of time.

The largest decrease in CSA for the whole lung occurred at RLR_{20}, and the highest HU occurred at RLR_{30} – however there was very little difference between HU between these 2 time intervals.

The ventral third of the lobe was responsible for the greatest decrease in CSA (70%), also at LLR_{20}, however, the highest HU (-615) was measured in the middle third of the lobe, at RLR_{30}.

The highest measured HU (circular ROI), drawn in the middle third of the lobe peripherally and subpleurally (the most severe (visually) affected region), was -487.

4.3.5.10 Summary of results for all lungs lobes

The range of baseline HU (S_i) for all lobes at all slices, excluding the accessory lobe, ranged from -722 to -877, and fell within normal respiratory range. The accessory lobe range was markedly lower and ranged from -651 to -753.

Despite the sometimes wide variation in CSA measurement over time, the initial baseline (Si) CSA values at each slice for each lobe, taken prior to placement in each lateral recumbency, were largely within close range of each other (<1 cm^2 difference). The largest difference was again for the accessory lobe, with a difference of 2 cm^2.

The initially visible HU changes were only noted in the left lobes in LLR, except for the changes noted for the right caudal lobe in RLR. The left *pars cranialis*, when affected, was the first lobe to show visual attenuation changes by LLR_3 (Dog 2). This was followed by changes seen onwards from LLR_8 (4/7 times; *pars cranialis* in Dog 1, and left *pars caudalis* for Dogs 1, 2 and 5), and LLR_{13} (2/7 times; left *pars caudalis* for Dog 4 and left caudal lobe for Dog 1), and most often involving the ventral third of the lobe. There was only mild visual increase in perceived attenuation throughout lateral recumbency, with mild resolution when replaced in sternal recumbency. However there was never full resolution of the patchy increase HU, and in all cases was still noted at S_{20}. Of the affected left lobes, the left cranial lobe *pars caudalis* was most commonly affected (4/7 times), followed by the *pars cranialis* (2/7 times). The left caudal lobe was affected only once.

The most marked increases in HU were apparent on measured HU values by LLR_{13} (3/7 lobes; left *pars caudalis* in Dog 1 and 2, left *pars cranialis* in Dog 2), LLR_{30} (3/7 lobes; left *pars caudalis* Dog 1 and 4, and left caudal lobe for Dog 1), and LLR_{20} (1/7; left *pars caudalis* for Dog 1). The highest HU for any lobe third in the study was -391 (ventral third of the left *pars caudalis* lobe in Dog 1) at LLR_{30}, and highest value for the small circular ROI placed at the highest visible increased attenuation was -289 (same dog, placed in the ventral third of the left *pars caudalis*), also at LLR_{30}. None of the

measured values corresponded to the accepted criteria for atelectasis, and thus these lungs could only be referred to as “poorly ventilated”.

The decrease in cross-sectional area measurements ranged from a 20-53% decrease. The smallest cross-sectional area at any point in each dog always shared the highest HU value. The ventral third lobe usually contributed most to decreased cross-sectional area of the total lobe (5/7 times; left *pars cranialis* in Dogs 1 and 2, left *pars caudalis* in Dogs 1, 4 and 5) followed by the dorsal third (2/7 times; left caudal lobe in Dog 1 and left *pars caudalis* Dog 2).

Measured HU values at S_{20} in 5/7 lobes (Left *pars cranialis* for Dogs 1 and 2, left *pars caudalis* for Dogs 1, 2 and 5) remained higher than normal respiratory values. Thus in this study, the lungs did not return to their baseline S_i aeration. Statistical analysis supported this descriptive finding.

The most consistent significant statistical association was for time with HU and CSA in lateral recumbency, however in sternal recumbency these associations were not significant in the majority of lobes.

Chapter 5: Discussion

Computed tomography studies were conducted in healthy adult Beagle dogs, using changes in body position to determine the effects of lateral recumbency on the development of atelectasis and the effects of sternal recumbency on resolution of atelectasis. A standardized anaesthetic protocol was used.

5.1 General thoracic assessment and anatomical findings

As assessment of the images and data capture progressed after the study, certain factors which may have influenced the way measurements were done, and the repeatability of the measurements, were discovered. The most significant factor in this study was believed to be the unavoidable shift in the location of the five boxes that occurred when the dog was moved from lateral to sternal recumbency. It was believed that the most accurate comparisons could only be done within time intervals that fell within the first phase of the study (S_i to S_e) or during the second phase of the study (S_e to S_{20}), as the location of the five boxes were not changed for the duration of each phase.

Several thoracic structures were studied in order to explain the tracheal and aortic roots shift detected on measurements performed on the images. These structures included the pericardiophrenic ligament, heart, trachea, mediastinum and diaphragm.

There are no references pertaining to visualisation of the pericardiophrenic ligament in diagnostic imaging to the best of the author's knowledge. In this study, a fine soft tissue attenuating band of tissue was seen in some of the studies, extending on the thoracic midline from the caudoventral cardiac silhouette margin to the diaphragm. It appeared to be immediately dorsal to the thoracic floor, as opposed to lying on the floor, and was identified separately to the caudoventral mediastinal fold, which was associated with the slightly left-sided cardiac apex. This ligament was not easy to identify in most dogs as it was very small, and when the caudal cardiac silhouette was in contact with the diaphragm (as would occur in some normal dogs) it was obscured. It was best visualised when there was fat adjacent to it and often a fair degree of windowing was needed to be applied to the images to visualise it. The

presence of this soft tissue band could not be attributed to any other known thoracic structure (e.g. blood vessels), and is thus believed to be the pericardiophrenic ligament. Unfortunately, this could not be confirmed as no post mortem studies were conducted. Because the ligament could not be visualised in all the dogs in this study, its function within the thorax could not be determined.

When placed in lateral recumbency, the cardiac silhouette (at the level of the aortic root) shifted towards the dependent side, away from its ventral midline position (normally at a 5:30 to 6:00 location, using a clock face analogy). The canine heart has been found to be more mobile than the human heart[11] and thus these findings were perhaps not surprising. It is not certain to what degree nor in which direction the pericardiophrenic ligament can restrict cardiac motion,[53] but it is believed from this study that it is only gross motion that is affected. In LLR, the cardiac silhouette was located towards the left (from 6 to 8 o'clock, with left to the left of the image on TRA) and when in RLR, was located towards the right (from 4 to 6 o'clock). The shift that occurred to either side was of equal magnitude, and thus recumbent side did not appear play a role.

However, when comparing the cardiac apex/ventral mediastinum, there appeared to be a mild asymmetrical shift between LLR and RLR. The cardiac apex normally is positioned slightly to the left of the midline.[52] In LLR, the cardiac apex/ventral mediastinum made contact with the left ventro-lateral thoracic wall (7 o'clock, using the same clock face analogy). However when in RLR, the cardiac apex either appeared in its normal position, or displaced only mildly towards the right into a midline position (6 o'clock), and the cardiac silhouette did not make contact with the right ventro-lateral thoracic wall. The degree of displacement towards the left appeared in excess of what could be contributed to the normal resting left-sided position of the apex. Proposed "checking" of cardiac apex movement by the pericardiophrenic ligament when in RLR has been mentioned briefly in the literature,[47] however at that time the ligament and the caudoventral mediastinal fold were identified as the same structure. Thus whether the apparent restriction of rightwards motion in RLR was due to the caudoventral mediastinal fold, the pericardiophrenic ligament or other cardiac-associated structures (e.g. CVC), could not be determined. The effect of left versus right cardiac ventricular wall thickness and pliability may also play a role in cardiac displacement, but this was not investigated. The effect of mild rotation of the heart in dependency, due to the apex shift, was also not investigated.

There were certain observations made when dogs were in RLR, which were not noted when in LLR. When placed in RLR, the total thoracic width decreased mildly as expected due to change in body position. The distance from the left parietal pleural margin to the centre of the trachea (as done in all measurements) also decreased, but to a greater degree than the total thoracic width. An example can be used to illustrate this fact. If the total thoracic width in sternal recumbency was 10 cm, and the distance from the centre of the trachea to the parietal pleural margin was 6 cm, a ratio of 0.6 would indicate a right-sided position of trachea, as is consistent with its normal position. With placement in RLR, the approximate decrease of 5% in total thoracic width and the decrease in 20% of trachea to left parietal pleural margin would result in measured values of 9.5 cm and 4.8 cm respectively. This gives a ratio of 0.5, which indicates that the trachea has shifted towards the left and is now located on the midline. This resultant decreased ratio (which was the method use to determine tracheal shift) thus indicated a leftwards shift despite being in RLR.

The findings above could not be consistently found for measurements done in LLR. The distance from the left parietal pleural margin to the centre of the trachea was more inconsistent and was increased, decreased or unchanged to variable degrees compared to the change in thoracic width. This is believed to be due the greater mobility of the cardiac apex in LLR, which may have resultant in less consistent results. Further causes remain obscure at this stage.

When the width of the dorsal mediastinum in the region of the cardiac base was assessed, it was found to decrease by variable degrees when the dogs were lying in RLR or LLR compared to the width when in sternal recumbency. This was believed to the due to mild tension on the mediastinum due to the relative dorsoventral elongation of the thorax when in lateral recumbency, and from the heart's apex shifting dependently. This was not further assessed for magnitude of decrease in RLR versus LLR.

Overall, the general thoracic changes that were noted during altered positioning appear complex and multi-factorial and needed to be taken into account during image and data analysis. Nevertheless, they were subtle findings and were unlikely to be of clinical significance.

5.2 Trachea

The subtle changes in tracheal position with change in recumbency were believed to be due to changes in the position of the apex of the heart, and although were likely to be true findings, were not as result of mediastinal shift secondary to atelectasis or decreased lung aeration. The trachea appeared to shift more prominently when in RLR, versus in LLR where the shift was very mild. It was believed that as the cardiac apex moved dependently, it caused a resultant mild opposite displacement of the cardiac base, which is relatively more fixed, with similar displacement of the trachea. This resulted in the apparent shift of the trachea away from the dependent side. Hence when in RLR, the trachea appeared to shift leftwards and when in LLR, appeared to shift rightwards.

Additionally, when in lateral recumbency with an unsupported natural head position, the trachea enters the thoracic inlet with a gentle curve away from the recumbency the dog was in (e.g. LLR the trachea curves mildly towards the right to enter the thorax). This was more pronounced for LLR, and in RLR the trachea was often only subtly curved. This was believed to be due to neck position, but also due to the greater leftwards cardiac apex shift when in LLR (as above).

In RLR, there was less rightwards motion of the heart resulting in less curvature of the trachea as it enters the thorax, and thus less leftwards displacement of the trachea would have been expected. However in RLR, there was a greater degree of shift compared to LLR. This was believed to be due to the thoracic changes (and example given) as discussed (under 5.1), which resulted in a greater perceived left-sided shift. However, upon careful thoracic evaluation a cause for this greater perceived shift could not be elucidated.

In LLR, there was more pronounced leftwards cardiac motion, with a resultant more rightwards curved entry of the trachea into the thorax. However, tracheal shift towards the right was of lesser magnitude than could be explained by these findings. It is believed that there likely is a limit on the degree of right lateral movement that can occur, as the trachea already is located towards the right of the midline. The greater variation in thoracic cage changes that occurred in LLR (see 5.1), may also contribute to this findings of this decreased degree of shift.

Overall, the tracheal positional changes were small, not easily visualised on images, and thus considered overall insignificant.

The large degree of overlap between the subjective assessment (i.e. position of the trachea, or to either side of the midline) and the actual measured values was believed to be because the actual measured values fell within a very narrow range which tended to be centred around the midline of the thorax (for example, for the trachea 30% of the measurements ranged from 0.47, i.e. left of the midline, to 0.53, i.e. right of the midline), which may be too small for the human eye to be able to differentiate. Any small variation or inaccuracy in measurement may also have shifted the location of the structure from one side of the thorax to the other, or to the midline. Additionally, as discussed, the thoracic conformation had a different appearance in sternal (wider) versus lateral (narrower) recumbency, which may have caused unconscious differences in subjective evaluation.

The reason why the trachea tended to be more right-sided, from S_e onwards, compared to baseline values after being in RLR, and after LLR tended to more towards the midline than the original baseline values, is uncertain. It is believed to be due to measurement discrepancies between lateral and sternal recumbencies, as already discussed. The possibility of residual decreased aeration in the dependent lobes (and thus decreased area) after lateral recumbency may result in this perceived shift, but this is unclear and could not be visualised subjectively.

5.3 Aortic root

The reasons for the changes in aortic root position with change in recumbency was believed to be due gravity (dependency) and due to changes in the position of the apex of the heart and thus considered insignificant.

In RLR, the aortic root initially shifted unexpectedly towards the left, but then shifted towards the right with time in RLR as would be expected. The reason for the rightwards shift could not be determined.

In LLR, the aortic root behaved as expected for a change in body position, whilst the trachea shifted in the opposite direction (already discussed). The degree of shift towards the left was greater than the degree of shift towards the right in RLR, which supports the findings that the cardiac apex is more mobile in LLR.

The degree of aortic and tracheal shift was similar for LLR, however for RLR the minimal degree of aortic shift could not be correlated to the large degree of tracheal shift. This has been explained already (see 5.2).

It is believed that measurement discrepancies between lateral and sternal recumbencies (as already discussed) also played a role in assessment of aortic root position and that the two time ranges cannot be compared accurately.

5.4 Diaphragm

The point where the crura intersected the ventral vertebral bodies (from caudal T12 to cranial L1) was consistent to what has been described in normal dogs.[47]

The findings of a symmetrical diaphragmatic cupular appearance in a larger proportion of dogs versus slightly cranially displaced right crus, did not correlate entirely with findings reported in radiology.[48] Reasons for this may be due to the level at which the cupula was measured on CT, where there is no superimposition, versus a superimposed image obtained with radiographs. In radiology, the appearance is also due to the divergent nature of the x-ray beam and where in the patient it is centred, which usually for the thorax or abdomen,[47] whilst in CT the beam is collimated narrowly to detectors that are in line with the x-ray source. Mild cupular asymmetry (e.g. <0.25 ICS) or an undulating cupular margin, may have unintentionally affected the way measurements were done and thus the cupula erroneously visualised as being symmetrical. Mild angulation of the dorsal plane reference line on the MPRs was also found to mildly affect the cupular symmetry. The reason for the somewhat contradictory cupular findings was likely due to these factors in combination.

The left diaphragmatic crus was always located in a more cranial position compared to the right. This is in accordance with radiological studies that have shown that the left crus is normally more cranially situation in the standing or sternal recumbent dog.[47] The CT images on which the diaphragm were assessed were obtained in sternal recumbency.

There was no correlation between the cranial locations of the cupula, nor the crura, with gastric filling in the dogs that were starved for a shorter time period than the rest, when in sternal recumbency. This is in accordance with findings by Grandage

(1974), who noted that a food-filled stomach does not selectively push the left crus cranially.

Dorsal displacement of the crura has not been described to the best of the author's knowledge in canines. In this study, the dependent diaphragmatic crus, in addition to cranial displacement, demonstrated a marked dorsal displacement. This was most pronounced when the dogs were in LLR, most likely as result of the stomach located caudally to the left crus. Likewise, when in RLR, the right crus was often only mildly more dorsal than the left one due to the absence of the stomach caudally to it. In Dog 6, which was inadequately starved for the RLR study, both crura were nearly symmetrical dorsoventrally, indicating the ingesta-filled stomach did perhaps push the left crus more dorsally.

Overall, diaphragmatic excursion was not felt to affect tracheal and aortic root position, and findings were not believed to be significant in this study.

5.5 Lungs

5.5.1 Measurement technique

The most significant factor affecting measured HU and CSA values in this study again was believed to be due to shift in the location of the five boxes occurring with dog movement from lateral to sternal recumbency, as already discussed.

On slices "c", "d" and "e", the lungs demonstrated HU and CSA findings that were consistent with what would be expected for a dependent versus non-dependent lobes (i.e. increase in measured HU and concomitant decrease in CSA when dependent, and *vice versa* when non-dependent). No correlation between tracheal and aortic root movement, and lung changes, could be demonstrated.

Slice "a", and rarely slice "b", tended to show more variable and somewhat contradictory results. For slice "a", this was attributed to the small thoracic size at the thoracic cupula, which resulted in much smaller imaged lung regions compared with the caudal slices. The lung borders here were often less well defined due to mediastinal fat, and the intrusion of the *left pars caudalis* into the slice further decreased the size of the left *pars cranialis* lobe. The breath hold technique may also have a more significant effect at slice "a", where a relatively small increase in pressure

could have caused a more significant increase in cranially directed lung excursion, resulting in a “larger” lobe, making measurement easier. This was also believed to have resulted in the atypical left cranial *pars cranialis* lung graphs, which did not behave as expected, because measurement may have been done on different regions of the lung. The thoracic position change between lateral and sternal recumbency, as discussed above, was very likely to result in a greater degree of measurement variation in the most cranial slices, where the lungs rapidly become smaller in a cranial direction. The statistical evaluation for slice “a” for the individual lobes supported these findings and there was never an association between time and measured HU at this level. At slice “b”, the right cranial lobe demonstrated the most inconsistent pattern only at one time point for CSA, and only when in RLR. The reason for this is not clear and was attributed to an error in measurement technique.

Additional less important factors that were believed to affect lung measurements included the following:

1. CSA measurements:

- There was a reasonable likelihood for small differences between measurements to occur due to variation in lung boundaries due to poorly defined borders (for example, the accessory lobe) or human error. The effect of these errors may have contributed to the overall variation in CSA measurements within and between dogs, resulting in some graphs with a wide measured range between individual dogs or lack of obvious pattern.
- It was believed that the smaller CSA measurements (e.g. around only a portion of a lobe, dorsal, middle or ventral thirds) may be more accurate than measuring the whole lobe (owing to more room for error with larger free-hand measurements).
- Measurements done at different locations between dogs and between studies were very likely and could be due to slightly different locations in planning of the boxes (human error), and variation in exact lobe anatomy due to breath-holds (the lung moves relative to the “fixed” vertebral bodies).

2. HU measurements:

- HU and HU standard deviation values were consistent, even with small errors in CSA measurements, and even if the region of interest accidentally included a portion of osseous or soft tissue.
- This statement could be made because in cases where the region of interest was felt to include too much non-lung tissue, it was redrawn and the HU and standard deviation found not to change significantly.

5.5.2 Overall lung findings

The range of baseline HU values was consistent with what has been described for normal lung in the literature.[35] The accessory lobe values were always below this range, due to inclusion of the CVC when ROIs were drawn and due to the effect of partial volume averaging. The effect of partial volume averaging was also noted in the measured CSA and is believed to be the reason for the wider range in baseline CSA values compared to the other lung lobes. The accessory lobe values were however not considered to be abnormal, nor did the lobe appear abnormal on visual assessment.

On the whole, the dependent lobes demonstrated an increase in HU with a concomitant decrease in CSA (consistent with a decrease in aeration), and the non-dependent lobes demonstrated a decrease in HU and concomitant increase in CSA (consistent with improved aeration). These findings were best appreciated on slices “c”, “d” and “e” and were in accordance with statistical analysis.

None of the lungs, even with using a small circular ROI in the worst affected region, had HU values that were consistent with the values expected in atelectic lung (-100 to +100), and thus at best we noted a moderate to marked decrease in aeration. None of the most severely affected lobes demonstrated a corresponding change in aortic root, tracheal or diaphragmatic position.

The right lung lobes were never affected, except in the dog (Dog 6 in RLR) that was not adequately starved prior to CT. The periphery of the right caudal lobe was affected, however the caudal lobes are the least likely to be affected by atelectasis.[9] Therefore, the ingesta-filled stomach was believed to have indirectly caused extra compression on the right dependent lobes via possibly extra weight acting on the

diaphragm - although the right half of the cupula was still positioned more cranially than the left one when in RLR. It was thus believed that the HU changes in this lung were likely not significant for the purpose of the study, and could not be correlated to the findings in the other dogs. Interestingly, the right middle lobe never demonstrated any visible attenuation changes despite being reported as most prone to any sort of collapse, including atelectasis.[9,10] It is speculated that there is less compression of this lobe by the heart in RLR due to less cardiac apex displacement, and perhaps due to the prominent cardiac notch[57] which exposes the right heart to the thoracic wall and thus results in less lung being compressed by the heart.

The lobes that demonstrated visual increases in HU, were always the left lobes in LLR. The left *pars cranialis* was the first lobe to show visible attenuation changes, within 3 minutes, and correlates with the findings in the literature.[9] The left cranial *pars cranialis* was also visually most extensively affected. However, the *pars caudalis* had the highest HU for the most affected ventral portion of the lobe (-391, versus -410 for the *pars cranialis*), but the *pars cranialis* had the highest HU for the entire lobe (-560, versus -605 for the *pars caudalis*). The highest HU for the circular ROI was located in the ventral third of the *pars caudalis*, and the ventral thirds of the lobes were commonly the most severely affected, which is due to the large surface area to volume ratio at this location.[10] The left cranial *pars caudalis* lobe was over represented, which may be expected as it is adjacent to the heart and thus would be compressed more, relative to the other left lobes.[10]

The caudal lobes are rarely reported to be affected[9] and the findings in Dog 1 in this regard was unexpected as the dog was not in dorsal recumbency as these lobes appear to be predisposed with a dorsally recumbent body position.[4]

Visible decreased pulmonary aeration developed predominantly within 3 to 8 minutes (4/7 times) in the dependent lobes after placement in lateral recumbency, which correlated well with the literature findings of 5 minutes (human studies) to 7 minutes (canine studies).[5,11,20] All the visually affected lobes demonstrated only very mild, if any, progression at 30 minutes post general anaesthesia, and did not resolve within 10 minutes after return to sternal recumbency. No complete resolution was noted even at 20 minutes. Thus in this study, the lungs did not return to their baseline S_i aeration, as expected within ten minutes according to relevant literature.[11,20] Statistical analysis supported this descriptive finding. A difference in study design was possibly the reason for the contradictory return to baseline attenuation values. In

positional CT studies where dogs were spontaneously breathing room air,[11] and positional radiological studies assessing oxygen supplementation versus room-air,[5] the inspired air composition was probably the reason for the fairly rapid resolution of atelectasis, as oxygen supplementation is a major factor in atelectasis formation.[4] The Beagles in this study received 100% oxygen supplementation for the duration of the study, and thus a degree of ongoing resorption hypoattenuation was expected.[3,10,22]

The accessory lobe changes in this study were interesting. Due to inclusion of the CVC in the ROIs and the effect of partial volume averaging, assessment of accessory lobe was believed to be less reliable than other lobes. However as it was serially scanned, compared to itself, and served as its own control over time, there would have been a fair degree of accuracy in its assessment. The accessory lobe, although situated on the midline in the mediastinal recess, is considered one of the right lung lobes.[57] The mediastinal recess is located between the diaphragm caudally, the heart cranially, the CVC and *plica vena cava* on the right, and the caudoventral mediastinum separating it from the left caudal lobe, on the left. The accessory lobe also showed the largest visual degree of shape variation of the lobes between sternal and lateral recumbencies, and became mildly dorsoventrally elongated (“tall”) and narrow in width when in either lateral recumbency. This is probably due to the concurrent thoracic cage shape changes, as well as some displacement of the diaphragm and cardiac silhouette away from the midline region usually occupied by the accessory lobe. Whether the dog was placed in RLR or LLR did not affect the HU or CSA plots. There appeared to be improved aeration initially with placement in either lateral recumbency, but over time the HU increased gradually and repositioning in sternal recumbency had no effect on aeration. The HU and CSA plots did not correlate at all; with placement in either recumbency, a decrease in CSA was noted. Over the remainder of the study, the CSA gradually also increased, but repositioning in sternal recumbency had no effect on its values. The findings are difficult to interpret for this lobe, and it is uncertain how much variation may be due to unavoidable errors in drawing the ROIs. The accessory lobe possibly shows some overall displacement away from the dependent side, which may become occupied by cupula and the cardiac apex, and this may explain the improved aeration (HU) initially seen. The CSA values of individual dogs in either recumbency were haphazard and perhaps less importance should be imparted on them. Although CSA decreased in either recumbency, decreases were noticeably larger when the dogs were in RLR. The reason for this is

also unclear, but may be due to the lesser cardiac displacement away from the midline in RLR, resulting in a similar degree of occupation of the accessory lobe region by heart and not by lung. It is uncertain as to why the CSA should decrease in either recumbency, and may have to do with cranial diaphragmatic excursion.

In this study, the significant causes of increased attenuation was believed to be poorly aerated lung, expiratory phase of respiration (towards the cranial slices when the dogs were breathing against the breath-hold technique), inclusion of blood vessels in the ROI, and partial volume artefact. The partial volume artefact was only particularly problematic in the accessory lobe and sometimes for the cranial lobes at slice “a”, as already mentioned. Because blood vessels were included consistently for each lung when measurements were done, they were not felt to hamper evaluation of the lungs and could be visually identified as vessels, and thus not confused as an abnormal cause of increased HU.

There was always a statistically significant relationship of measured HU as well as CSA with lung lobe portion (dorsal, middle or ventral) in both sternal and lateral recumbency. The dorsal third had the most negative HU (best aerated), and the ventral third had the highest values (least aerated), and the middle third was in between. This was found overall for all lobes, including the dogs with visual attenuation changes. The ventral lobe had the smallest CSA, followed by the dorsal lobe. The middle lobe had the largest CSA. These findings are partly consistent with findings in a previous CT study.[11] In that study, only HU was assessed, and the same HU gradient as found in this current study could be demonstrated for dogs in dorsal recumbency. Interestingly, in that study the same gradient could not be demonstrated in sternal recumbency but a reason could not be established. The current study demonstrates the same gradient in sternal and lateral recumbency, thus indicating that dorsal versus sternal versus lateral recumbency has no effect on this gradient. An explanation for this likely has to do with the surface CSA to volume ratio of each lung lobe portion (for example, the ventral lobe will have to largest surface CSA to volume ratio regardless of the dog’s body position) with resultant decreased degree of aeration.[10]

The significance of decrease in CSA described may be questionable, as it only refers to a single slice through a lobe. However, utilizing serial measurements at approximately the same points was felt to give some insight into the changes that occur in the lung with change in recumbency. Unfortunately, our data could not be compared to other studies, for example that by Ahlberg,[11] which stated a 50%

decrease in volume with lateral recumbency, because we measured CSA only and not volume. Our findings state that there is a range in decrease in CSA. The smallest CSA at any point in each dog always shared the highest HU value, as would be expected. The ventral lobe appeared to contribute the most to the decreased CSA of the total lobe (4/7 times), and always had the lowest HU of all thirds. A small CSA change often had a large corresponding change in HU, but this was likely due to the wide scale of HU ranges present in the lungs, and thus the two cannot be exactly correlated.

5.6 Limitations of the study

- The main limitation to this study was the low number of animal investigated. Although each animal was used as its own control, statistically the number of studies was undesirable.
- Because we followed protocols commonly used in thoracic CT in daily studies, we believe there may be a possibility that the breath-hold technique may itself have been responsible for prevention of severe atelectasis to some degree. However, positive pressure of 40 cm H_20 for 7-8 seconds is needed to re-inflate atelectic lung in man.[58] Although a pressure of 15 cm H_20 should not result in any effect on atelectasis formation, each breath-hold was of long duration (approximately 35 seconds) and the influence of this is uncertain.
- Moving the dogs from lateral to sternal recumbency, and repeating the topogram and re-planning scan sites, led to mismatches in exact slice measurement position (despite best efforts to align them anatomically), which led to obvious differences in measured values between these time period, as noted on the graphs.
- Only one person (the primary investigator) assessed the images and performed the measurements, thus inter-interpreter consistency could not be assessed. The measurements were only performed once, thus intra-observer consistency also could not be determined.
- The vast amount of data took very long to capture and interpret, which was a major drawback to the study.
- The study did not look at dogs of other body conditions (especially obesity) or thoracic anatomical differences (e.g. Bulldog), and it is suspected that this may

have a noticeable effect of the outcome of the study. Studies in support of increased atelectasis with obesity[5,16] are available.

- The effect of the GA protocol (compared to other potential combinations of drugs) was not assessed, but if compared to previous studies that utilised only sedation or no breath-hold, it is expected that the breath-hold technique (as discussed) may indeed have some effect on atelectasis formation. The dogs in this study received the same drugs and thus were their own control.

5.7 Clinical applications

The current study has found that lateral recumbency in a healthy medium-sized breed, of normal body condition, does not result in true atelectasis, nor hypoinflation that is severe enough to hamper pulmonary evaluation, especially if the dog has only been in lateral recumbency for a short period of time (< 3 minutes).

Visible attenuation changes always occurred in the left lobes in LLR, and thus the recommendation could be made that all general thoracic studies should be performed in RLR as the chance of radiologically or CT visible changes would be expected to be absent or negligible. Obviously this recommendation can only be made if the choice of RLR versus LLR for thoracic studies (as part of orthogonal views) is equivocal.

In the dogs that did have some degree of hypoinflation of the lungs (and thus visible increased attenuation), the changes persisted despite repositioning in sternal recumbency. In these cases, where there is doubt with regards to the presence of pathology in the affected lung, ventilatory strategies can be applied to the lungs to resolve atelectasis.

An ingesta-filled stomach was believed to result in mild visible CT attenuation changes, and thus adequate patient starvation was proven to important prior to imaging.

The study supports the recommendation that general anaesthesia be induced in sternal recumbency; however anaesthesia in lateral recumbency (particularly RLR) should not preclude CT scanning. Although not investigated in this study, this recommendation may be more significant in obese dogs or dogs that have pre-existing pulmonary pathology.

5.8 Future studies

The following future studies have been identified based on this study:

- The development and resolution of atelectasis in large-breed or obese dogs.
- The development and resolution of atelectasis in dogs with atypical thoracic conformations, for example the English bulldog.
- The development and resolution of atelectasis in dogs with respiratory conditions that may hamper normal respiration (e.g. brachycephalic airway syndrome).
- The development and resolution of atelectasis in dogs given 100% oxygen versus room air via endotracheal tube during general anaesthesia, using the protocol used in this study.
- The development and resolution of atelectasis in dogs if anaesthesia is induced in LLR or RLR.

To refine the study further, it would be recommended to acquire CT software that can perform automated lung segmentation techniques[59] in order to rapidly acquire HU measurements for all slices of the scan which would decrease the time taken to collect data.
A method to assess lungs in cases of true atelectasis is proposed, and the following measurements could be performed as follows (Fig. 54):

- The total lung border would be manually drawn by the operator (as described) using a computer mouse, to obtain a lung CSA in cm^2 and a mean HU of the total lung. The same guidelines pertaining to blood vessels and bronchi as already discussed would be applied.
- Regions of subjective increased soft tissue attenuation will also be manually outlined by the operator to obtain a CSA (cm^2) and mean HU.
- The percentage of affected lung would be calculated by dividing the CSA of atelectic lung by the total lung CSA for each slice.
- The difference in HU and CSA of total lung will be compared with previous time intervals to detect a change in these parameters, either seen as progression of

atelectasis with lateral recumbency or resolution with repositioning in sternal recumbency.

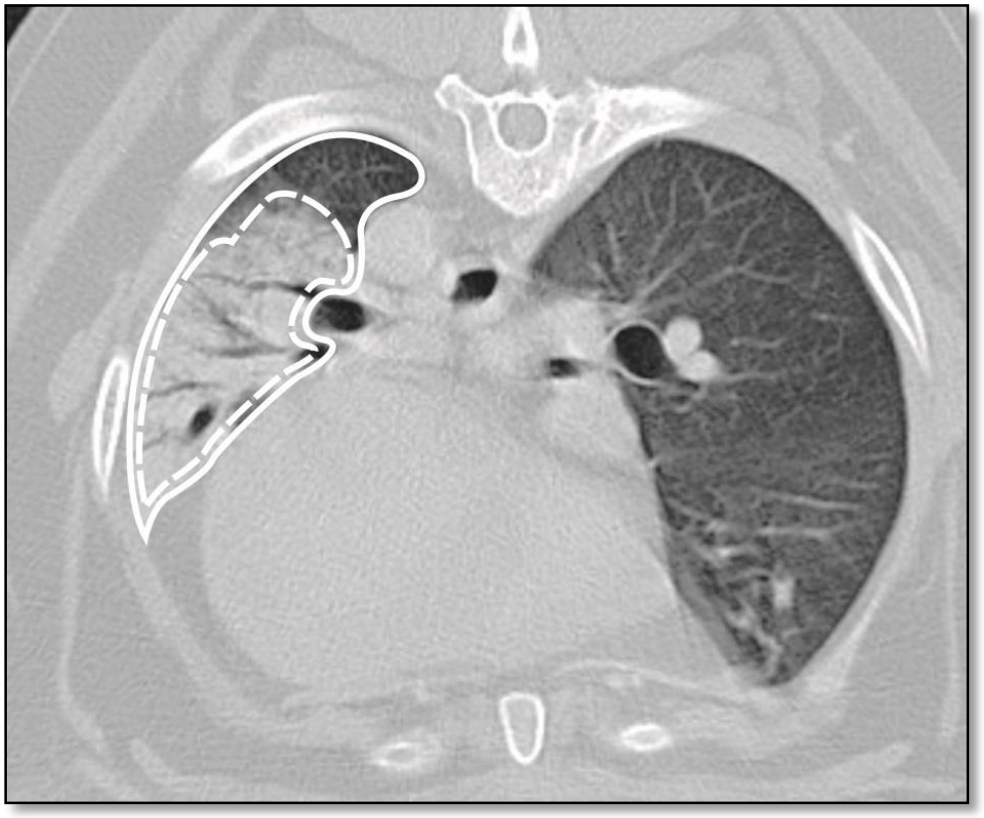

FIG. 54. Transverse plane image indicates the method employed to measure the total lung CSA (solid white outline) and the region of increased HU (dashed outline), determined visually. The image was obtained over the caudal cardiac silhouette in an obese Labrador which presented for an axillary mass (determined to be a benign lipoma) and thoracic CT to check for metastasis. The dog had been in LLR under general anaesthesia, prior to the thoracic CT. The ventral two-thirds of the left caudal lobe demonstrated marked increased soft tissue attenuation and air bronchograms, believed to be due to atelectasis. The image was windowed from a lung window (WL -600, WW 1200) and the left of the image corresponds to the dog's left. Image acquired in sternal recumbency.

Chapter 6: Conclusion

The following conclusions were deduced from this study:

- The degree of attenuation changes in healthy Beagles was minimal, and the study did not support the hypothesis that lateral recumbency would induce true pulmonary atelectasis. Anaesthesia in lateral recumbency should not preclude CT scanning.
- Visible attenuation changes did not resolve with repositioning in sternal recumbency, however were not found to be severe enough to hamper evaluation.
- There were very few visible HU and no CSA changes in this study, and the most severe HU changes indicated moderate to marked decrease in aeration (up to -391) but not atelectasis, per definition.
- The baseline HU measurements for the lungs were all within normal ranges for respiration reported in the literature.[35]
- The significant changes that could be visualised all occurred in the left lobes, when the dogs were in LLR, and were most severe ventrally.
- The right middle lobe was never affected.
- The left cranial *pars caudalis* lobe was affected most often, but the *pars cranialis* and *pars caudalis* could be affected equally in severity.
- The first lobe to show visible attenuation changes was the left cranial *pars cranialis* lobe at 3 minutes in LLR.
- The location of the attenuation changes was mainly in the periphery of the lobes, especially the ventral third, which was also affected first.[10] The middle third also demonstrated appreciable changes, sometimes to a similar degree.
- Visible decreased pulmonary aeration developed predominantly within 3 to 8 minutes in the dependent lobes after placement in lateral recumbency (after induction of anaesthesia using a standardised anaesthetic protocol commonly used in the section of diagnostic imaging), and:
    - Showed only very mild, if any, progression at 20 minutes post general anaesthesia (even up to 30 minutes), and

  - Did not resolve within 10 minutes after return to sternal recumbency. No complete resolution was noted even at 20 min.
- The lack of resolution of the visible increased attenuation was not consistent with previous canine lung CT studies. The most likely explanation for this was the difference in anaesthetic or sedative protocols used between studies, as well as the possibility of a different study population (age, breed) between studies.
- For the dogs with visually detectable HU changes, a gradient occurred for HU and CSA findings from the ventral to the dorsal thirds most often when in lateral recumbency, as follows:
  - The dorsal third had the most negative HU, the ventral third had the highest HU values, and the middle third was in between.
  - The dorsal third most often had the largest CSA values, followed by the middle third, with the ventral lobe having the smallest CSA.
- In general, the dependent lobes demonstrated an increase in HU (consistent with a decrease in aeration), and the non-dependent lobes demonstrated a small decrease in HU (consistent with improved aeration). Changes were most obvious on the graphs at S_i to LLR_3/RLR_3, and when repositioned in sternal recumbency from LLR_{30}/RLR_{30} to S_e. Minimal change in HU and CSA over time was seen.
- HU and CSA graphs correlated well (i.e. an increase in HU was seen with a decrease in CSA, as seen with decreased aeration, and vice versa).
- The trachea was always located to the right of the midline, and the aortic root was positioned closely around the midline. In lateral recumbency, tracheal and aortic root movement was assigned to body and cardiac positional changes, and movement was too mild to be visualised.
- There was no concurrent tracheal, aortic root or diaphragmatic changes (as seen with mediastinal shift) associated with decreased aeration.
- Diaphragmatic findings were considered normal in this study and no conclusion could be drawn with regards to position versus stage of respiration, although the findings correlated to those in previous radiological studies.
- The study design was believed to be adequate for the research questions posed, and the limitations have been identified and addressed.

References

1. Ohlerth S, Scharf G. Computed tomography in small animals - basic principles and state of the art applications. Vet J 2007;173:254–271.
2. Brooks-Brunn J. Postoperative atelectasis and pneumonia. Heart Lung 1995;24:94–115.
3. Duggan M, Kavanagh BP. Pulmonary atelectasis: a pathogenic perioperative entity. Anesthesiology 2005;102:838–854.
4. Staffieri F, Franchini D, Carella G, et al. Computed tomographic analysis of the effects of two inspired oxygen concentrations on pulmonary aeration in anesthetized and mechanically ventilated dogs. Am J Vet Res 2007;68:925–931.
5. Barletta M, Almondia D, Williams J, et al. Radiographic evaluation of positional atelectasis in sedated dogs breathing room air versus 100% oxygen. Can Vet J 2014;55:985–991.
6. Morandi F, Mattoon JS, Lakritz J, et al. Correlation of helical and incremental high-resolution thin-section computed tomographic imaging with histomorphometric quantitative evaluation of lungs in dogs. Am J Vet Res 2003;64:935–944.
7. Brainard BM, Alwood AJ, Kushner LI, et al. Postoperative pulmonary complications in dogs undergoing laparotomy: anesthetic and perioperative factors. J Vet Emerg Crit Care 2006;16:184–191.
8. Alwood AJ, Brainard BM, LaFond E, et al. Postoperative pulmonary complications in dogs undergoing laparotomy: frequency, characterization and disease-related risk factors. J Vet Emerg Crit Care 2006;16:176–183.
9. Suter P, Lord P. Lower airway and pulmonary parenchymal disease. In: Suter P, Lord P (eds): Thoracic radiography: a text atlas of thoracic disease in the dog and cat. Wettswil, Switzerland: P. Suter, 1984;640–650.
10. Mai W, O'Brien R, Scrivani P, et al. The lung parenchyma. In: Schwarz T, Johnson V (eds): BSAVA Manual of canine and feline thoracic imaging. Gloucester: BSAVA, 2008;283–286.
11. Ahlberg NE, Hoppe F, Kelter U, et al. A computed tomographic study of volume and x-ray attenuation of the lungs of Beagles in various body positions. Vet Radiol 1985;26:43–47.

12. Robinson N. Section VIII: Respiratory function. In: Cunningham J, Klein B (eds): Textbook of veterinary physiology. 4th ed. St. Louis: Elsevier Saunders, 2007;565–610.
13. Corcoran BM. Respiratory pathophysiology. In: Fuentes VL, Johnson LR, Dennis S (eds): BSAVA Manual of cardiorespiratory medicine. 2nd ed. Gloucester, BSAVA; 2010;108–111.
14. Delaunois L. Anatomy and physiology of collateral respiratory pathways. Eur Respir J 1989;2:893–904.
15. Thrall DE. Principles of radiographic interpretation of the thorax. In: Thrall DE (ed): Textbook of veterinary diagnostic radiology. St. Louis: Elsevier Saunders, 2013;474–488.
16. Mosing M, German A, Holden S, et al. Oxygenation and ventilation characteristics in obese sedated dogs before and after weight loss: a clinical trial. Vet J 2013;198:367–371.
17. O'Donohue W. Prevention and treatment of postoperative atelectasis. Chest 1985;87:1–2.
18. Canfrán S, Gómez se Segura I, Cediel R, et al. Effects of a stepwise lung recruitment manoeuvre and positive end-expiratory pressure on lung compliance and arterial blood oxygenation in healthy dogs. Vet J 2012;194:89–93.
19. Lundquist H, Hedenstierna G, Strandberg A, et al. CT-assessment of dependent lung densities in man during general anaesthesia. Acta Radiol 1995;36:626–632.
20. Brismar B, Hedenstierna G, Lundquist H, et al. Pulmonary densities during anesthesia with muscular relaxation - a proposal of atelectasis. Anesthesiology 1985;62:422–428.
21. Guyton AC, Hall JE. Regulation of respiration. In: Guyton AC, Hall JE (eds): Textbook of medical physiology. Philadelphia: Elsevier Inc. 2006;514–523.
22. Hedenstierna G, Edmark L. Mechanisms of atelectasis in the perioperative period. Best Pract Res Clin Anaesthesiol 2010;24:157–169.
23. Rothen H, Sporre B, Engberg G, et al. Prevention of atelectasis during general anaesthesia. Lancet 1995;345:1387–1391.
24. Rusca M, Proietti S, Schnyder P, et al. Prevention of atelectasis formation during induction of general anesthesia. Anesth Analg 2003;97:1835–1839.

25. Eichenberger A, Proietti S, Wicky S, et al. Morbid obesity and postoperative pulmonary atelectasis: An underestimated problem. Anesth Analg 2002;95:1788–1792.
26. Lundquist H, Hedenstierna G, Ringertz H. Barbiturate anaesthesia does not cause pulmonary densities in dogs: a study using computerized axial tomography. Acta Anaesthesiol Scand 1988;32:162–165.
27. Prather A, Berry C, Thrall D. Use of radiography in combination with computed tomography for the assessment of noncardiac thoracic disease in the dog and cat. Vet Radiol Ultrasound 2005;46:114–121.
28. Cai H, Gong H, Zhang L, et al. Effect of low tidal volume ventilation on atelectasis in patients during general anesthesia: a computed tomographic scan. J Clin Anesth 2007;19:125–129.
29. Giglio RF, Winter MD, Reese DJ, et al. Radiographic characterization of presumed plate-like atelectasis in 75 nonanesthetized dogs and 15 cats. Vet Radiol Ultrasound 2013;54:326–331.
30. Simon BA. Non-invasive imaging of regional lung function using x-ray computed tomograpy. J Clin Monit Comput 2000;16:433–442.
31. Magnusson L, Spahn D. New concepts of atelectasis during general anaesthesia. Br J Anaesth 2003;91:61–72.
32. Staffieri F, DeMonte V, DeMarzo C, et al. Influence of abdominal surgery on pulmonary atelectasis formation in dogs. In: Pugliese A, Gaiti A, Boiti C (eds): Veterinary science: Current aspects in biology, animal pathology, and clinical food hygiene. Heidelberg: Springer-Verlag Berlin Heidelberg 2012;141–145.
33. Strang C, Hachenberg T, Freden F, et al. Development of atelectasis and arterial to end-tidal PCO_2-difference in a porcine model of pneumoperitoneum. Br J Anaesth 2009;103:298–303.
34. David M, Karmrodt J, Bletz C, et al. Analysis of atelectasis, ventilated, and hyperinflated lung during mechanical ventilation by dynamic CT. Chest 2005;128:3757–3770.
35. Schwarz T, Johnson V. Lungs and bronchi. In: Schwarz T, Saunders J (eds): Veterinary computed tomography. West Sussex: John Wiley and Sons Ltd, 2011;261–276.
36. Drummond G. Computed tomography and pulmonary measurements. Br J Anaesth 1998;80:665–671.

37. Wandtke JC, Hyde RW, Fahey PJ, et al. Measurement of lung gas volume and regional density by computed tomography in dogs. Invest Radiol 1986;21:108–117.
38. Woodring J. Determining the cause of pulmonary atelectasis: A comparison of plain radiography and CT. Am J Roentgenol 1988;150:757–763.
39. Brenner DJ, Hall EJ. Computed tomography - An increasing source of radiation exposure. N Engl J Med 2007;29:2277–2284.
40. Israel GM, Cicchiello L, Brink J, et al. Patient size and radiation exposure in thoracic, pelvic, and abdominal CT examinations performed with automatic exposure control. Am J Roentgenol 2010;195:1342–1346.
41. Johnson V, Corcoran B, Wotton P, et al. Thoracic high-resolution computed tomographic findings in dogs with canine idiopathic pulmonary fibrosis. J Small Anim Pract 2005;46:381–388.
42. Schild H, Weitz M, Strunk H, et al. Computertomographie der atelektase. Fortschr Geb Rontgenstr Nuklearmed 1987;147:493–497.
43. Evans HE, de Lahunta A. Miller's anatomy of the dog. Evans HE, de Lahunta A (eds):, St. Louis: Elsevier Saunders, 2013.
44. Suter P, Lord P. Thoracic radiography: A text atlas of thoracic disease of the dog and cat. Suter P, Lord P (eds): Wettswil: Peter F. Suter, 1984.
45. Schwarz T, Johnson V. BSAVA manual of canine and feline thoracic imaging. Schwarz T, Johnson V. (eds) Gloucester: BSAVA, 2008.
46. Saunders J, Schwarz T. Veterinary computed tomography. Saunders J, Schwarz T (eds): West Sussex: John Wiley and Sons Ltd, 2011.
47. Grandage J. The radiology of the dog's diaphragm. J Small Anim Pract 1974;1–17.
48. Dennis R, Kirberger RM, Barr F, et al. Lower respiratory tract. In: Dennis R, Kirberger RM, Barr F (eds): Handbook of small animal radiology and ultrasound. 2nd ed. St Louis: Elsevier Ltd, 2010;145-147.
49. Baines E. The mediastinum. In: Schwarz T, Johnson V (eds): BSAVA Manual of canine and feline thoracic imaging. Gloucester: BSAVA, 2008;177–199.
50. Frame A, King A. The pleural space. In: Schwarz T, Johnson V (eds): BSAVA Manual of canine and feline thoracic imaging. Gloucester: BSAVA, 2008;322.
51. Thrall DE. The mediastinum. In: Thrall DE (ed): Textbook of veterinary diagnostic radiology. 6th ed. St. Louis: Elsevier Saunders, 2013;551–570.

52. Bezuidenhout A. The heart and arteries. In: Evans H, de la Hunta A (eds): Miller's anatomy of the dog. St. Louis: Elsevier Saunders, 2013;428–438.
53. Dyce K, Sack W, Wensing C. The cardiovascular system. In: Dyce K, Sack W, Wensing C (eds): Textbook of veterinary anatomy. St. Louis: Elsevier Saunders, 2010;225.
54. Davis H, Jensen T, Johnson A, et al. 2013 AAHA/AAFP fluid therapy guidelines for dogs and cats. J Am Anim Hosp Assoc 2013;49:149–159.
55. Hall L, Clarke K, Trim C. Patient monitoring and clinical measurement. In: Hall L, Clarke K, Trim C (eds): Veterinary anaesthesiology. 9th ed. London: Harcourt Publishers Limited, 2001;35–36.
56. Soulsby SN, Holland M, Hudson JA, et al. Ultrasonographic evaluation of adrenal gland size compared to body weight in normal dogs. Vet Radiol Ultrasound 2015;56:317–326.
57. Evans H, de Lahunta A. The respiratory system. In: Evans H, de Lahunta A (eds): Miller's anatomy of the dog. 4th ed. St. Louis: Elsevier Saunders, 2013;338–360.
58. Hedenstierna G, Rothen HU. Atelectasis formation during anaesthesia: Causes and measures to prevent it. J Clin Monit 2000;16:329–335.
59. McEvoy FJ, Buelund L, Strathe AB, et al. Quantitative computed tomography evaluation of pulmonary disease. Vet Radiol Ultrasound 2009;50:47–51.

Appendices

Appendix A: Beagle data

Dog	Age (months)	Weight (kilograms)	Body condition score	Recumbency first CT scan	Recumbency second CT scan	DLP total	CDTI total
1	108	11.2	5 to 6	Right	Left	1116	267.04
2	105	13.7	5 to 6	Right	Left	1294	284.31
3	97	13.7	5 to 6	Right	Left	1223	269.27
4	104	10.8	5	Left	Right	1189	265.33
5	100	12.8	5 to 6	Left	Right	1236	274.97
6	100	13.3	5 to 6	Left	Right	1226	273.27

DLP – dose length product; CTDI – computed tomography dose index

Appendix B: Timed scanning intervals

Dog	Study (1 or 2)	Time (minutes) from induction to survey helical scan	Time (minutes) taken to lateral scan after repositioning from sternal to lateral recumbency	Time (minutes) taken to sternal scan after repositioning from lateral to sternal recumbency
1	1	5	4	2
	2	5	2	2
2	1	6	3	2
	2	8	2	2
3	1	4	3	1.5
	2	5	3	2
4	1	6	4	1
	2	7	2	2
5	1	5	3	1
	2	8	2	1
6	1	5	2	2
	2	4	1	2